SAND2020-10742R

United States Department of Energy
National Nuclear Security Administration
Nuclear Criticality Safety Program

PITCH VARIATION EXPERIMENTS IN WATER-MODERATED SQUARE-PITCHED U(6.90)O_2 FUEL ROD LATTICES WITH FUEL TO WATER VOLUME RATIOS SPANNING 0.08 TO 0.67

Integral Experiment Request 230
CED-3b Summary Report

Critical and Subcritical Experiment Design Team (C_EdT)

David E. Ames (SNL), C_EdT Lead
Gary A. Harms (SNL), C_EdT Experiment Member
Michael L. Zerkle (NNL), C_EdT NDAG Member
Justin B. Clarity (ORNL), C_EdT Methods Member
David P. Heinrichs (LLNL), C_EdT Member
Isabella Duhamel (IRSN), C_EdT Member

September 30, 2020

SANDxxxx-xxx

Sandia National Laboratories is a multimission laboratory managed and operated by National Technology and Engineering Solutions of Sandia LLC, a wholly owned subsidiary of Honeywell International Inc. for the U.S. Department of Energy's National Nuclear Security Administration under contract DE-NA0003525.

Nearly Blank Page

PITCH VARIATION EXPERIMENTS IN WATER-MODERATED SQUARE-PITCHED U(6.90)O_2 FUEL ROD LATTICES WITH FUEL TO WATER VOLUME RATIOS SPANNING 0.08 TO 0.67

Integral Experiment Request 230
CED-3a Summary Report

Critical and Subcritical Experiment Design Team (C_EdT)

David E. Ames (SNL), C_EdT Lead
Gary A. Harms (SNL), C_EdT Experiment Member
Michael L. Zerkle (NNL), C_EdT NDAG Member
Justin Clarity (ORNL), C_EdT Methods Member
David P. Heinrichs (LLNL), C_EdT Member
Isabella Duhamel (IRSN), C_EdT Member

September 30, 2020

1.0 DETAILED DESCRIPTION

1.1 Overview of Experiment

The US Department of Energy (DOE) Nuclear Energy Research Initiative funded the design and construction of the Seven Percent Critical Experiment (7uPCX) at Sandia National Laboratories. The start-up of the experiment facility and the execution of the experiments described here were funded by the DOE Nuclear Criticality Safety Program. The 7uPCX is designed to investigate critical systems with fuel for light water reactors in the enrichment range above 5 % ^{235}U. The 7uPCX assembly is a water-moderated and -reflected array of aluminum-clad square-pitched U(6.90 %)O_2 fuel rods. Other critical experiments performed in the 7uPCX assembly are documented in LEU-COMP-THERM-078, LEU-COMP-THERM-080, LEU-COMP-THERM-096, LEU-COMP-THERM-097, and LEU-COMP-THERM-101.

The fuel used in these experiments was fabricated using unirradiated 6.90 % enriched UO_2 fuel pellets from fuel elements designed to be used in the internal nuclear superheater section of the Pathfinder boiling water reactor operated in South Dakota by the Northern States Power Company in the 1960s. The fuel elements were obtained from The Pennsylvania State University where they had been stored for many years. The fuel pellets in those fuel elements were removed from the original Incoloy cladding and reclad in 3003 aluminum tubes and end caps for use in the experiments reported here.

The purpose of these experiments was to measure the effects of decreasing the fuel-to-water volume ratio on the critical array size. This was accomplished by removing fuel rods from fully fueled configurations, effectively increasing the pitch of the fuel arrays in the assembly. The fuel rod pitch variations provided assembly configurations that ranged from strongly undermoderated to slightly overmoderated.

The critical experiments were done using the two existing sets of grid plates available at the Sandia Critical Experiments (SCX), each having 2025 fuel rod locations configured in a 45 x 45 square-pitched array. The grid plates were designed for investigating fuel configurations with fuel-to-water ratios in the same range as

are present in the current US inventory of pressurized water reactors. As a result, the hole-to-hole spacing (i.e. fuel rod pitch when loaded with fuel) for both sets of grid plates produce fuel rod arrays that are strongly undermoderated. The pitch values for the two sets of grid plates are 0.315 in (0.8001 cm) and 0.3366 in (0.854964 cm). The corresponding fuel-to-water volume ratios for each are 0.67 and 0.52.

The fuel rod pitch for each set of grid plates was effectively increased by a factor of $\sqrt{2}$ and a factor of two. To accomplish this, consider the case in which all 2025 fuel rod locations are occupied. Then, by removing every other fuel rod in a staggered pattern, the original square pitch is rotated by 45 degree and increased by a factor of $\sqrt{2}$. Now, again considering the case with all 2025 fuel rods loaded, this time by removing every other row and column of fuel rods, the original pitch is doubled. The process described above provides four additional fuel rod pitch values at 0.445477 in (1.131512 cm), 0.476024 in (1.209102 cm), 0.63 in (1.6002 cm), and 0.6732 in (1.709928 cm). The corresponding fuel-to-water volume ratios for each are 0.23, 0.19, 0.10, and 0.08.

The twenty-seven critical experiments in this series were performed in 2020 in the SCX at the Sandia Pulsed Reactor Facility. The experiments are grouped by fuel rod pitch. Case 1 is a base case with a pitch of 0.8001 cm and no water holes in the array. Cases 2 through 6 have the same pitch as Case 1 but contain various configurations with water holes, providing slight variations in the fuel-to-water ratio. Similarly, Case 7 is a base case with a pitch of 0.854964 cm and no water holes in the array. Cases 8 through 11 have the same pitch as Case 7 but contain various configurations with water holes. Cases 12 through 15 have a pitch of 1.131512 cm and differ according to the number of water holes in the array, with Case 12 having no water holes. Cases 16 through 19 have a pitch of 1.209102 cm and differ according to number of water holes in the array, with Case 16 having no water holes. Cases 20 through 23 have a pitch of 1.6002 cm and differ according to number of water holes in the array, with Case 20 having no water holes. Cases 24 through 27 have a pitch of 1.709928 cm and differ according to number of water holes in the array, with Case 24 having no water holes. As the experiment case number increases, the fuel-to-water volume ratio decreases.

All twenty-seven critical experiments are judged to be acceptable as benchmark experiments.

1.2 Description of Experimental Configuration

1.2.1 Design of the Critical Assembly – A schematic of the critical assembly as it was configured for the experiments evaluated in LEU-COMP-THERM-079 is shown in Figure 1. The same assembly tank was used for the experiments evaluated here though the assembly core was modified. Figure 2 shows a view of the critical assembly configured for the current experiments. The assembly core resides in an elevated assembly tank that is connected to a moderator dump tank at a lower elevation. When the assembly is not being operated, the moderator resides in the dump tank. When the assembly is being brought to critical, the moderator is pumped from the dump tank into the assembly tank. The moderator can be released by gravity to the dump tank through two large-diameter pneumatically-operated normally-open dump valves. During operation, the moderator is continually circulated between the dump tank and the assembly tank. The level of the moderator in the assembly tank is maintained by overflow into one of two overflow standpipes. One is set at a fixed height that allows the core tank to fill to a level that fully reflects the fuel in the critical assembly. The other overflow standpipe is remotely adjustable to set the water level in the core below the fully-reflected level. For the experiments described here, the adjustable standpipe was set to a level above that of the fixed standpipe. A heater is included in the dump tank to keep the moderator at a constant temperature set by a controller at the assembly control system. The purity of the water moderator is maintained by pumping it from the dump tank through a clean-up loop consisting of a pump, two particulate filters, a resin bed, a resistivity water quality monitor, and the associated piping.

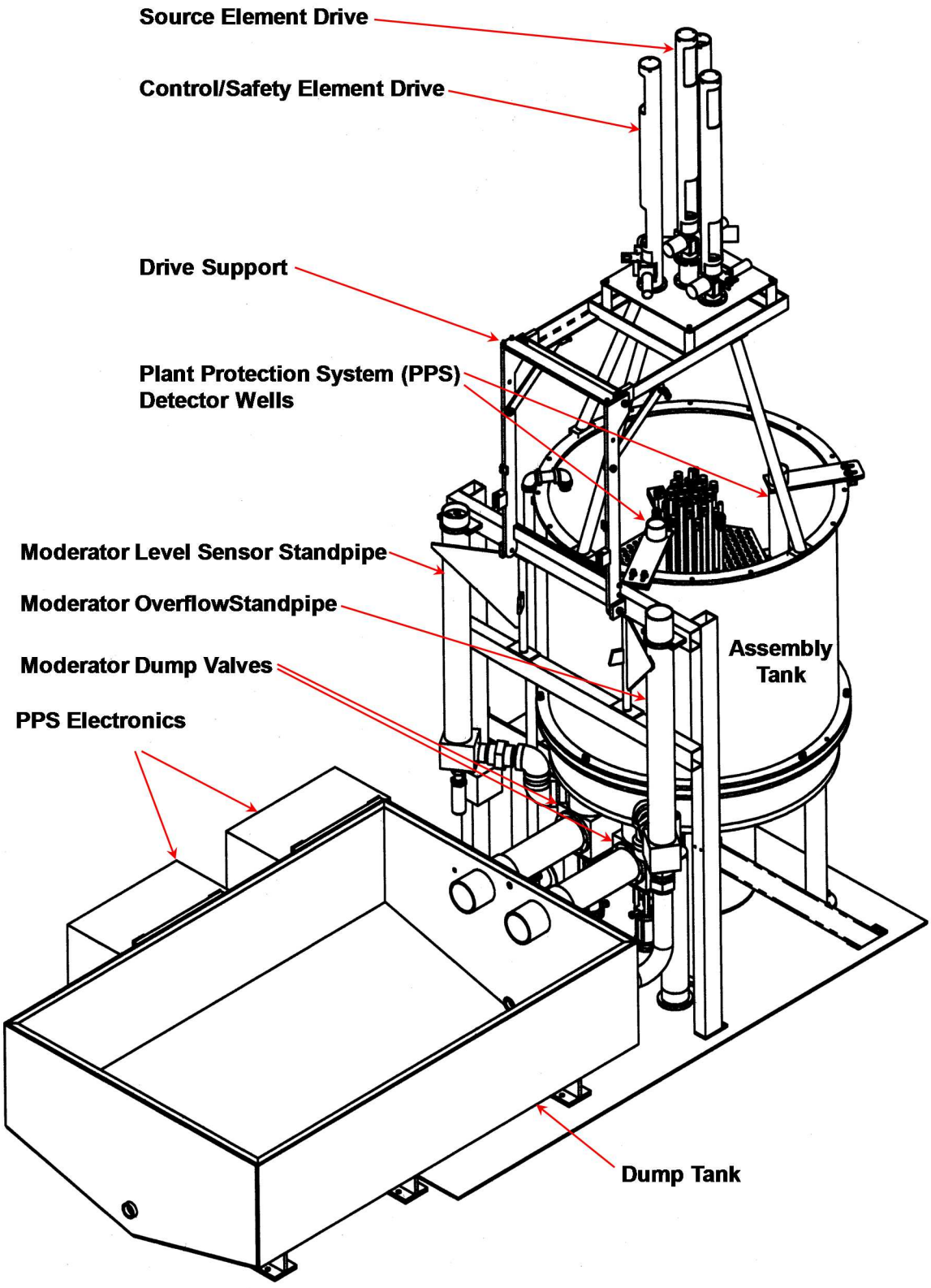

Figure 1. A Schematic of the Critical Assembly.

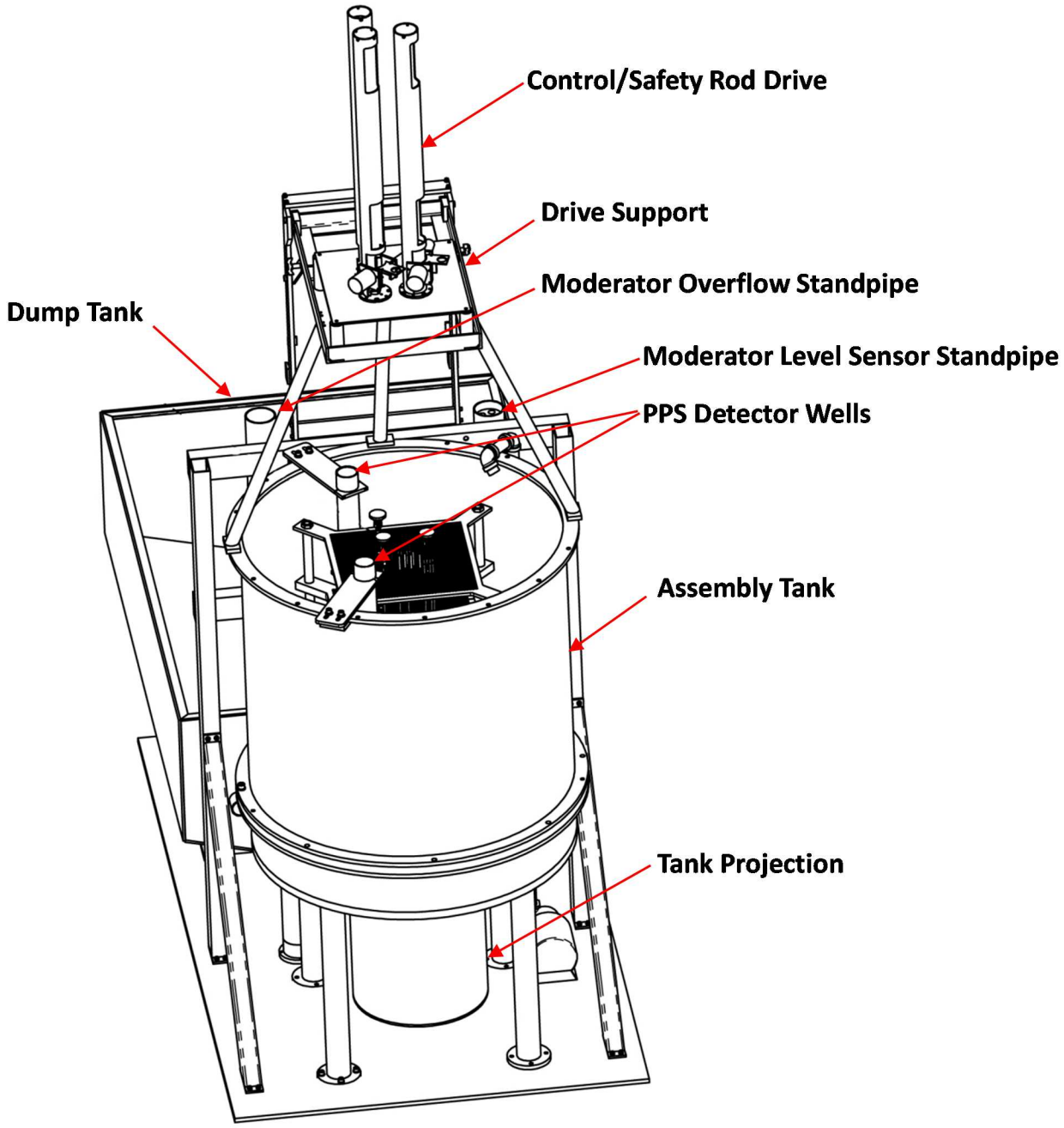

Figure 2. View of the Critical Assembly.

A cut-away view of the critical assembly is shown in Figure 3. The assembly fuel is supported in the assembly tank by two 1 in (2.54 cm) thick aluminum grid plates. A guide plate, used to align the fuel rods in the assembly during insertion, is located above the upper grid plate. The assembly core is situated in the tank to provide a 6.5 in (16.51 cm) thick water reflector below the lower grid plate. The diameter of the tank provides a radial water reflector around the assembly greater than 6 in (15.24 cm). The fixed assembly tank standpipe is set to provide an upper reflector approximately 6 in (15.24 cm) thick when the assembly tank is full.

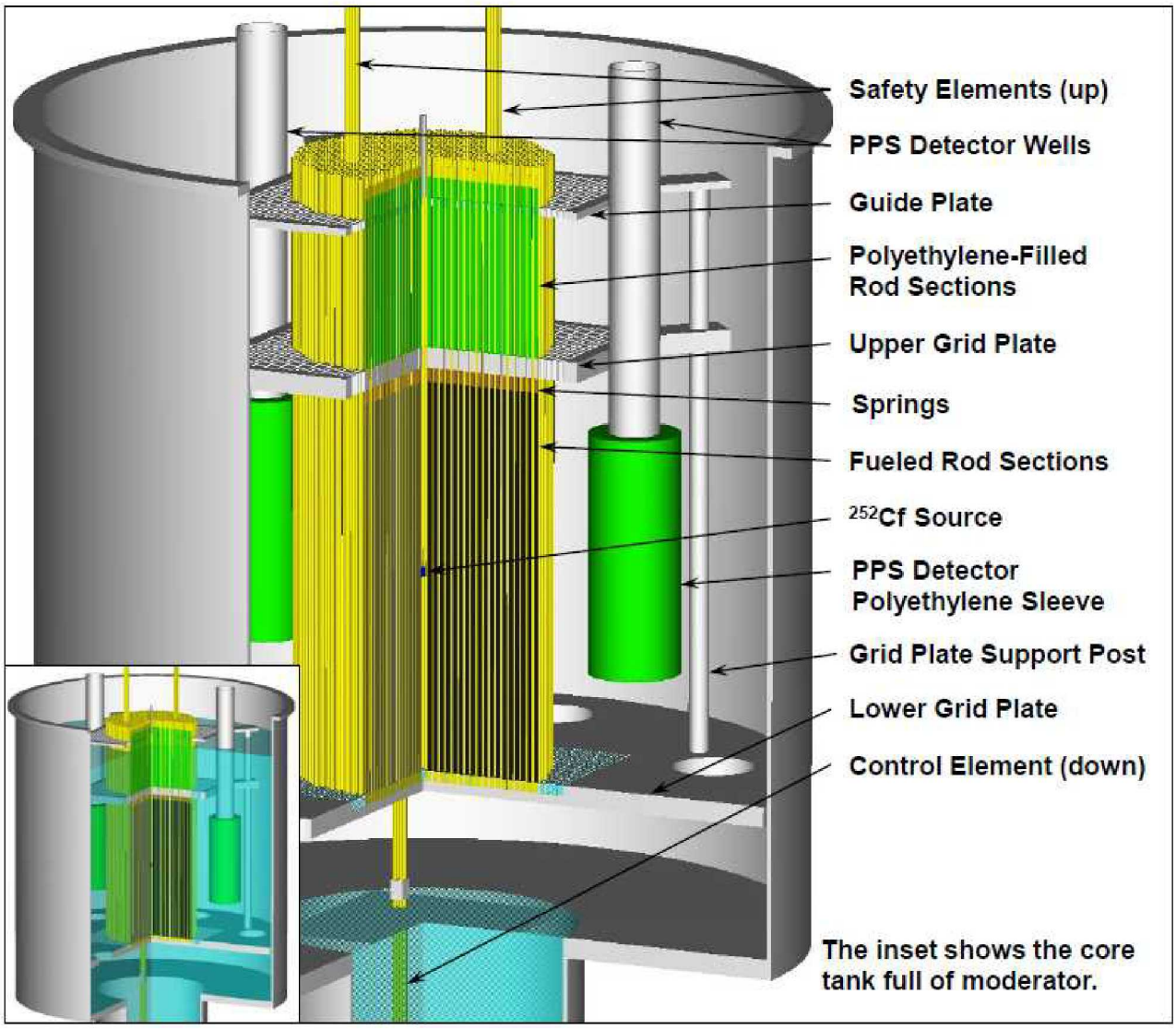

Figure 3. Cut-Away View of the Critical Assembly Core Tank (Case 8).

The assembly has one control and two safety elements of identical design. Each of these elements has a B_4C-filled absorber section separated from a fuel follower by a polyethylene-filled decoupler section. When each of the elements is fully withdrawn, the fuel follower is in the assembly and the absorber is above the surface of the assembly moderator. The two types of elements are differentiated by the way in which they are used. During operations, the two safety elements are held in the most reactive position and provide a redundant shutdown mechanism that can be rapidly inserted by gravity drop. The control element is used to make fine adjustments to the reactivity of the assembly during operations. During the measurements reported here, all three elements were fully withdrawn to their most reactive positions. The three control/safety elements are attached to the control/safety element drives through electromagnets. The control/safety element drives are supported above the assembly tank by the drive support.

Figures 4 through 6 show photographs of three of the cores in the assembly. At the time that the photographs were taken, the moderator had been drained from the core tank. Figure 4 shows an overall view of the critical assembly core in the assembly tank. In this view, the control element is down and attached to the control element drive. Both safety elements are down, and the safety element drives are withdrawn out of the picture. The lower grid plate is visible at the bottom of the tank with the upper grid plate above it. The guide plate is visible above the upper grid plate. The upper grid plate and the guide plate have checkerboard markings to aid in the placement of the fuel rods in the assembly grid. The guide plate has been etched so that each

column and row in the grid pattern can be identified. The markings are visible in the figures. The two dry wells that house the fission chambers for the assembly instrumentation are visible in the picture. The handle of the neutron source, which stands above the tops of the fuel rods, is visible at the center of the core.

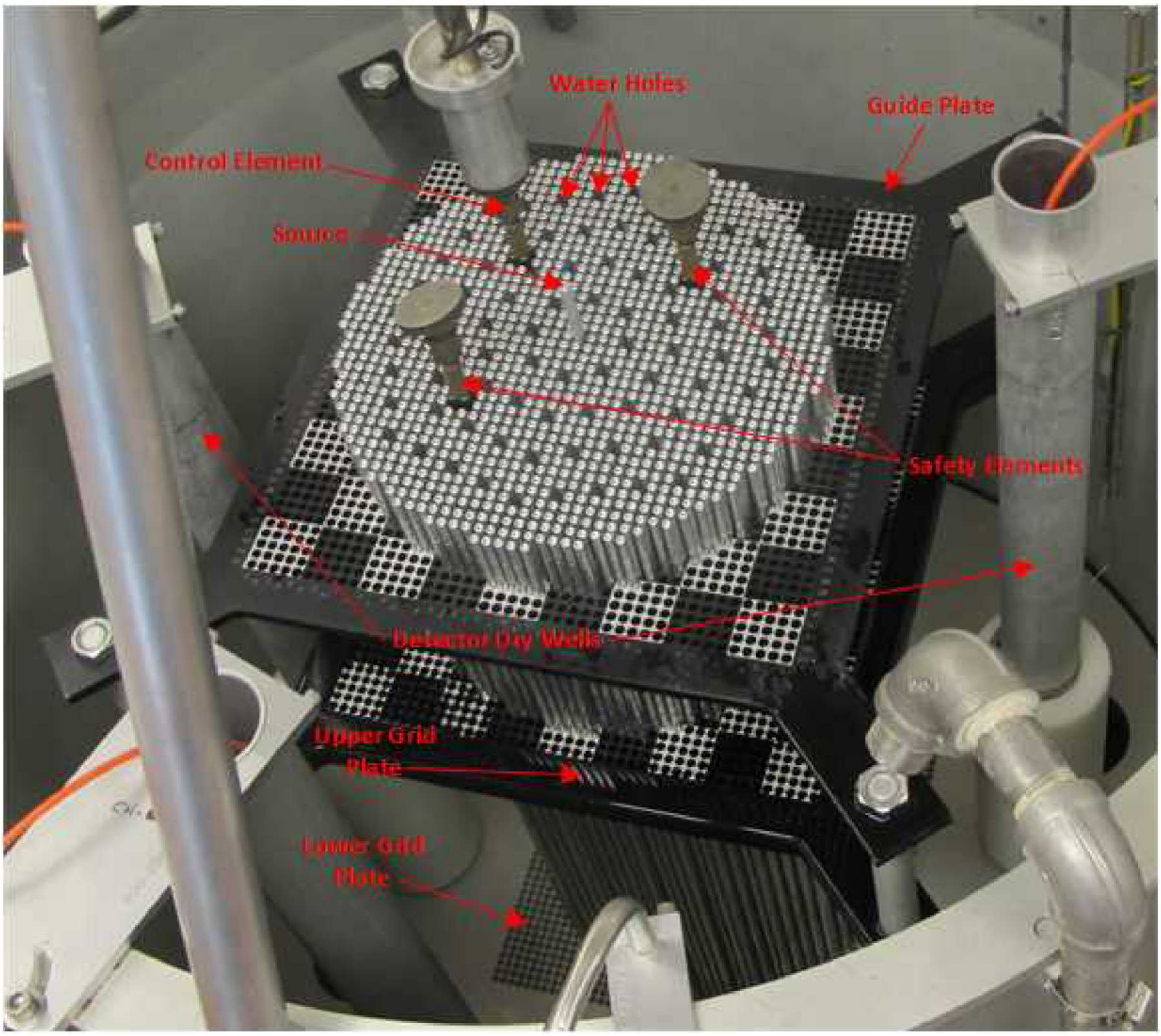

Figure 4. View of One of the Critical Configurations (Case 6).

Figure 5 shows a view of the top of the core for a different configuration. In this view, grid plate holes within the fueled region are left empty to effectively increase the fuel rod pitch by a factor of $\sqrt{2}$. The fuel rods fill every other location on a grid plate row and are staggered on the adjacent rows. The pitch it is rotated by 45° in this configuration compared to Figures 4 and 6. In this view, the control element and both safety elements are down and attached to the control element drive.

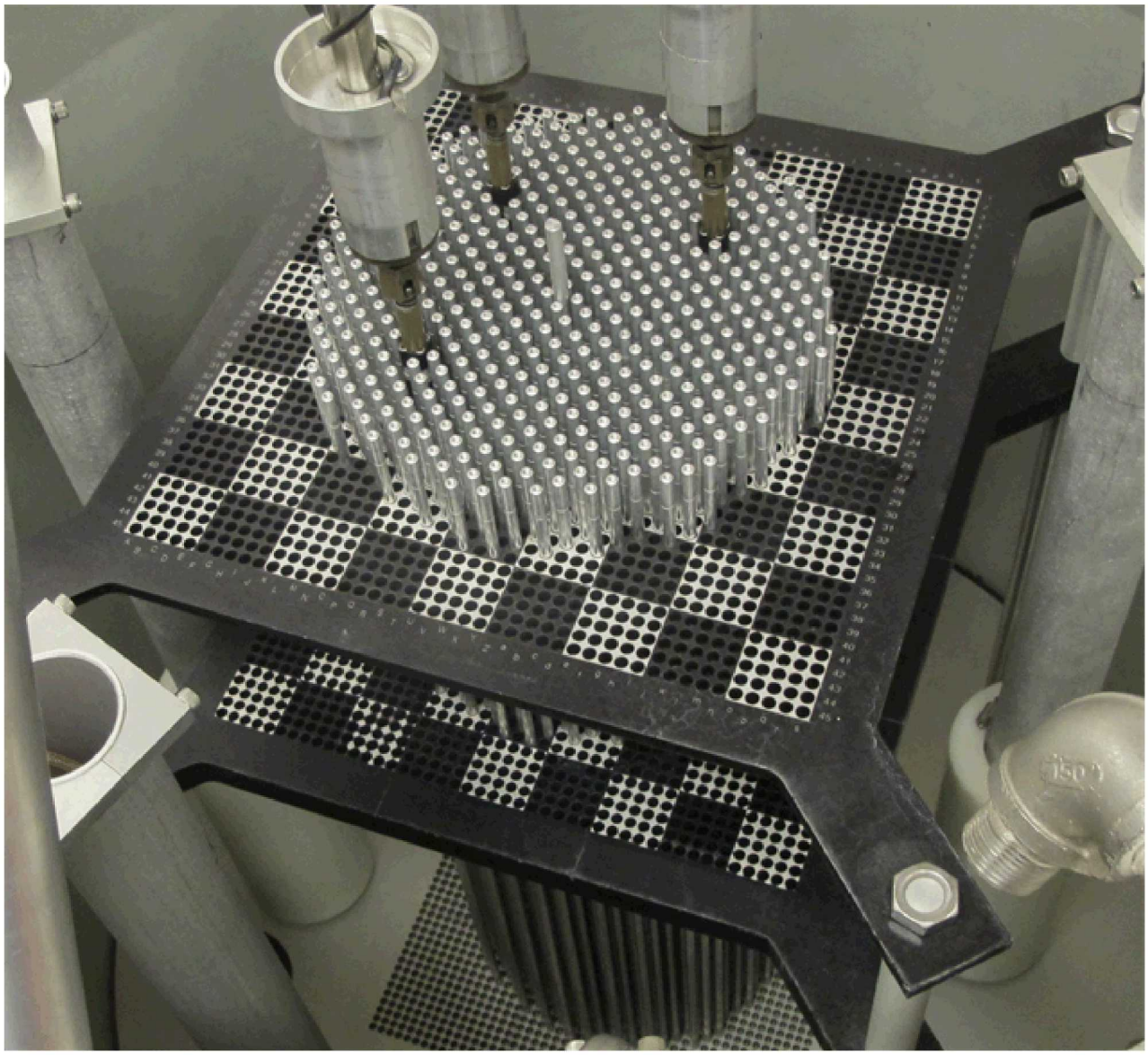

Figure 5. View of One of the Critical Configurations (Case 12).

Figure 6 shows a view of the top of the core for a different configuration. In this view, every other row and column of grid plate holes within the fueled region are left empty to effectively increase the original fuel rod pitch by a factor of two.

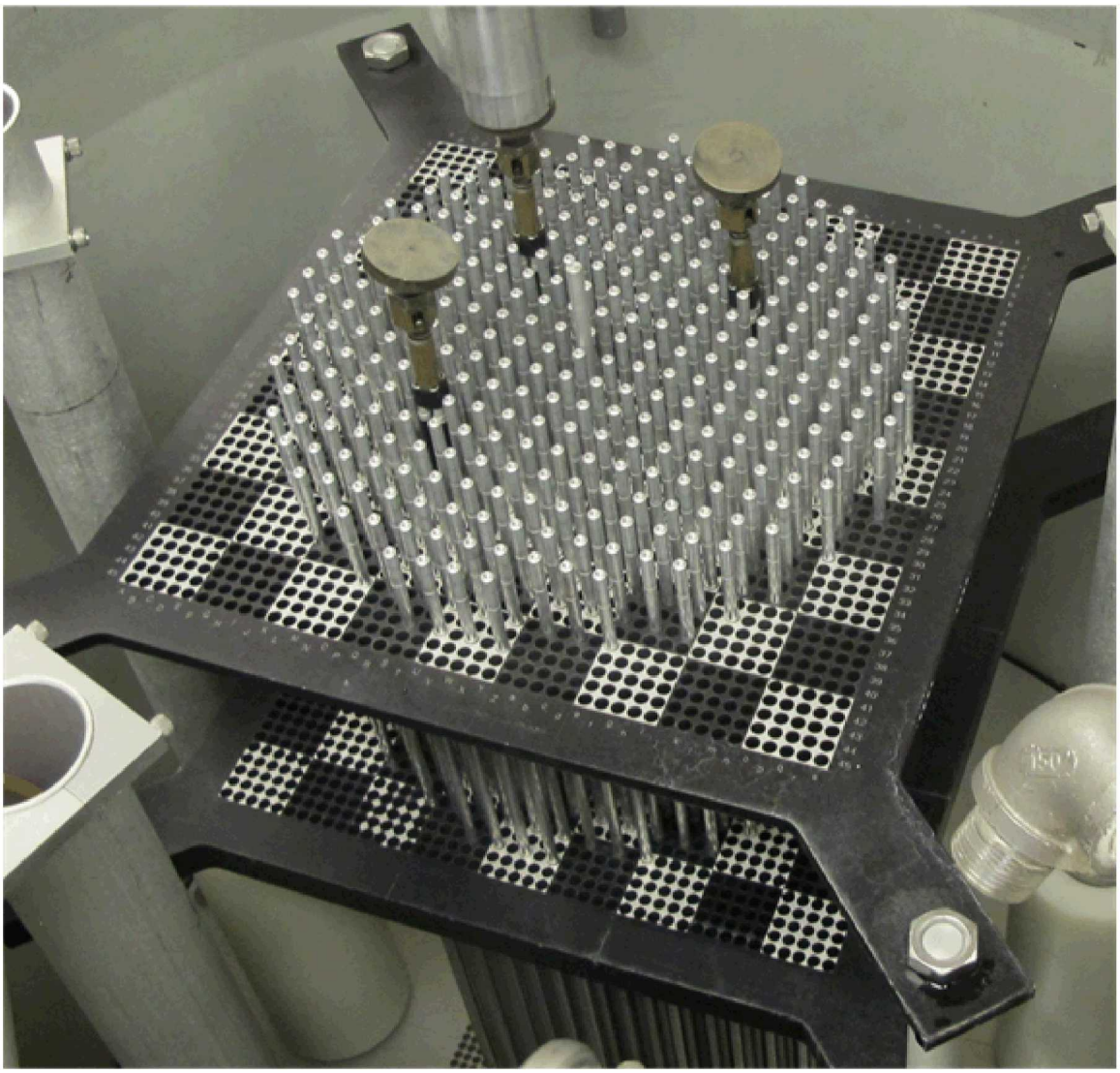

Figure 6. View of One of the Critical Configurations (Case 20).

1.2.2 Reactor Room – The critical experiments were performed in the reactor building at the Sandia Pulsed Reactor Facility. The reactor building is a large thick-walled, steel-reinforced concrete structure with a base in the shape of a cylinder having an inside diameter of approximately 30 ft (9.1 m) and capped with a hemispherical shell. A large steel and concrete door is present in the wall. Inside the building, the reactor room is lined on the walls and the dropped ceiling by 8 in (20.32 cm) of gypsum. The 4 in (10.16 cm) of gypsum that is nearest the concrete walls is borated. The floor is an 8 in (20.32 cm) thick concrete slab, the upper 4 in (10.16 cm) of which is borated. The ceiling is about 12 ft 5 in (378.46 cm) above the floor. A view of the critical assembly in the reactor room is shown in Figure 7.

Figure 7. View of the Critical Assembly in the Reactor Room.

1.2.3 Assembly Tank - The assembly tank supports the assembly and contains the moderator during approach-to-critical experiments. The tank is cylindrical with a coaxial cylindrical projection out of the bottom to accommodate the motion of the fuel-followed control/safety elements. The assembly tank consists of two welded flanged sections joined through a ring that supports the lower grid plate of the assembly. All parts of the tank were fabricated from 6061 aluminum.

The upper tank section is essentially a flanged tube. The inside dimensions of the upper tank are 40 in (101.6 cm) tall by 36.88 in (93.6752 cm) diameter. The upper tank is 6061 aluminum. It has a radial wall thickness of 0.25 in (0.635 cm). The lower flange is drilled to match the flange on the lower tank section and the grid plate support ring. The upper flange is drilled to connect to the support structure for the control/safety and source element drives.

The lower tank section has the same inner diameter and wall thickness as the upper tank section and has a 1 in (2.54 cm) thick floor that provides support for the assembly tank. The floor is drilled and tapped to

accommodate the tank supports and has holes to connect to the two moderator dump valves. The floor also has a large central hole for the projection. The inside dimensions of the projection are 21.75 in (55.25 cm) tall by 15 in (38.1 cm) diameter. The radial wall thickness and floor thickness of the projection are both 0.25 in (0.635 cm). The lower tank section has a flange at the top with an O-ring groove used for connection to the grid plate support ring. The flange is drilled and tapped to match the lower flange in the upper tank section and the grid plate support ring.

The grid plate support ring fits between the upper and lower tank sections and has an O-ring groove in the surface that mates with the lower flange on the upper tank section. The lower grid plate attaches to the grid plate support ring.

The assembly tank is connected to two standpipes. One standpipe contains a linear moderator level sensor. The other contains an overflow pipe that determines the moderator level. The assembly tank also has a float switch used to indicate that the tank is full of moderator.

1.2.4 Grid Plates – The two 6061 aluminum grid plates support and maintain the spacing of the fuel rods in the critical assembly. A third grid plate, similar to but thinner than the upper grid plate, is located above the upper grid plate to guide the fuel rods as they are being inserted into the assembly. The guide plate was fabricated from cast aluminum tooling plate, a standard aluminum product known for its dimensional stability. The upper and lower grid plates are 1 in (2.54 cm) thick while the guide plate is 0.375 in (0.9525 cm) thick. The lower grid plate is circular, 36.5 in (92.71 cm) in diameter, and is supported by the grid plate support ring that is part of the assembly tank. The lower grid plate has six 4.00 in (10.16 cm) diameter holes in it equally spaced on a 28 in (71.12 cm) diameter circle to allow passage of the moderator when the dump valves are opened. The upper grid plate is a 16.50 in ± 0.06 in (41.91 cm ± 0.1524 cm) square with four support bosses at the corners. The support bosses are rectangular projections of the grid plates and are visible in Figures 4 through 6. The upper grid plate is supported above the lower grid plate by four 1 in (2.54 cm) diameter threaded aluminum standoffs that attach to the bosses. The standoffs maintain a spacing of 19.88 in ± 0.02 in (50.4952 cm ± 0.0508 cm) between the top of the lower grid plate and the bottom of the upper grid plate. The standoffs are placed on a 28 in (71.12 cm) diameter circle centered on the center of the grid plates. Similar standoffs maintain a 7.00 in ± 0.02in (17.78 cm ± 0.0508 cm) spacing between the top of the upper grid plate and the bottom of the guide plate.

Two sets of three grid plates – lower, upper, and guide – were fabricated, one set with the holes on a 0.3150 in (0.8001 cm) square pitch and one set with holes on a 0.3366 in (0.854964 cm) square pitch. These plates have provisions for 2025 fuel rods in the 45 × 45 square-pitched critical array. The tolerance on the absolute location of each fuel rod position in the grid is 0.005 in (0.0127 cm). The two lower grid plates each have 2013 0.5 in (1.27 cm) deep holes bored in them to support and locate the bottom of the fuel rods. The upper grid plates and guide plates have matching through holes in them to locate the top of the fuel rods. The diameter of the grid plate holes is 0.260 +0.005/–0.000 in (0.6604 + 0.0127/–0.0000 cm). All six plates have three through holes – square in shape with rounded corners – machined in them to allow for passage of the four-rod control/safety elements. Excerpts from the design drawing for the two upper grid plates are shown in Figures 8 and 9.

The rows and columns of holes in the guide plates are marked for identification. The guide plates and the upper grid plates are anodized in a checkerboard pattern to assist in identifying the grid locations.

Table 1 shows the axial locations of the grid/guide plates under the assumption that the origin is at the top of the lower grid plate.

Table 1. Axial Locations of the Grid and Guide Plate Surfaces as Installed in the Critical Assembly.

Part	Location	Axial Position Relative to the Top of the Lower Grid Plate	
		Position (in)	Position (cm)
Lower Grid Plate	Bottom of the lower grid plate	-1	-2.5400
	Bottom of the fuel rod support holes	-0.5	-1.2700
	Top of the lower grid plate	0	0.0000
Upper Grid Plate	Bottom of the upper grid plate	19.88	50.4952
	Top of the upper grid plate	20.88	53.0352
Guide Plate	Bottom of the guide plate	27.88	70.8152
	Top of the guide plate	28.255	71.7677

1.2.5 Radiation Detectors – Two cylindrical fission chambers that are part of the facility plant protection system were used to obtain count-rate data during the experiments. The active material in the fission chambers was uranium enriched to about 93 % ^{235}U. The fission chambers have a 9.75 in (24.765 cm) length and 2 in (5.04 cm) OD. They are constructed of aluminum with an overall mass of 793.79 g. The detectors were placed in dry wells outside the fuel array. The dry wells were fabricated from aluminum 6061-T6511 tubing 2.50 in (6.35 cm) OD with 0.125 in (0.3175 cm) wall. The bottom of the tube was closed with a 0.250 in (0.635 cm) thick welded aluminum 6061-T6 or –T651 plate. The bottom of the tube was in contact with the top of the lower grid plate. The detector tubes were surrounded by an annulus of polyethylene 11.82 in (30.0228 cm) tall with an inner diameter of 2.603 in (6.61162 cm) and an outer diameter of 4.535 in (11.5189 cm). The bottom of the polyethylene was 0.3 in (0.762 cm) above the top surface of the lower grid plate. The mass of each of the polyethylene annuli was measured on a balance with the following specifications given by the manufacturer: repeatability 0.01 g, linearity 0.02 g, readability 0.01 g. The average mass of the two annuli was 2017.28 g. The vertical axis of one detector tube, using the orientation of the upper grid plate shown in Figures 8 and 9, was 28.94 cm to the right of and 6.4122 cm above the center of the grid plate. The second detector was 28.94 cm to the left of and 6.4122 cm below the center of the grid plate, as the grid plate is shown in the figure. The detectors were placed axially at the bottom of the dry wells with the axes of the detectors parallel to the axis of the tank. A third fission chamber, located below and immediately adjacent to the bottom of the core tank, was used in the experiments.

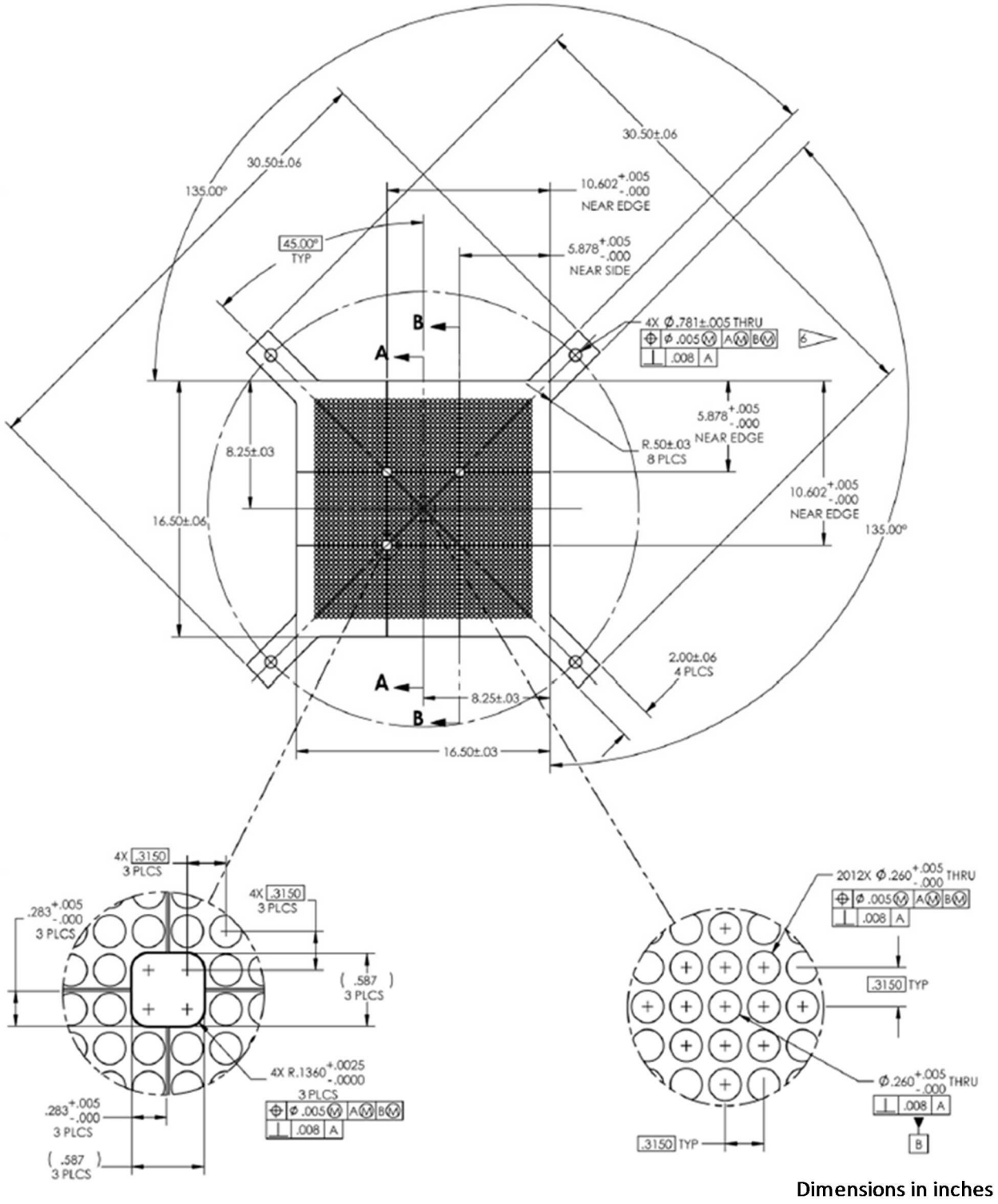

Figure 8. Excerpt from the Design Drawing for the Upper Grid Plate (Pitch 0.315 in).

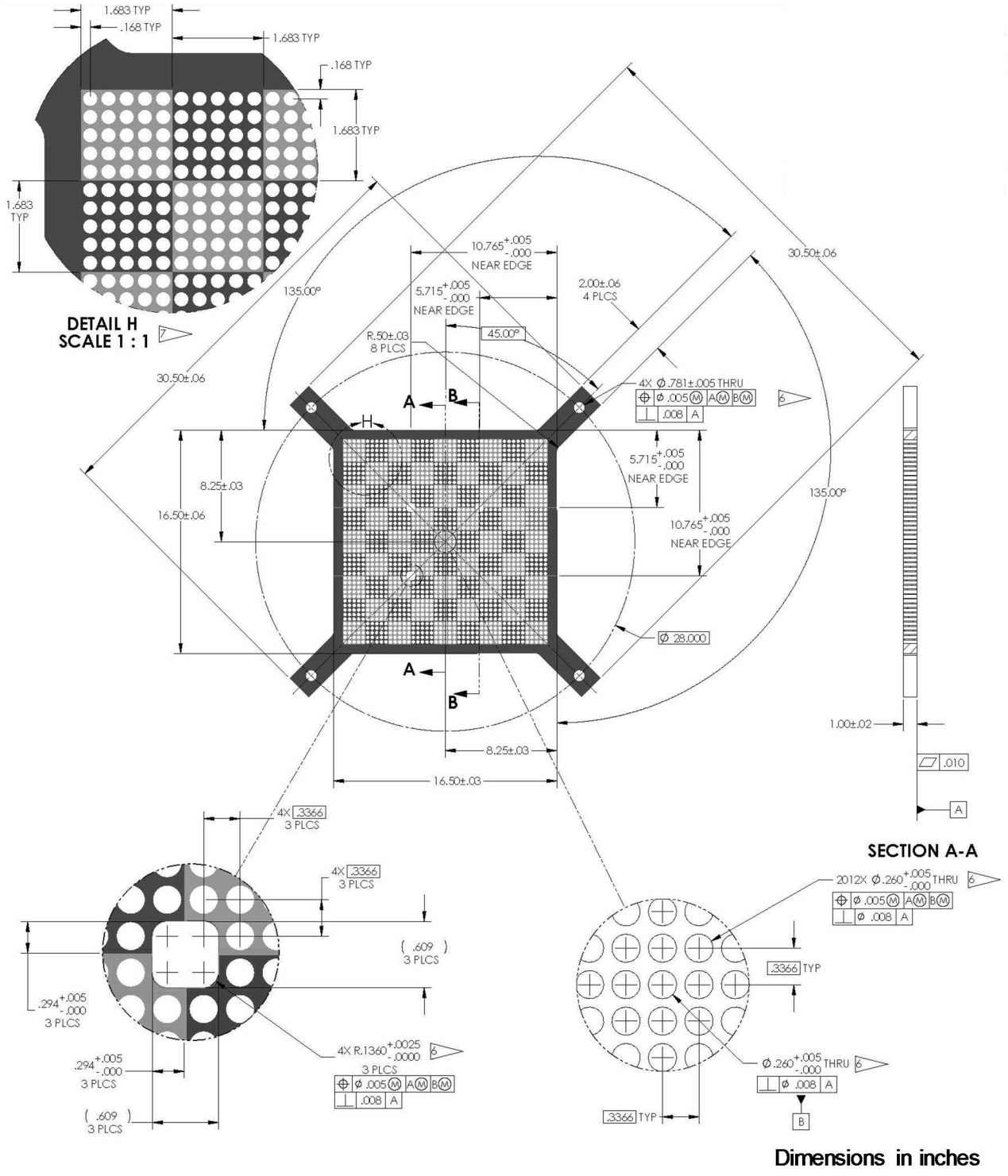

Figure 9. Excerpt from the Design Drawing for the Upper Grid Plate (Pitch 0.3366 in).

1.2.6 Water Moderator and Reflector – As noted above, the lower grid plate was supported in the core tank so that the core was reflected on the bottom by a 6.5 in (16.51 cm) thick layer of water. The bottom surface of the water in the core tank is 7.5 in (19.05 cm) below the upper surface of the lower grid plate. The level of the water in the core tank was controlled by the fixed overflow standpipe. It was adjusted so that the surface of the water in the core tank was 6 in (15.24 cm) above the upper grid plate. At this level, the moderator surface is 26.88 in (68.2752 cm) above the top of the lower grid plate. The remotely-adjustable

standpipe was set at a level above the fixed standpipe. The diameter of the core tank was sufficient that the core was reflected radially by more than 6 in (15.24 cm) of water for all cores. There was nothing that is not described above within 6 in (15.24 cm) of the fuel rods.

Water can be pumped from the dump tank to the core tank through two pumps of differing capacity. When the core tank is being filled initially, water is pumped through the "fast" fill pump. This pump is active until the level of the water in the core tank reaches a predetermined level at which a float switch is activated. When the float switch is first activated, the fast-fill pump is disabled by an interlock in the assembly control system. From that point, water may only be added to the core tank through the "slow" fill pump. The volumetric capacity of the slow-fill pump is set to limit the maximum reactivity addition rate. The slow-fill pump runs continuously through the rest of the operation. The outlet of the line from the slow pump is set so the continuous flow of water mixes the water in the core tank to promote temperature homogenization of the water in the tank. The level of the water in the core tank is limited by overflow into the lower of the two overflow standpipes.

The temperature of the water in the core tank is monitored by three thermocouples mounted in the assembly reflector at three different levels near the outer wall of the core tank. Another thermocouple in the dump tank monitors the temperature of the water there. The dump tank has an electrically-operated heater. The dump tank thermocouple signal is provided to a controller that switches the power to the heater on and off to maintain a constant water temperature in the dump tank.

1.2.7 Fuel Rods – With the exception of the fueled sections of the control and safety elements, the fuel rods in the critical assembly were all of the same design. The design of the fuel rods is shown in Figure 10. The fuel rods were fabricated in 2004 at Sandia National Laboratories from existing UO_2 fuel pellets removed from "Pathfinder" fuel assemblies obtained from The Pennsylvania State University. The fuel rods in the Pathfinder fuel assemblies were separated from the assemblies and the fuel pellets were removed from the original cladding tubes and fabricated into new fuel rods using 3003 aluminum tubing welded to end plugs of the same aluminum alloy.

The cladding tubes are welded to the lower caps. During fabrication, each weld was subjected to and certified to have passed a helium leak test. Passing the helium leak test assured that the water moderator would not enter the fuel rods. The material stack in the fuel rods, starting at the bottom, is as follows: a 0.500 in (1.270 cm) aluminum 3003 lower cap; a nominal 19.257 in (48.91278 cm) stack of fuel pellets; a corrosion-resistant steel compression spring 0.180 in (0.4572 cm) outside diameter, 0.138 in (0.35052 cm) inside diameter, 0.875 in (2.2225 cm) uncompressed length whose length adjusts according to the actual length of the fuel stack; a 1.000 in (2.540 cm) aluminum 6061 spacer 0.207 in ± 0.010 in (0.52578 cm ± 0.02540 cm) diameter, an 8.38 in ± 0.02 in (21.2852 cm ± 0.0508 cm) long high-density polyethylene spacer also 0.207 in ± 0.010 in (0.52578 cm ± 0.02540 cm) diameter, and a 1.000 inch (2.540 cm) aluminum 3003 top cap. Table 2 lists the axial locations of the interfaces between the fuel rod components when the fuel rods are installed in the critical assembly.

The cladding tubes used in the fuel rods have a nominal outer diameter of 0.250 in (0.635 cm) with a nominal 0.014 in (0.03556 cm) wall. The lower cap of the fuel rods is 0.500 in (1.270 cm) long.

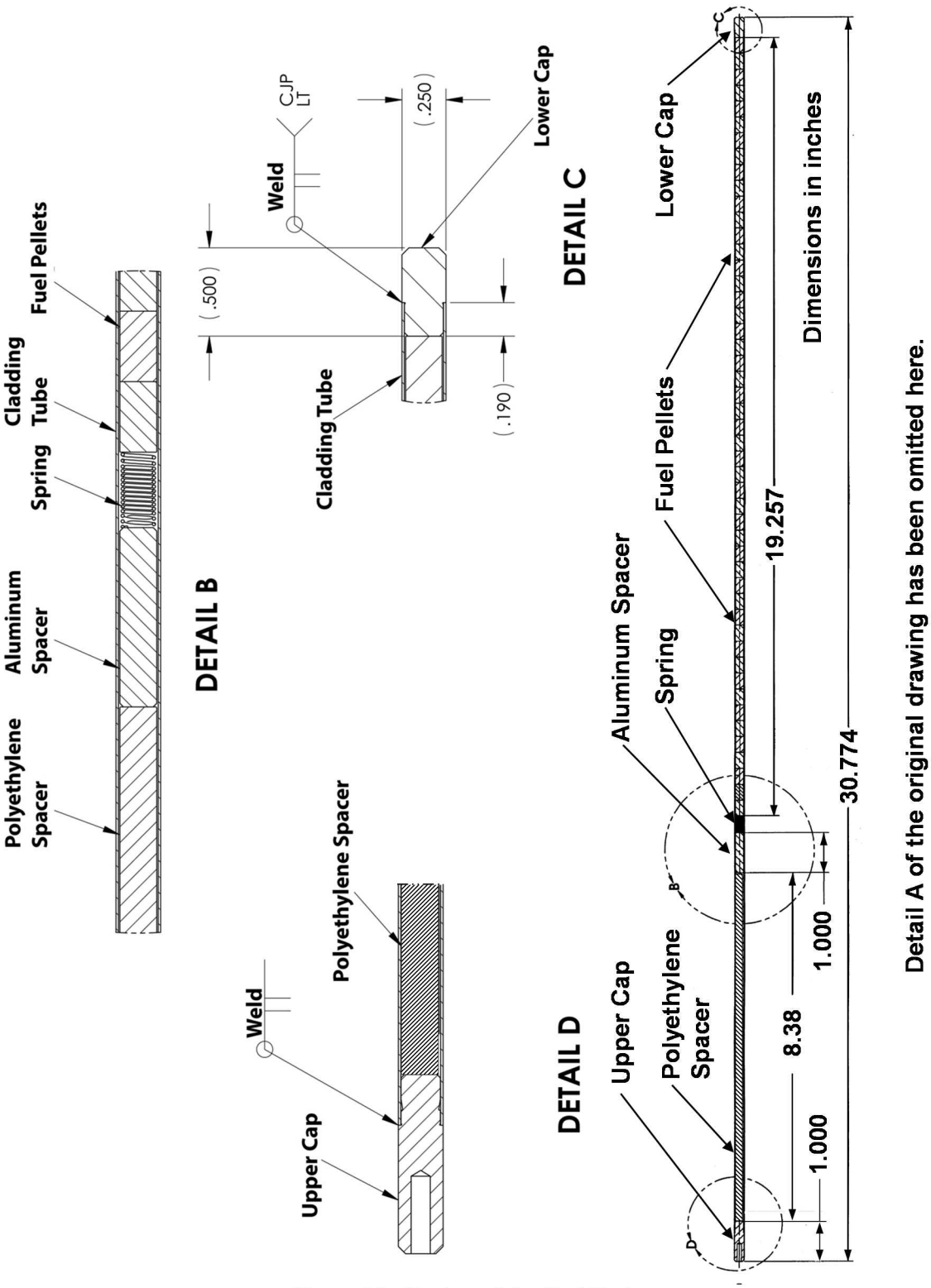

Figure 10. Design of the Fuel Rod.

Table 2. Axial Locations of the Interfaces in the Fuel Rods as Installed in the Critical Assembly.

Location	Axial Position Relative to the Top of the Lower Grid Plate	
	Position (in)	Position (cm)
Bottom of the lower grid plate	-1.00	-2.54
Bottom of the fuel rod	-0.50	-1.27
Bottom of the fuel pellet stack	0.00	0.00
Top of the fuel pellet stack (measured)	19.2045	48.780 [(a)]
Bottom of the aluminum spacer	19.894	50.53076
Top of the aluminum spacer	20.894	53.07076
Top of the polyethylene spacer	29.274	74.35596
Top of the fuel rod	30.274	76.89596

(a) This is the mean measured fuel column length, different from the 19.257 in (48.91278 cm) nominal length. The measured length in inches is this value (48.780) divided by 2.54.

Before the fuel rods were fabricated, the masses of 100 of each non-fuel components of the fuel rods were measured. The mass measurements were made on a balance with the following specifications given by the manufacturer: repeatability 0.01 g, linearity 0.02 g, readability 0.01 g. The results of the mass measurements are summarized in Table 3. The sixth row in the table gives the results for 100 sets of all five parts. It can be seen that the variability in the mass sum is dominated by the variability in the mass of the polyethylene spacer. The variability is attributed to the manufacturing process used to fabricate the polyethylene spacers. The last (seventh) row in the table gives the results for 100 sets of parts without the polyethylene spacers.

Table 3. Measured Mass Data for the Fuel Rod Components.

Component	Average Mass (g)	Standard Deviation (g)
Cladding Tube/Lower Cap Assembly	13.824	0.027
Corrosion-Resistant Steel Springs	0.1923	0.0095
Aluminum Spacer	1.4368	0.0043
Polyethylene Spacer	4.524	0.094
Upper Cap	1.8350	0.0052
Sum of Five Parts for 100 Sets	21.813	0.094
Sum Without Polyethylene Spacer	17.289	0.027

During the fabrication of the 2199 fuel rods available for the experiments, the following quantities were measured for each fuel rod: total rod mass, polyethylene spacer mass, and fuel pellet column length. The mass measurements were made on a balance with the following specifications given by the manufacturer: repeatability 0.01 g, linearity 0.02 g, readability 0.01 g. The length measurements were made to the nearest 0.1 cm. The values of the measured masses and lengths were preserved for each fuel rod. The mass of the fuel pellets in each rod was obtained by subtracting the measured mass of the polyethylene spacer plus the 17.289 g average mass of the remaining hardware given in Table 3 from the total mass of the fuel rod. Table 4 lists average values of UO_2 fuel mass and fuel pellet stack length for the entire population of 2199 fuel rods. The linear fuel mass in each fuel rod was obtained from the UO_2 mass and the fuel pellet stack length for each fuel rod. The average value of the linear fuel mass is also listed in the table, as is the average polyethylene spacer mass.

Table 4. Population Averages for the 2199 Fuel Rods

Characteristic	Average Value	Standard Deviation
UO_2 Mass (g)	108.7165	0.323
Fuel Pellet Stack Length (cm)	48.780	0.125
Linear Fuel Mass (g/cm)	2.2287	0.0050
Polyethylene Spacer Mass (g)	4.454	0.102

After the fuel rods were fabricated, the outer diameter of each fuel rod was measured using a high-precision laser micrometer system. The system consisted of three micrometer heads and the hardware required to position the fuel rods in the micrometer heads. The micrometer heads were located to measure the fuel rod outside diameter at 6.4 in (16.256 cm), 10.15 in (25.781 cm), and 13.9 in (35.306 cm) above the bottom end of the fuel rod. This gave a fuel rod outer diameter measurement at about the midplane of the fuel pellet stack and 3.75 in (9.525 cm) above and below the midplane. Each micrometer made two simultaneous orthogonal diameter measurements. For each fuel rod, a measurement was taken, the fuel rod was rotated by 45°, and another measurement was taken. Thus, the outer diameter of each fuel rod was measured at three axial locations in four azimuthal orientations. The manufacturer's specifications indicated that the laser micrometers had a resolution of 0.000001 in (0.00000254 cm) and a repeatability of 0.000005 in (0.0000127 cm). The bias in the micrometer measurements was established using a pin gage standard with a calibration traceable to the US National Institute of Standards and Technology. The diameter measurements had a systematic uncertainty of 0.000022 in (0.00005588 cm) which is the sum in quadrature of the 0.000015 in (0.0000381 cm) uncertainty in the pin gage standard with the maximum in the random variations in the measurement of the standard on any axis for the three micrometers. The fuel rod diameter measurements were made in a number of sessions over the course of several months. The stability of the measurement system was monitored by repeatedly measuring two 12 in (30.48 cm) long pin gages during each of the sessions. These measurements also showed that the diameter measurements had a random reproducibility uncertainty of about 0.000030 in (0.0000762 cm). Of the 2199 fuel rods fabricated for the experiment, five were removed from service and not used. The average measured fuel rod diameter for the remaining population of 2194 fuel rods is 0.249980 in (0.634948 cm as rounded from the original data) with a standard deviation of 0.000086 in (0.000218 cm).

The design documents for the fuel elements from which the fuel pellets were removed specified the diameter of the fuel pellets as 0.207 in (0.52578 cm). The outer diameter of a sample of 123 fuel pellets, drawn randomly from the fuel pellet stock used in the fuel rods, was measured using one of the laser micrometers described above. The average measured diameter was 0.20694 in (0.52563 cm) with a standard deviation for the 123 measurements of 0.00019 in (0.00048 cm).

The fuel rods were designed to be supported by the two 1 in (2.54 cm) thick grid plates. The lower cap fits in a 0.5 in (1.27 cm) deep blind hole in the lower grid plate. The top of the lower cap is then aligned with the top of the grid plate to make the combination appear as a solid sheet of metal. With the appropriate grid plate spacing, the top and bottom of the aluminum spacers in the fuel rods are nearly aligned with the top and bottom of the upper grid plate.

1.2.8 Control and Safety Elements - The critical assembly has three identical fuel-followed control/safety elements, two operated as safety elements and one operated as a control element. Each control/safety element occupies four adjacent fuel rod positions in the critical assembly. Each element consists of four B_4C-loaded absorber sections followed by four polyethylene-filled decoupler sections followed by four fueled rod sections. These sections are joined into four-rod bundles by 6061 aluminum bundle plates. The three sections use the same 3003 aluminum tubing as the fuel rods. Each section has 3003 aluminum end caps at the top and bottom of identical design. When a control/safety element is fully withdrawn from the assembly, the fueled rod sections are in the core and are nearly identical neutronically to the other fueled positions in the critical assembly. The design of the control and safety elements is shown in Figure 11. The design of the lower bundle plate for the 0.315 in pitch grid plate is shown in Figure 12. The design of the middle bundle plate for the 0.315 in pitch grid plate, of which there are two in each control or safety element, is shown in Figure 13. The design of the upper bundle plate for the 0.315 in pitch grid plate is shown in Figure 14. The design of the lower bundle plate for the 0.3366 in pitch grid plate is shown in Figure 15. The design of the middle bundle plate for the 0.3366 in pitch grid plate, of which there are two in each control or safety element, is shown in Figure 16. The design of the upper bundle plate for the 0.3366 in pitch grid plate is shown in Figure 17. All of the bundle plates were fabricated from 6061 aluminum.

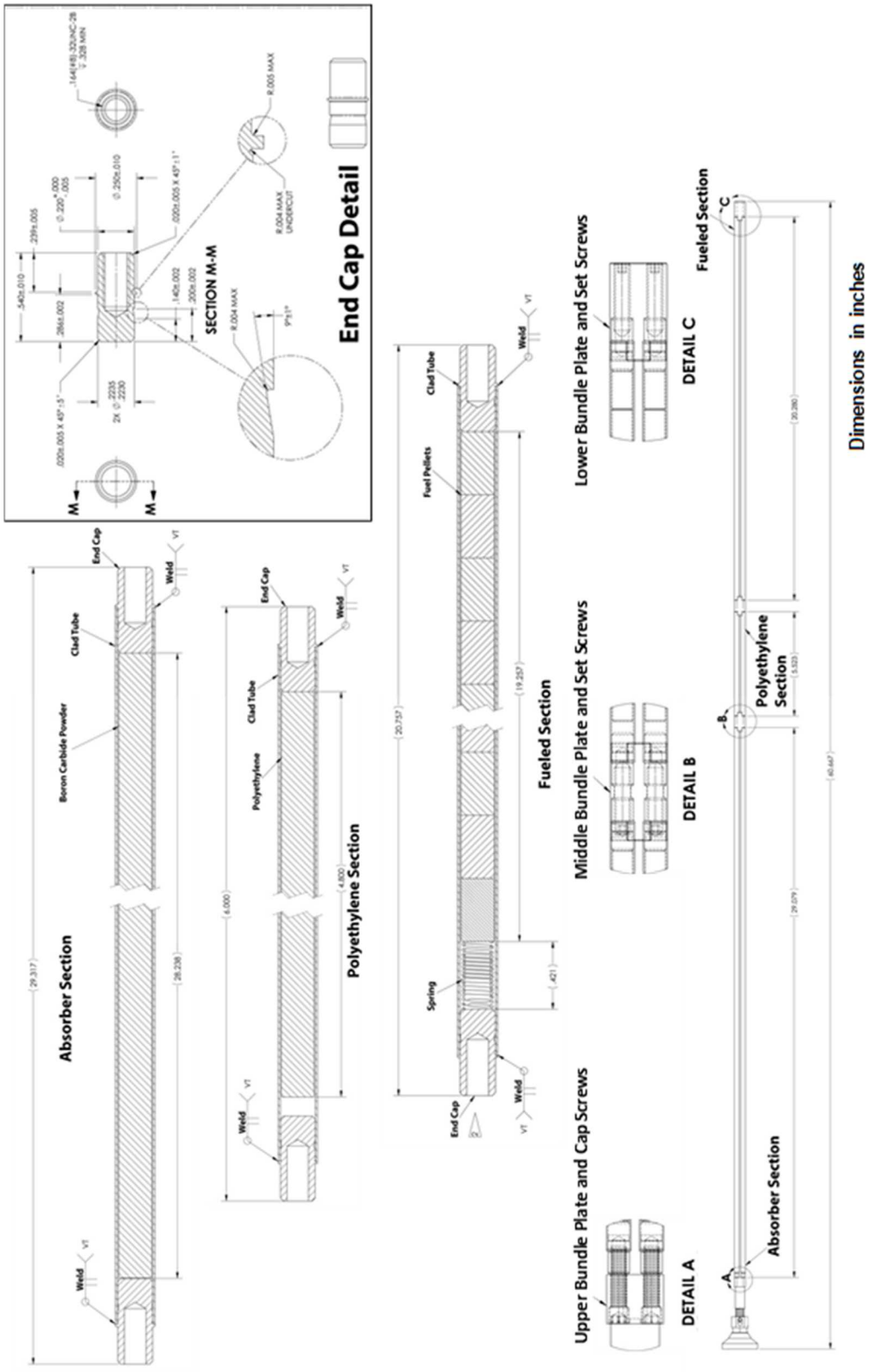

Figure 11. Design of the Control and Safety Elements.

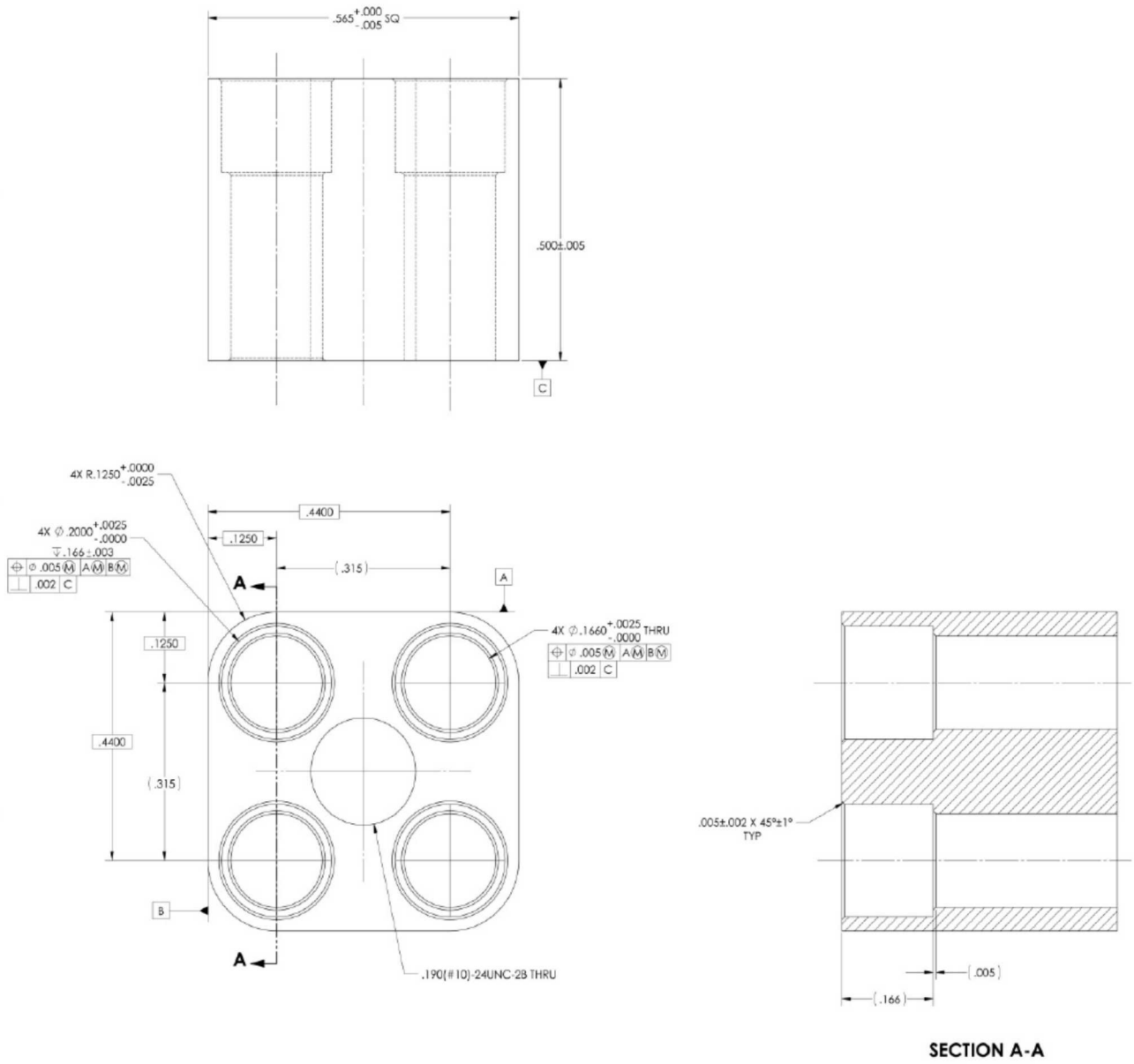

Figure 12. Excerpt from the Design Drawing for the Lower Bundle Plate (Pitch 0.315 in).

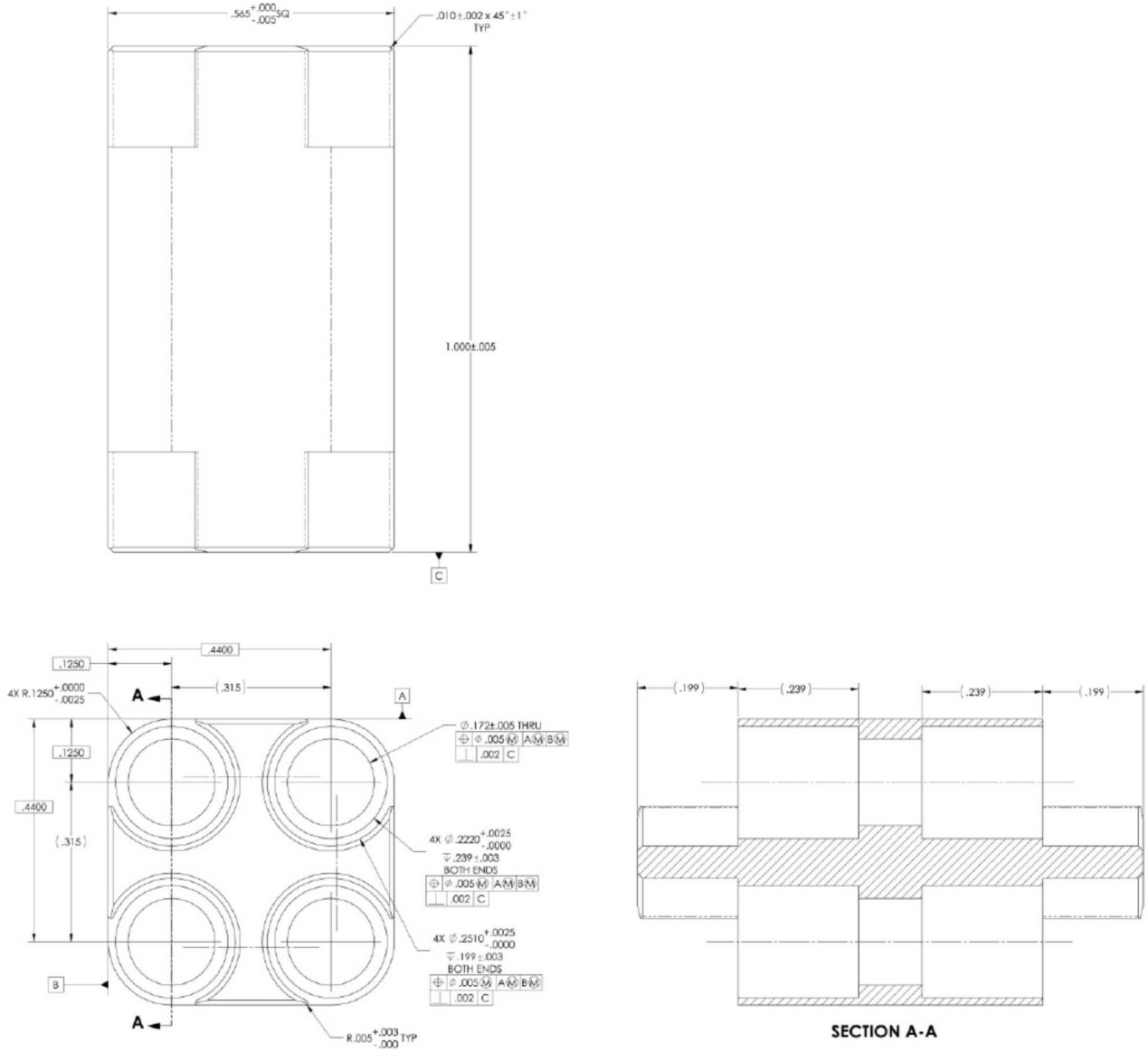

Figure 13. Excerpt from the Design Drawing for the Middle Bundle Plate (Pitch 0.315 in).

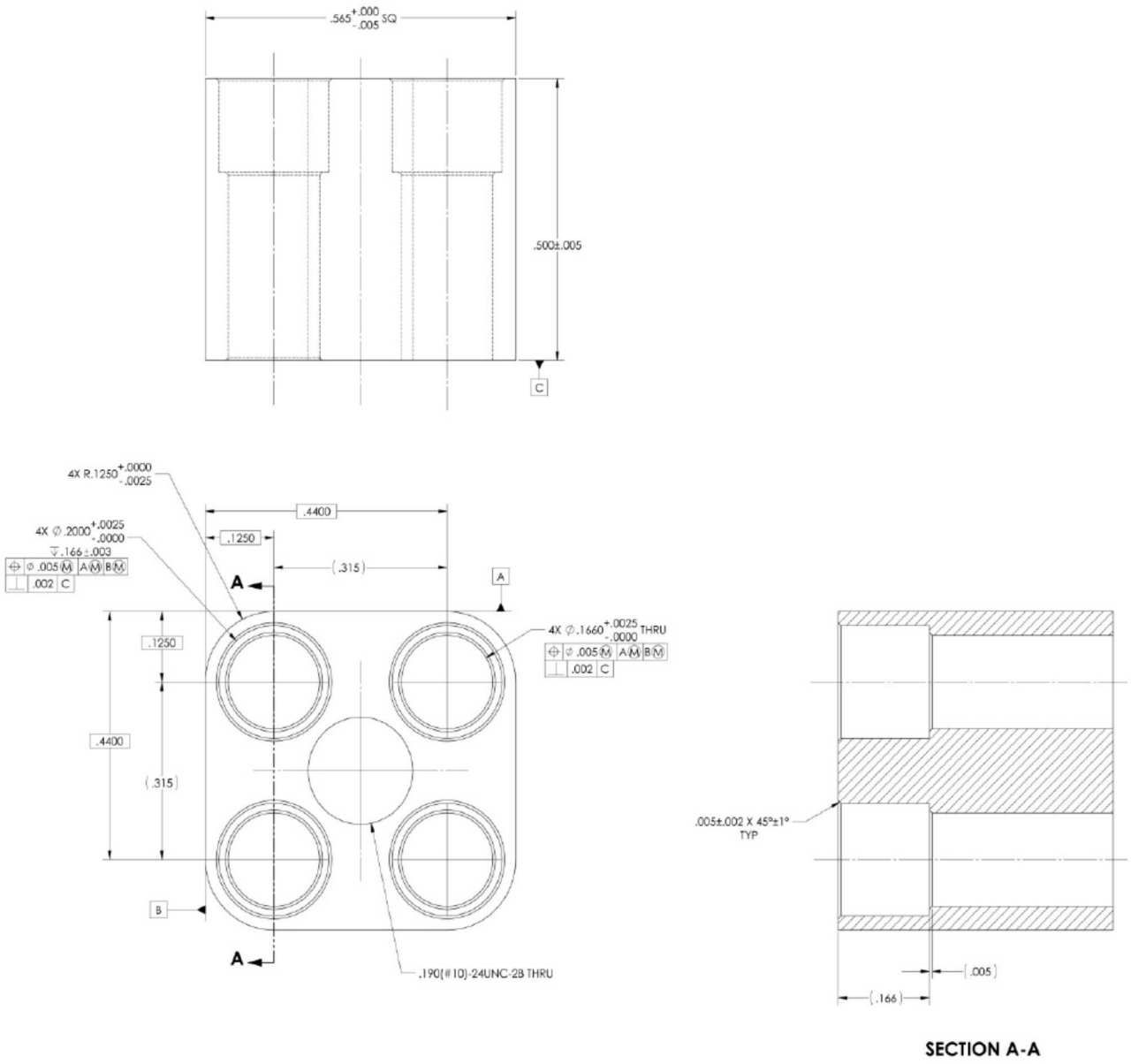

Figure 14. Excerpt from the Design Drawing for the Upper Bundle Plate (Pitch 0.315 in).

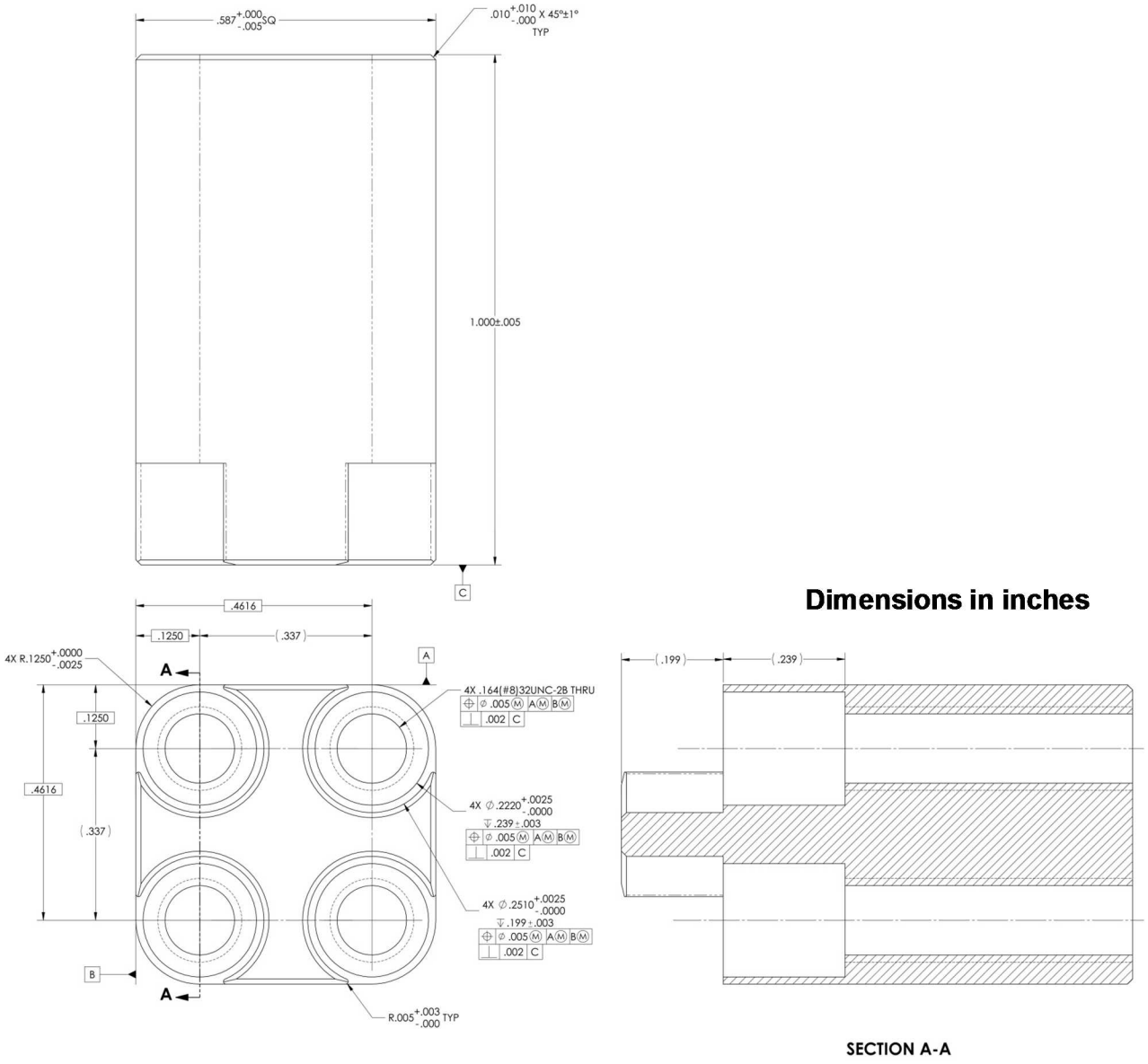

Figure 15. Excerpt from the Design Drawing for the Lower Bundle Plate (Pitch 0.3366 in).

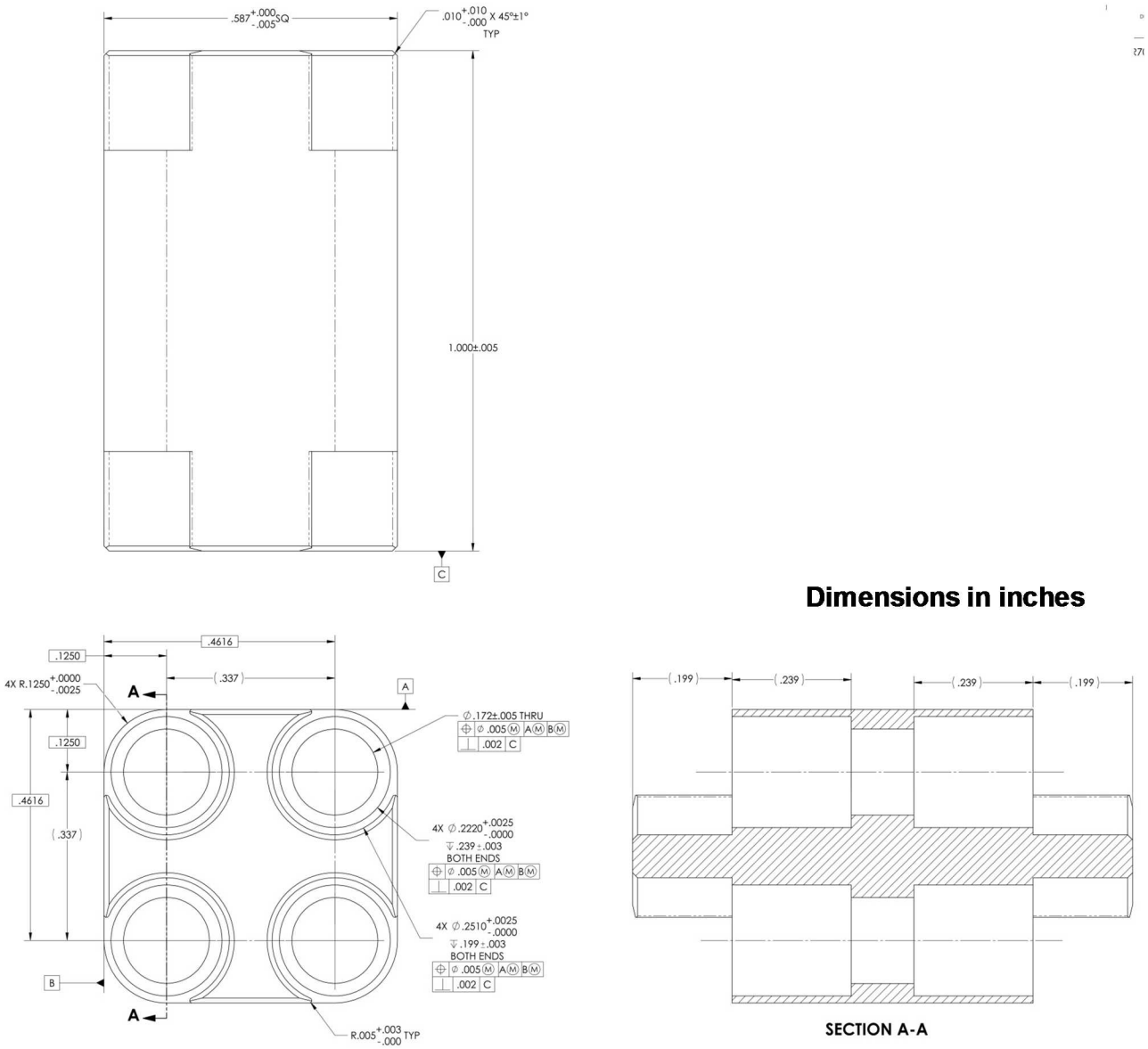

Figure 16. Excerpt from the Design Drawing for the Middle Bundle Plate (Pitch 0.3366 in).

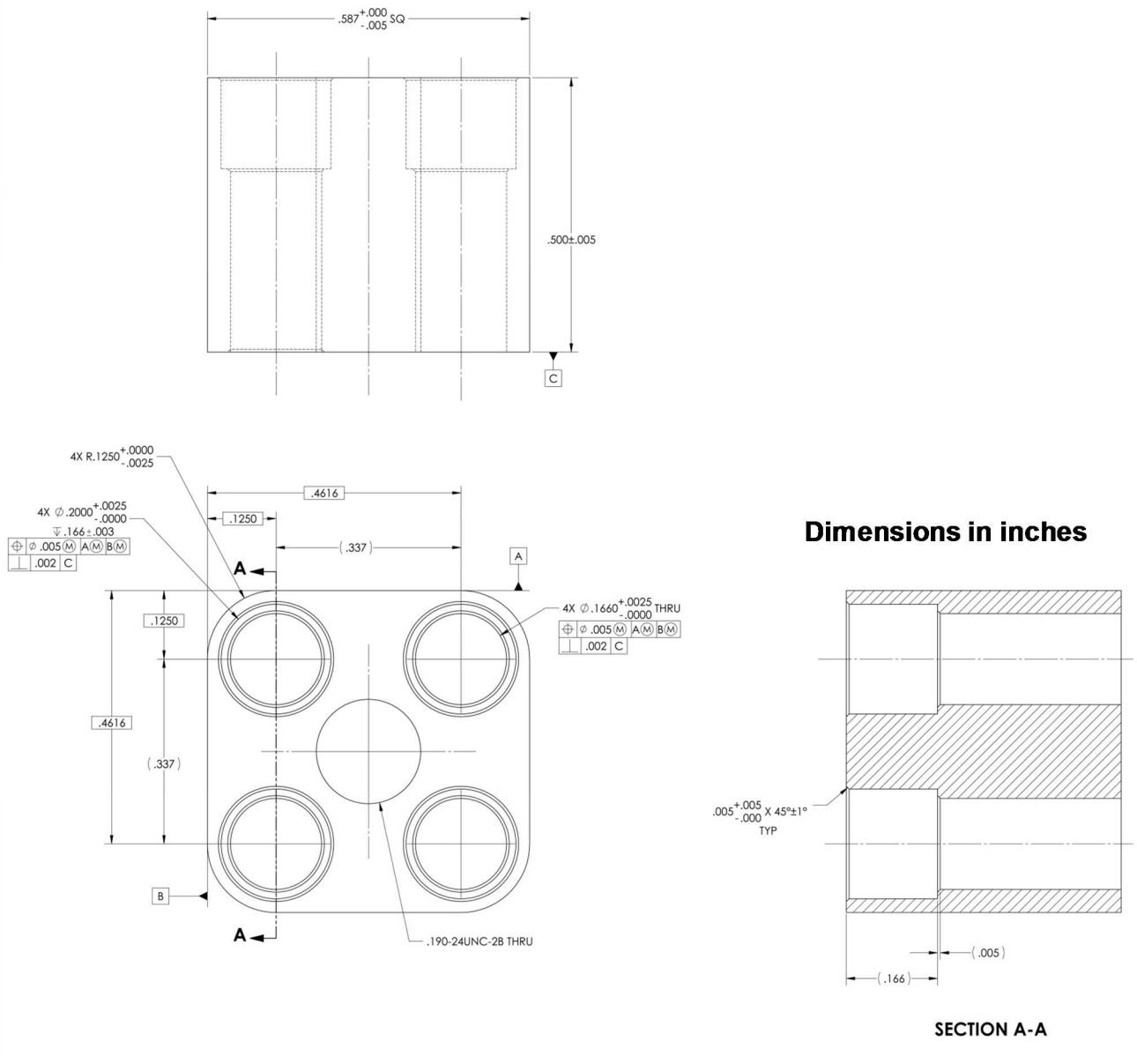

Figure 17. Excerpt from the Design Drawing for the Upper Bundle Plate (Pitch 0.3366 in).

The fueled section of the control/safety elements is similar to the fueled section of a fuel rod. The 3003 aluminum cladding tubes and end cap material are the same as were used in the fuel rods. In order to allow the elements to be lowered from the assembly, the lower grid plate has four-position through holes at the control/safety element positions as described above. The end caps on the fueled sections of the control/safety elements mate with a 6061 aluminum lower bundle plate that fills the hole in the lower grid plate. An 8-32 corrosion-resistant steel set screw 0.750 in (1.905 cm) long joins each fueled section to the bundle plate. Above the bottom end cap is a stack of fuel pellets and a spring similar to those in a fuel rod. The length and mass of the fuel pellet stack is known for each of the 23 fueled sections that were fabricated to the same precision as for the fuel rods. The relevant data on the fuel pellet stack for the population of 23 fueled sections is given in Table 5. The total mass of the UO_2 in the twelve fueled sections used in the experiments reported here is 1303.79 g and the total stack length is 584.7 cm.

Table 5. Population Averages for the 23 Control/Safety Element Fueled Sections.

Characteristic	Average Value	Standard Deviation
UO_2 Mass (g)	108.62	0.13
Fuel Pellet Stack Length (cm)	48.717	0.049
Linear Fuel Mass (g/cm)	2.2295	0.0020

The top end caps of the fueled sections are joined to the bottom end caps of the polyethylene-filled decoupler sections through a middle bundle plate using the same set screws as in the lower bundle plates. The length of the fueled sections is set so that, when the lower bundle plate upper and lower surfaces are in line with the surfaces of the lower grid plate, the upper and lower surfaces of the middle bundle plate are nearly in line with the upper and lower surfaces of the upper grid plate.

The decoupler sections contain 4.800 in (12.192 cm) long 0.207 in (0.52578 cm) diameter polyethylene rods inside the same 3003 aluminum tubes used for the fuel rod cladding. The average polyethylene mass in the population of 24 decoupler sections is 2.531 g with a standard deviation of 0.037 g. The end caps on the decoupler sections are identical to those on the fueled section.

The bottoms of the absorber sections are joined to the tops of the decoupler sections through a middle bundle plate. The same corrosion-resistant set screws are used. The absorber sections are filled with boron carbide powder. Two lots of boron carbide powder, each with a different average particle size, were mixed in equal parts prior to loading into the absorber sections. During loading, the powder was compacted by vibrating the tubes. The loading procedure specified that the absorber sections be filled to within about 0.3 in of the top of the tube. The top caps of the sections extend 0.286 in into the tubes. Thus the gap between the bottom of the cap and the top of the powder was small. The average boron carbide mass in the population of 23 absorber sections that were fabricated is 26.37 g with a standard deviation of 0.22 g. After filling, the top caps were welded to the absorber section tubes.

The top of each absorber section is joined to the upper bundle plate by a modified 8-32 socket head cap screw 1.125 in (2.8575 cm) tall. Table 6 lists the axial positions of the interfaces in the control and safety elements when the elements are fully withdrawn from the assembly to the positions in which the measurements reported here were made.

Table 6. Axial Locations of the Interfaces in the Control and Safety Elements when the Elements are Fully Withdrawn from the Critical Assembly.

Part	Location	Axial Position Relative to the Top of the Lower Grid Plate	
		Position (in)	Position (cm)
Lower Bundle Plate	Bottom of the lower bundle plate	-1.000	-2.54000
	Bottom of the 0.222 in ID hole	-0.438	-1.11252
	Bottom of the 0.251 in ID hole	-0.199	-0.50546
	Top of the lower bundle plate	0.000	0.00000
Fueled Section	Bottom of the fueled section	-0.438	-1.11252
	Bottom of the full-diameter clad	-0.199	-0.50546
	Bottom of the fuel pellet stack	0.102	0.25908
	Top of the fuel pellet stack	19.282	48.97608
	Bottom of the top end cap	19.78	50.24120
	Top of the full-diameter clad	20.081	51.00574
	Top of the fueled section	20.320	51.61280
Middle Bundle Plate 1	Bottom of the middle bundle plate 1	19.882	50.50028
	Top of the lower 0.251 in ID hole	20.081	51.00574
	Top of the lower 0.222 in ID hole	20.320	51.61280
	Bottom of the upper 0.222 in ID hole	20.444	51.92776
	Bottom of the upper 0.251 in ID hole	20.683	52.53482
	Top of the middle bundle plate 1	20.882	53.04028
Polyethylene Decoupler Section	Bottom of the decoupler section	20.444	51.92776
	Bottom of the full-diameter clad	20.683	52.53482
	Bottom of the polyethylene	20.984	53.29936
	Top of the polyethylene	25.784	65.49136
	Bottom of the top end cap	25.905	65.79870
	Top of the full-diameter clad	26.206	66.56324
	Top of the decoupler section	26.445	67.17030
Middle Bundle Plate 2	Bottom of the middle bundle plate 2	26.007	66.05778
	Top of the lower 0.251 in ID hole	26.206	66.56324
	Top of the lower 0.222 in ID hole	26.445	67.17030
	Bottom of the upper 0.222 in ID hole	26.569	67.48526
	Bottom of the upper 0.251 in ID hole	26.808	68.09232
	Top of the middle bundle plate 2	27.007	68.59778
Absorber Section	Bottom of the absorber section	26.569	67.48526
	Bottom of the full-diameter clad	26.808	68.09232
	Bottom of the absorber	27.109	68.85686
	Bottom of the top end cap	55.347	140.58138
	Top of the full-diameter clad	55.648	141.34592
	Top of the absorber section	55.887	141.95298
Upper Bundle Plate	Bottom of the upper bundle plate	55.887	141.95298
	Bottom of the 0.200 in ID hole	56.221	142.80134
	Top of the upper bundle plate	56.387	143.22298

Whenever moderator is present in the core tank during the execution of a critical experiment, the safety elements are held at their most reactive position with the absorber above the surface of the water and the fueled sections in the assembly core. In this position, a large negative reactivity is available to quickly shut down the assembly should the need arise. The absorber section in the elements is also well away from the assembly core and does not significantly affect the reactivity of the system. The control element is used during critical assembly operations to make fine adjustments in the reactivity of the assembly. When data are

taken during an approach-to-critical experiment, the control element is also fully withdrawn to its most reactive position so the absorber does not affect the system neutronically.

1.2.9 Neutron Source – The neutron source in the assembly is a small double-sealed 316L stainless steel capsule containing a ^{252}Cf spontaneous fission source. The source is attached to a fixture designed to be placed in a fuel rod location in the assembly grid structure or in a mounting location outside the grid plates. The source and fixture are shown in Figure 18. The bottom (source) end of the fixture is the bottom end cap, essentially a cylinder of aluminum 3003 0.540 in (1.3716 cm) long and 0.220 in (0.5588 cm) diameter that is drilled and tapped to accommodate a 3-48 steel set screw that is 0.313 in (0.79502 cm) long. The bottom of the source fixture and top of the source capsule are 5.099 in (12.95146 cm) above the top of the lower grid plate. An aluminum 3003 tube identical to the fuel rod cladding tubes (nominally 0.250 in outer diameter, 0.0014 in wall) covers the top 0.254 in (0.64516 cm) of the bottom end cap and extends above the moderator where it connects to a handle that rests on the guide plate. The tube is slotted at the ends so that it fills with moderator when the critical assembly is filled.

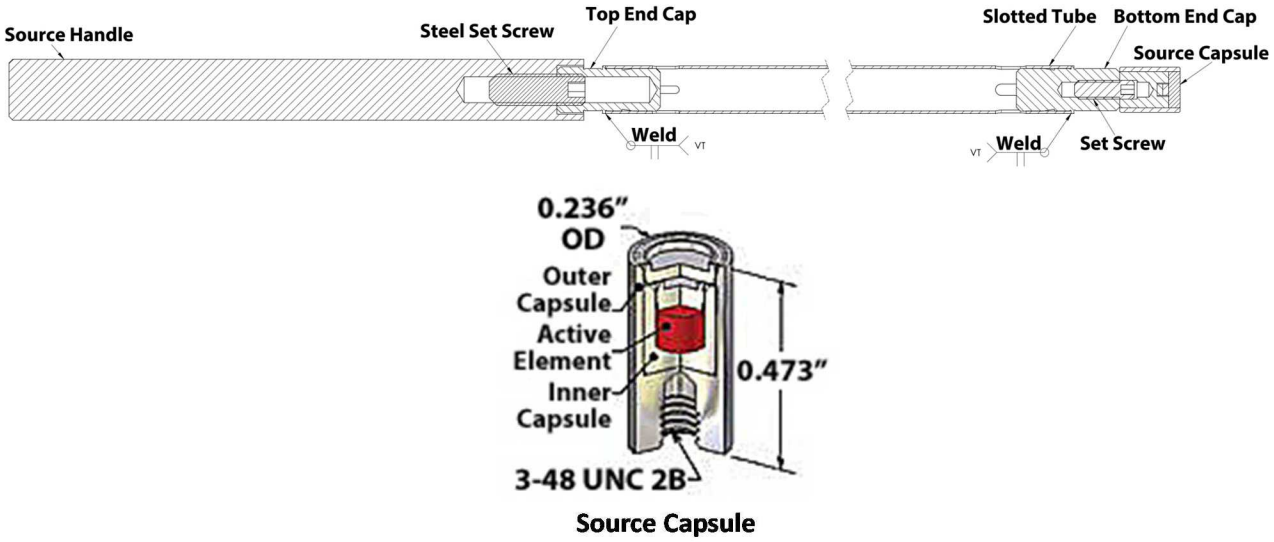

Figure 18. The Neutron Source and Supporting Fixture.

Table 7 shows the axial locations of the surfaces of the neutron source under the assumption that the origin is at the top of the lower grid plate.

Table 7. Axial Locations of the Interfaces in the Neutron Source as Installed in the Critical Assembly.

Part	Location	Axial Position Relative to the Top of the Lower Grid Plate	
		Position (in)	Position (cm)
Source Capsule	Bottom of the source capsule	4.626	11.75004
	Bottom of the set screw hole	5.016	12.74064
	Top of the source capsule	5.099	12.95146
Lower Set Screw	Bottom of the set screw	5.016	12.74064
	Top of the set screw	5.329	13.53566
Bottom End Cap	Bottom of the bottom end cap	5.099	12.95146
	Top of the set screw hole	5.586	14.18844
	Top of the bottom end cap	5.940	15.08760
Slotted Tube	Bottom of the slotted tube	5.382	13.67028
	Top of the slotted tube	28.156	71.51624
Top End Cap	Bottom of the top end cap	27.855	70.75170
	Bottom of the hole in the top end cap	27.908	70.88632
	Top of the top end cap	28.395	72.12330
Upper Set Screw	Bottom of the upper set screw	28.255	71.76770
	Top of the upper set screw	28.755	73.03770
Handle	Bottom of the handle	28.255	71.76770
	Top of the end cap hole in the handle	28.395	72.12330
	Top of the set screw hole in the handle	28.885	73.36790
	Top of the handle	32.255	81.92770

1.2.10 Experimental Method – The focus of these critical experiments was to measure the effects of decreasing the fuel-to-water volume ratio on the critical array size.

The critical array size for each configuration was determined in an approach-to-critical experiment with the number of fuel rods in the array as a free parameter. The inverse count rate at successive fuel configurations for two or three detectors as a function of number of fuel rods was extrapolated to zero to obtain an estimate of the critical array size. During all measurements the control and safety elements were in their fully withdrawn or most reactive positions. Because the assembly tank was full of moderator during the measurements, the fuel rod array was fully reflected as described in Section 1.2.6.

The square-pitched arrays were loaded from the center toward the outside while maintaining a roughly cylindrical cross section of the array. The loading order was identical for each experiment. Each fuel rod was in the same array location in every configuration that included that fuel rod.

Four of the configurations, Cases 12, 16, 20 and 24, were each addressed with a full approach-to-critical experiment. The initial array in these configurations had a calculated effective multiplication factor of about 0.9 and the second array had a calculated effective multiplication factor of about 0.95. Subsequent measurements were guided by the count rate results. Early in each approach, the fuel increments were many fuel rods. The fuel increments decreased in size during the approach until the last few count rate measurements were made at increments of a small number of fuel rods.

Cases 1 and 7 are baseline configurations that are documented in LCT-080 and LCT-078. Cases 2 through 6 are variants of the configuration in Case 1, and Cases 8 through 11 are variants of the configurations in Case 7. The differences between the variants and the baseline configurations are the number and position of interior fuel rods removed. These configurations were addressed by unloading several fuel rods from the outside of the final configuration of a similar experiment and performing an approach-to-critical experiment while projecting inverse count rates as a function of number of rods in the core to zero. The difference for these configurations was that the approach-to-critical experiment covered a much narrower range of fuel

loadings near delayed critical. A similar method was used for the remaining configurations, such that Cases 13 through 15 are variants of the configuration in Case 12, Cases 17 through 19 are variants of the configuration in Case 16, Cases 21 through 23 are variants of the configuration in Case 20, and Cases 25 through 27 are variants of the configuration in Case 24.

For all configurations, a final approach-to-critical experiment was performed in which count rate measurements were taken for specific fuel arrays. The measured count rates were inverted. A linear fit to the inverse count rate as a function of number of fuel rods in the array was extrapolated to zero inverse count rate to estimate the critical configuration of the experiment. The extrapolated critical array sizes reported below were developed from inverse count rate data measured during these final experiments. It should be noted that the extrapolated critical array sizes apply only to the specific configurations in which the count rates were measured. The extrapolations only give the actual critical array size if all the fuel rods have the same reactivity worth in the interval from the smaller, but largest measured array size, to the actual critical array size. Because the reactivity worth of the fuel rods depends on position in the array, sometimes strongly, no claim is made that the array will be exactly critical with the extrapolated number of fuel rods.

Based on the k_{eff} values derived in Section 2.3, all of the final configurations had subcritical multiplications that significantly exceeded 100.

1.2.11 Experiment Arrays – During the approach-to-critical experiments, detailed records were kept of the location and identity of each fuel rod in each core. A given fuel rod was placed in the same grid location in each core in which it was used. The total number of fuel rod positions occupied, the mass of UO_2 in the core, and the total length of the fuel columns in all the fuel rods for the largest array measured in each of the twenty-seven configurations are listed in Table 8. Also listed in the table is the fuel rod pitch, the previous array size that is used for extrapolation to delayed critical, the extrapolated array size at delayed critical, and the temperature at which the experimental measurements were made. Table 9 lists the average fuel rod diameter with standard deviation for the set of fuel rods used in each benchmark experiment. The fuel rod arrangement in the largest array measured for each of the twenty-seven cores is shown in Figures 19 through 45. The locations of all fuel rods, control and safety elements, and the neutron source are indicated in the 45×45 array of holes in the grid plates. The locations of the fuel rods that make up the difference of the two array sizes listed in Table 8 are shown in the figures as incremental fuel rods.

Table 8. Fuel Rod Pitch, Measured and Extrapolated Array Sizes, Total UO_2 Mass and Column Length, and Assembly Temperature for the Twenty-Seven Cases.

Case	Fuel Rod Pitch (cm)	Largest Array			Previous Array Size (rods) [a]	Extrapolated Critical Array Size (rods) [a] [d]	Temp. (°C)
		Array Size (rods) [a]	UO_2 Mass (g) [b]	Fuel Column Length (cm) [c]			
1	0.8001	1461	158910.31	71261.60	1453	1465.659 ± 0.005	24.6
2	0.8001	1456	158367.29	71018.00	1452	1461.977 ± 0.006	24.8
3	0.8001	1424	154889.87	69456.10	1416	1429.983 ± 0.005	24.9
4	0.8001	1360	147933.62	66333.20	1356	1364.222 ± 0.004	24.7
5	0.8001	1284	139669.86	62628.60	1280	1286.593 ± 0.002	24.7
6	0.8001	1204	130961.49	58724.80	1200	1209.537 ± 0.006	24.7
7	0.8550	1057	114991.68	51561.70	1053	1061.658 ± 0.008	24.9
8	0.8550	1056	114882.82	51512.90	1052	1058.983 ± 0.002	24.1
9	0.8550	1028	111843.75	50148.10	1024	1032.528 ± 0.005	25.3
10	0.8550	980	106622.98	47807.50	972	986.918 ± 0.009	24.9
11	0.8550	928	100970.36	45272.80	924	929.952 ± 0.001	24.9
12	1.1315	465	50593.84	22681.50	459	465.788 ± 0.004	24.8
13	1.1315	464	50484.98	22632.70	462	464.501 ± 0.001	25.3
14	1.1315	456	49615.02	22242.80	454	456.914 ± 0.001	25.2
15	1.1315	444	48308.16	21657.70	442	445.275 ± 0.001	24.8
16	1.2091	413	44945.00	20146.00	411	414.630 ± 0.002	25.4
17	1.2091	412	44836.14	20097.20	410	413.944 ± 0.003	23.8
18	1.2091	408	44402.78	19903.00	406	409.354 ± 0.001	25.2
19	1.2091	398	43313.34	19415.50	396	400.450 ± 0.004	24.4
20	1.6002	338	36771.14	16485.50	336	338.667 ± 0.001	25.1
21	1.6002	339	36880.28	16534.10	337	340.269 ± 0.001	25.2
22	1.6002	345	37534.21	16825.80	343	347.007 ± 0.003	25.4
23	1.6002	347	37746.24	16923.10	345	347.832 ± 0.001	25.4
24	1.7099	346	37642.66	16874.90	344	347.621 ± 0.002	24.9
25	1.7099	349	37969.69	17020.90	345	349.879 ± 0.001	24.9
26	1.7099	361	39273.10	17607.80	357	361.574 ± 0.001	24.9
27	1.7099	367	39918.06	17899.30	365	368.030 ± 0.001	24.8

(a) Includes the twelve fueled sections in the control element and the two safety elements
(b) Sum of the UO_2 masses in the rods included in the configuration.
(c) Sum of the fuel column lengths in the rods included in the configuration.
(d) The critical array size determined from count-rate measurements made at the two array sizes given. The uncertainties listed are those attributed only to the stochastic nature of the radiation detection process.

Table 9. Grid Plate Hole Pitch, Fuel Rod Pitch, Fuel-to-Water Volume Ratio, Average Fuel Rod Diameter and Standard Deviation of the Distribution for the Fuel Rods in Each Case.

Case	Grid Plate Hole Pitch (cm)	Fuel Rod Pitch (cm)	Fuel-to-Water Volume Ratio	Array Size (rods)	Average Fuel Rod Outside Diameter (cm)	Standard Deviation (cm)	Number of Fuel Rods [(a)]
1	0.8001	0.8001	0.67073	1461	0.634980	0.000216	1449
2	0.8001	0.8001	0.66982	1456	0.634981	0.000216	1444
3	0.8001	0.8001	0.66245	1424	0.634983	0.000216	1412
4	0.8001	0.8001	0.64719	1360	0.634985	0.000215	1348
5	0.8001	0.8001	0.62364	1284	0.634989	0.000216	1272
6	0.8001	0.8001	0.59193	1204	0.634991	0.000217	1192
7	0.8550	0.8550	0.52373	1057	0.634990	0.000207	1045
8	0.8550	0.8550	0.52286	1056	0.634990	0.000207	1044
9	0.8550	0.8550	0.51577	1028	0.634989	0.000208	1016
10	0.8550	0.8550	0.50118	980	0.634987	0.000207	968
11	0.8550	0.8550	0.47910	928	0.634988	0.000209	916
12	0.8001	1.1315	0.22517	465	0.634989	0.000205	453
13	0.8001	1.1315	0.22453	464	0.634988	0.000205	452
14	0.8001	1.1315	0.21942	456	0.634988	0.000205	444
15	0.8001	1.1315	0.21186	444	0.634988	0.000207	432
16	0.8550	1.2091	0.18947	413	0.634985	0.000199	401
17	0.8550	1.2091	0.18888	412	0.634984	0.000199	400
18	0.8550	1.2091	0.18428	408	0.634981	0.000200	396
19	0.8550	1.2091	0.17751	398	0.634981	0.000202	386
20	0.8001	1.6002	0.09670	338	0.634996	0.000217	326
21	0.8001	1.6002	0.09638	339	0.634994	0.000218	327
22	0.8001	1.6002	0.09390	345	0.634995	0.000215	333
23	0.8001	1.6002	0.08935	347	0.634997	0.000217	335
24	0.8550	1.7099	0.08323	346	0.634994	0.000216	334
25	0.8550	1.7099	0.08296	349	0.634993	0.000217	337
26	0.8550	1.7099	0.08097	361	0.634995	0.000216	349
27	0.8550	1.7099	0.07732	367	0.634991	0.000217	355

(a) Each configuration also included 12 fueled sections in the control and safety elements.

During the course of the critical experiments, reproducibility data were taken for four of the configurations investigated (Cases 1, 7, 20, and 24). The maximum deviation from the mean extrapolated array size was about 0.025 % for these measurements with a standard deviation of about 0.018 %.

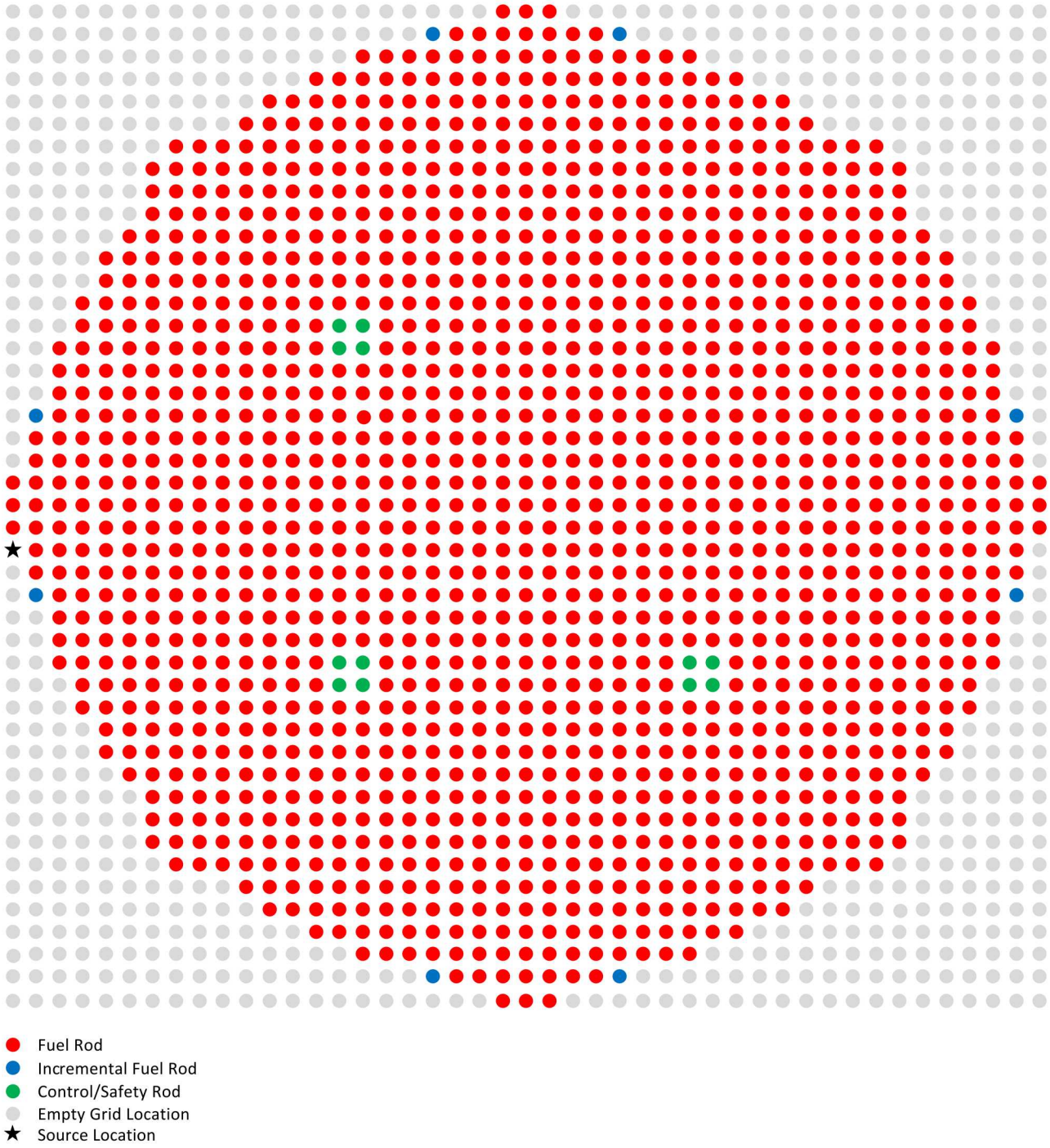

Figure 19. Fuel Rod Layout of the Largest Array Measured for Case 1.

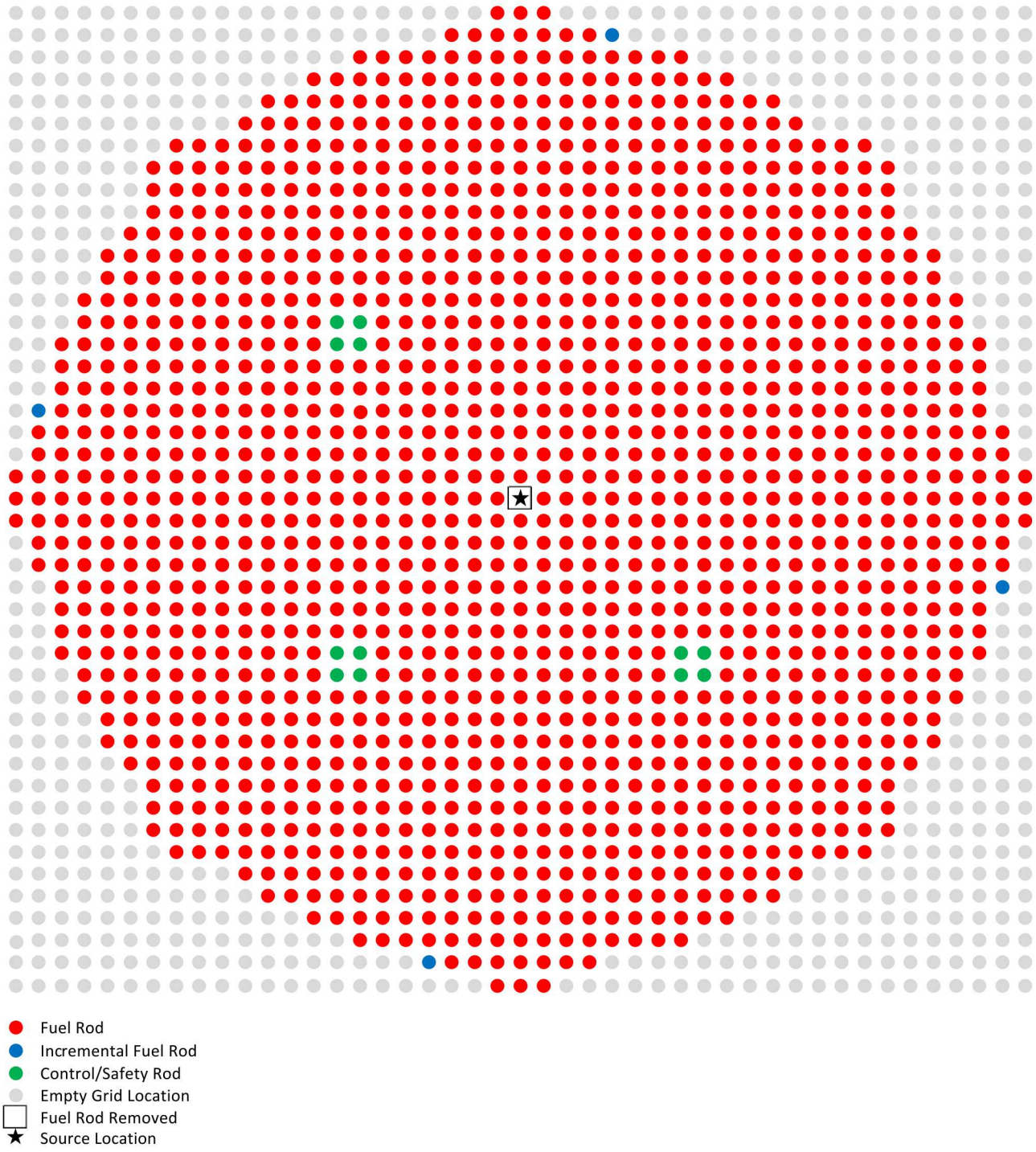

Figure 20. Fuel Rod Layout of the Largest Array Measured for Case 2.

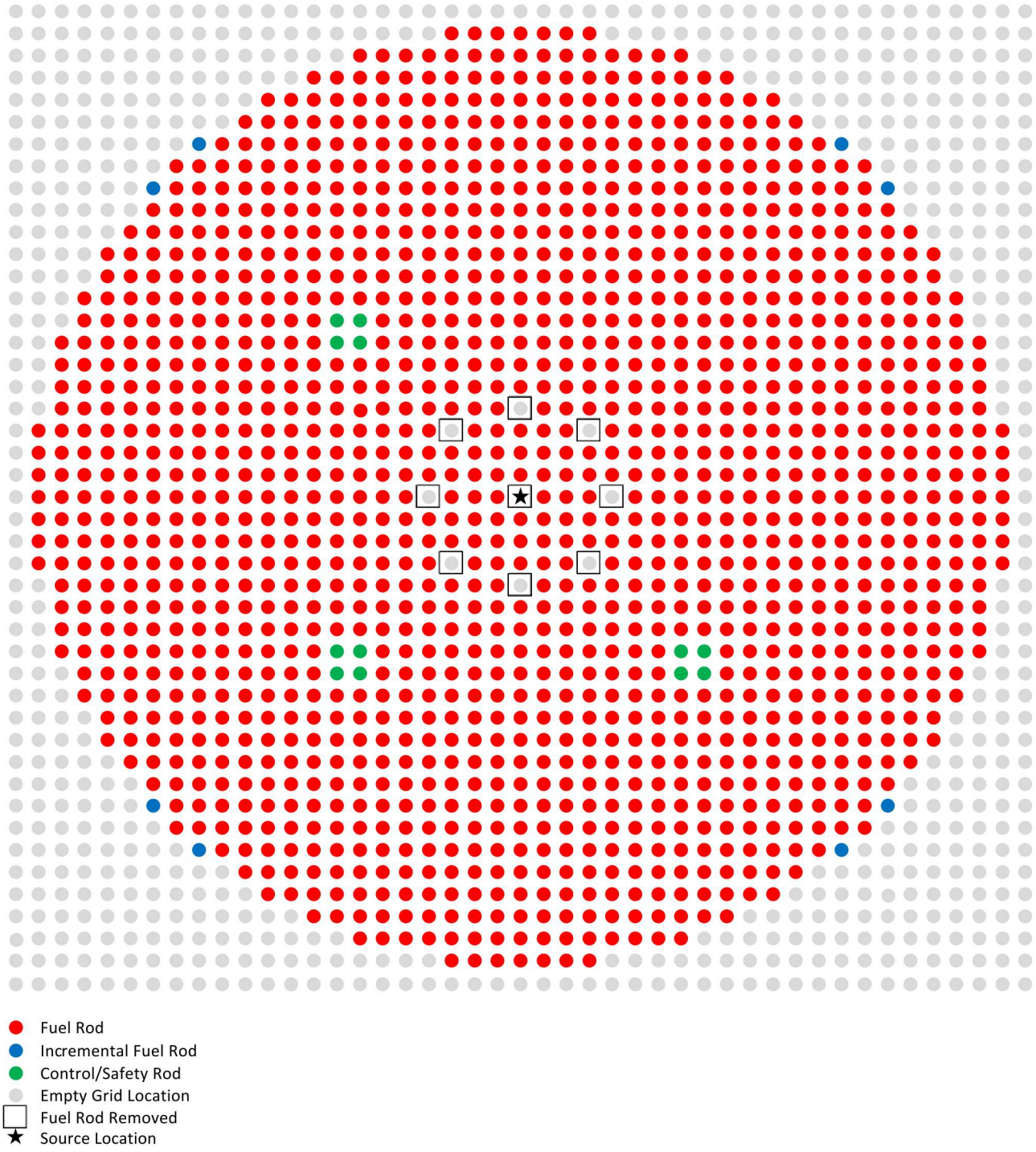

Figure 21. Fuel Rod Layout of the Largest Array Measured for Case 3.

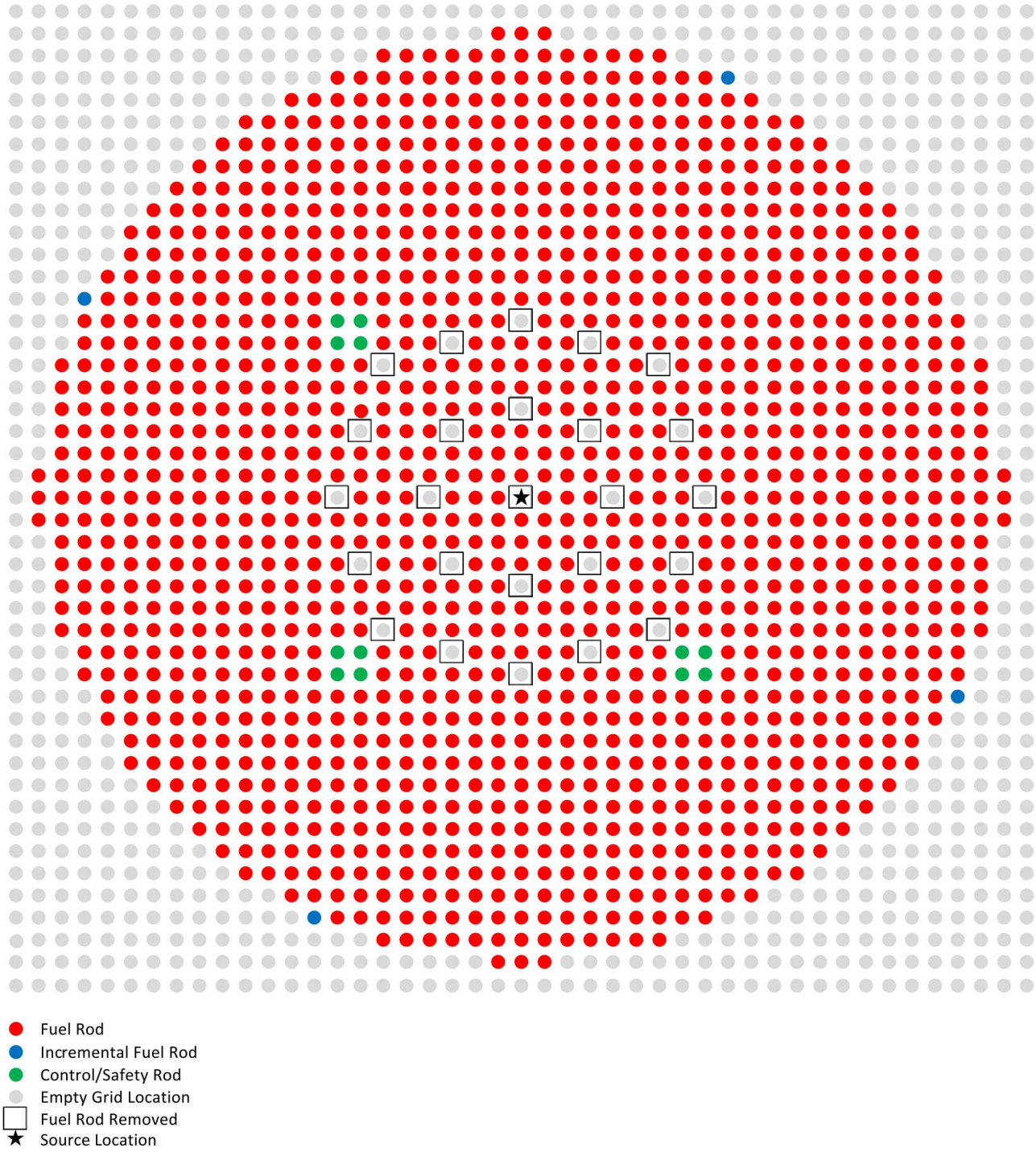

Figure 22. Fuel Rod Layout of the Largest Array Measured for Case 4.

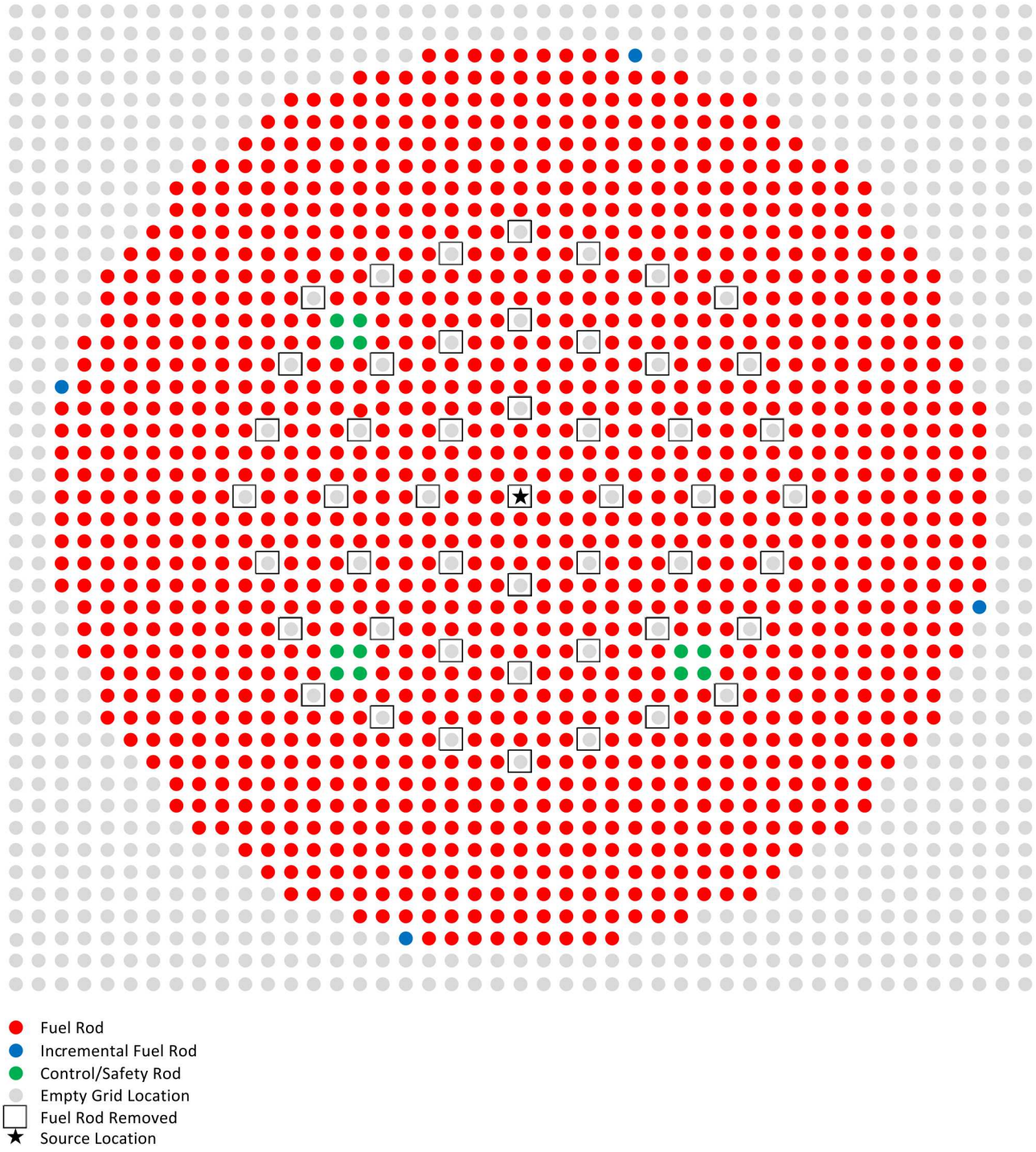

Figure 23. Fuel Rod Layout of the Largest Array Measured for Case 5.

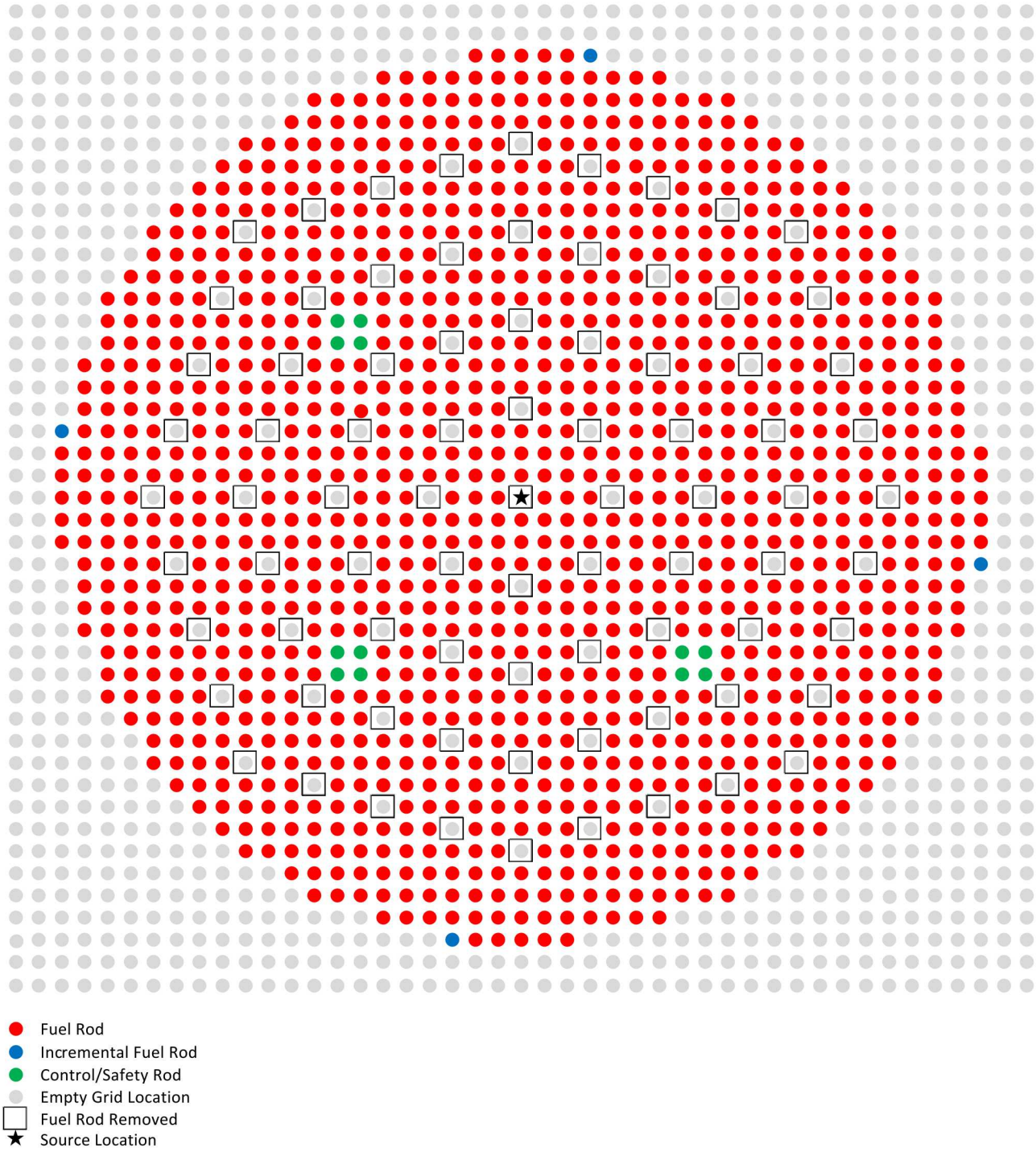

Figure 24. Fuel Rod Layout of the Largest Array Measured for Case 6.

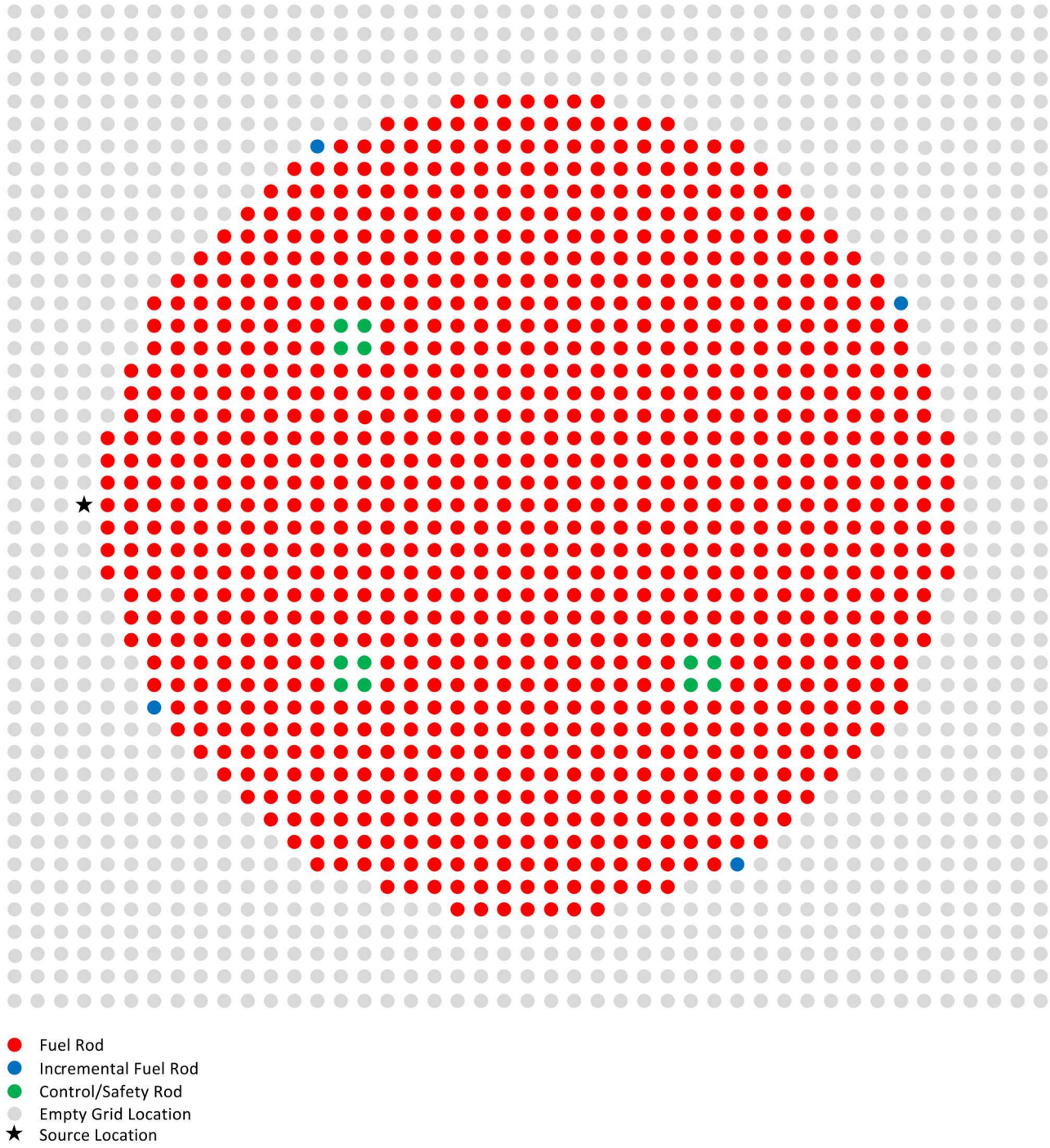

Figure 25. Fuel Rod Layout of the Largest Array Measured for Case 7.

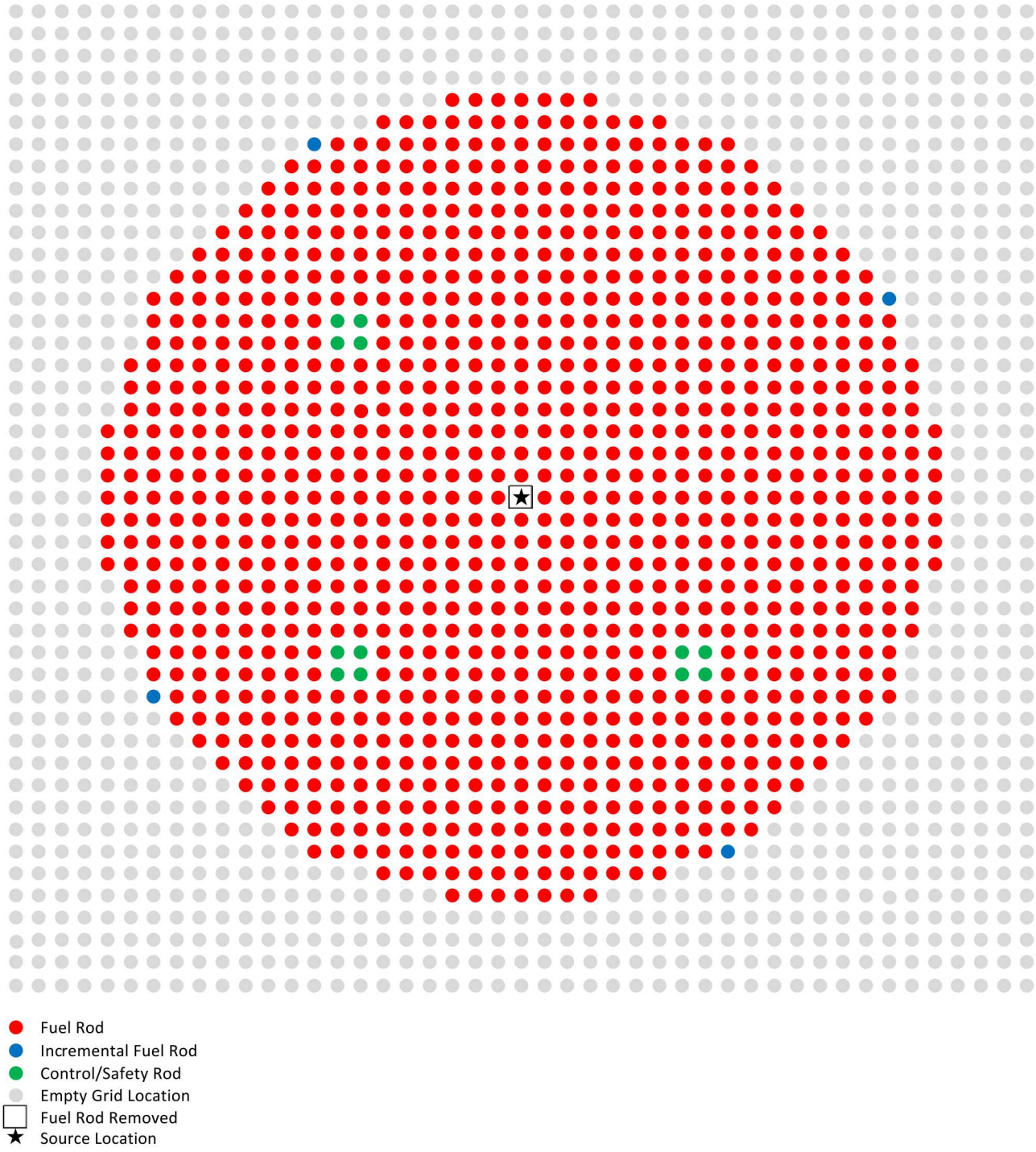

Figure 26. Fuel Rod Layout of the Largest Array Measured for Case 8.

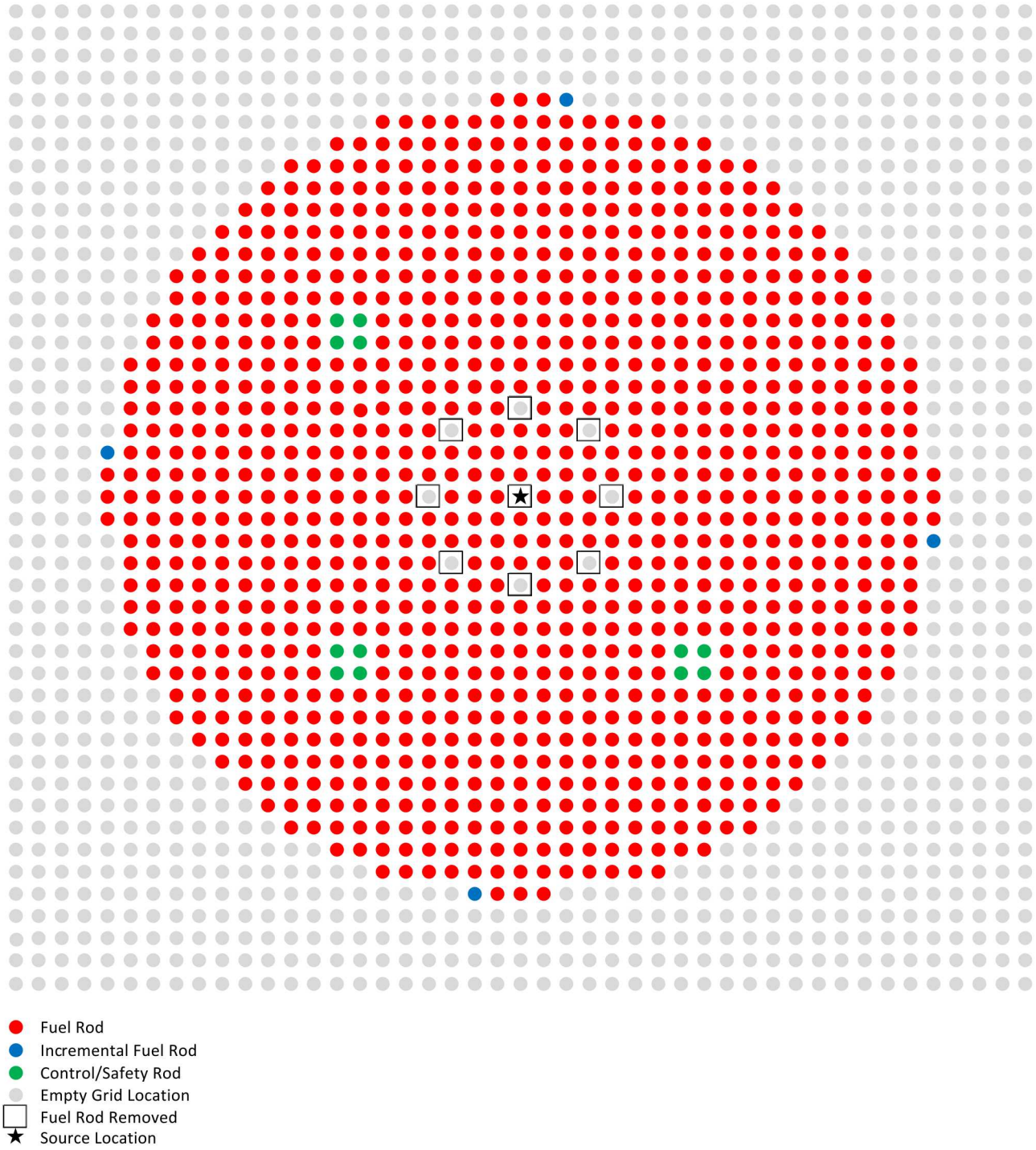

Figure 27. Fuel Rod Layout of the Largest Array Measured for Case 9.

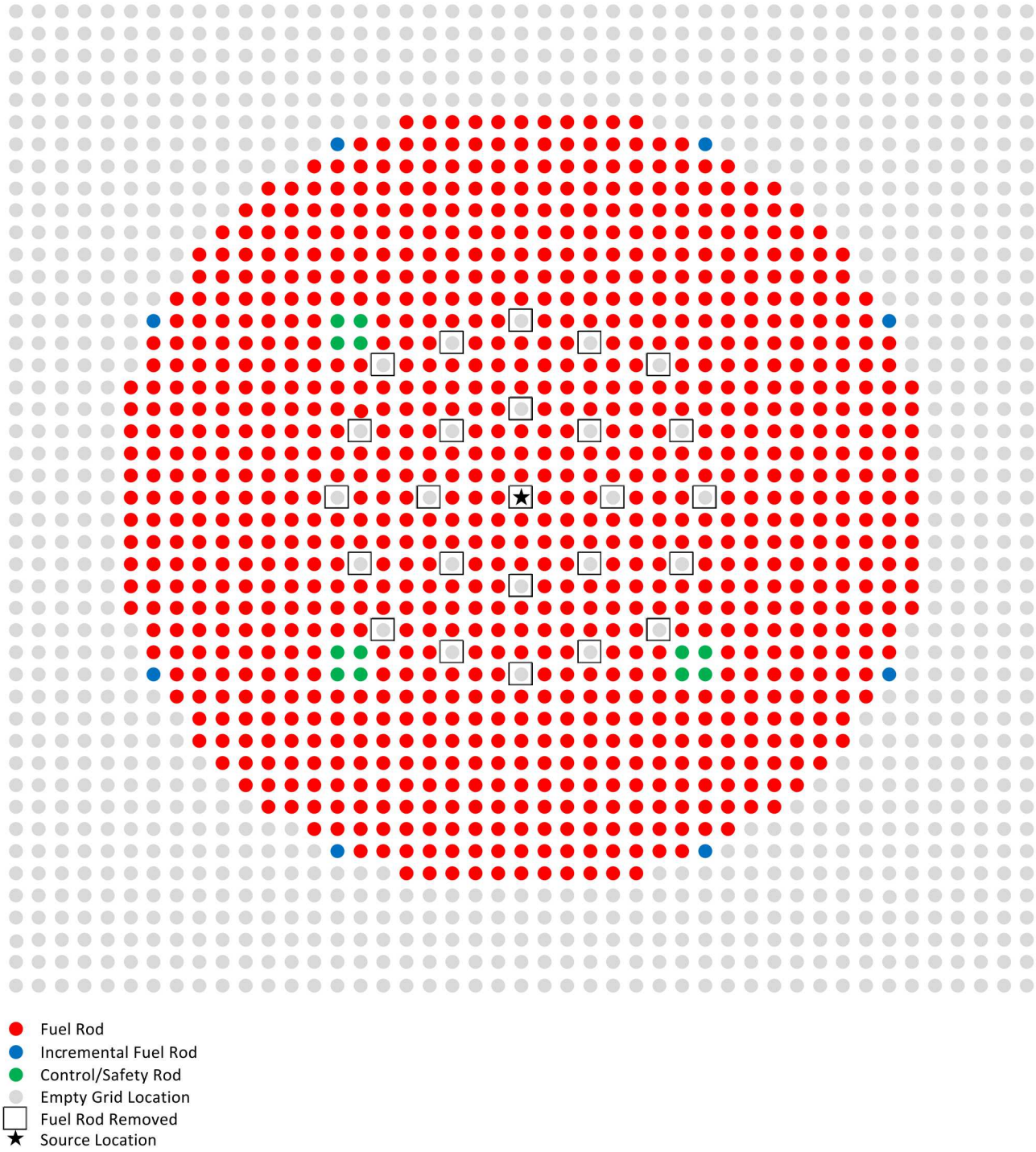

Figure 28. Fuel Rod Layout of the Largest Array Measured for Case 10.

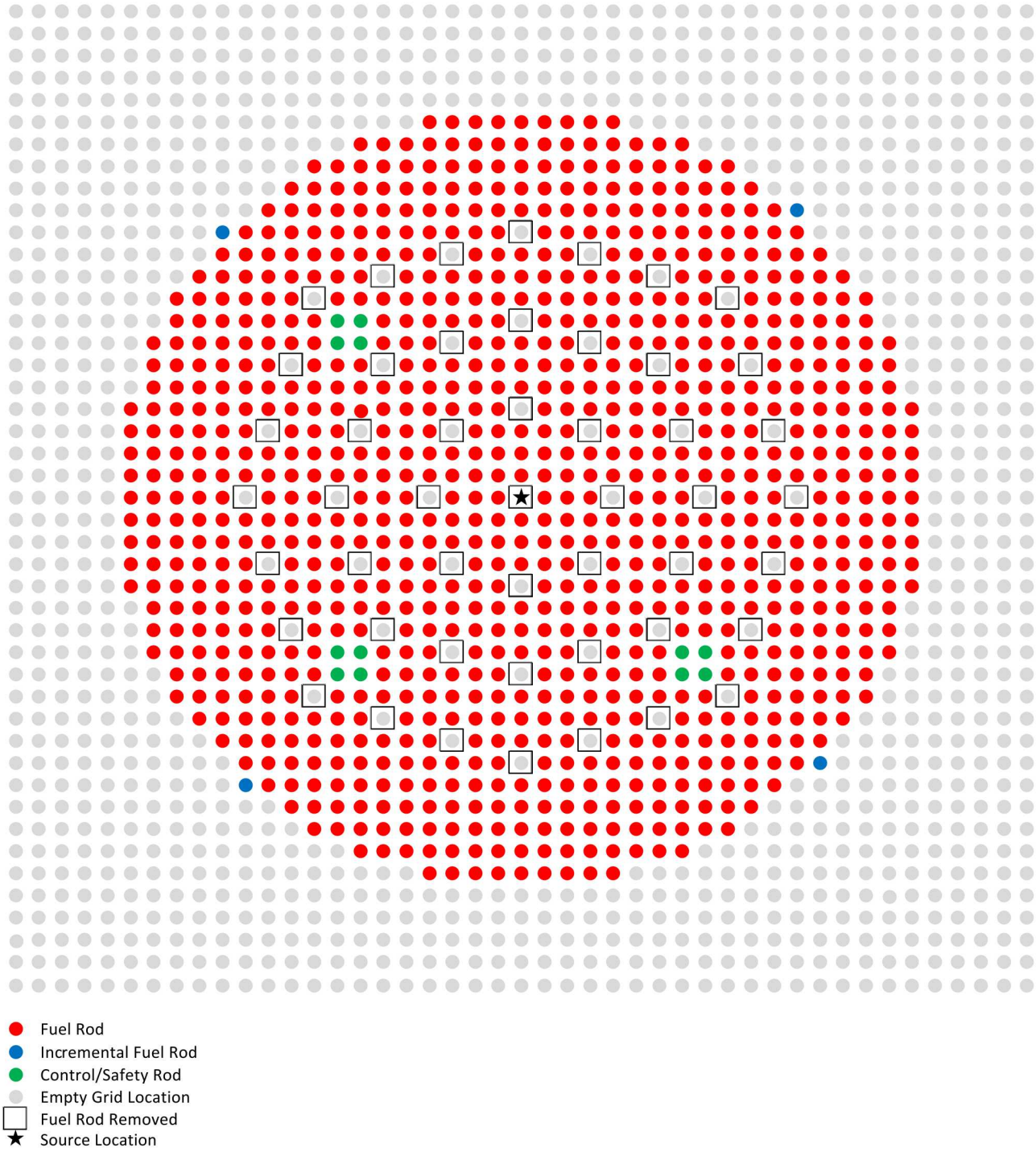

Figure 29. Fuel Rod Layout of the Largest Array Measured for Case 11.

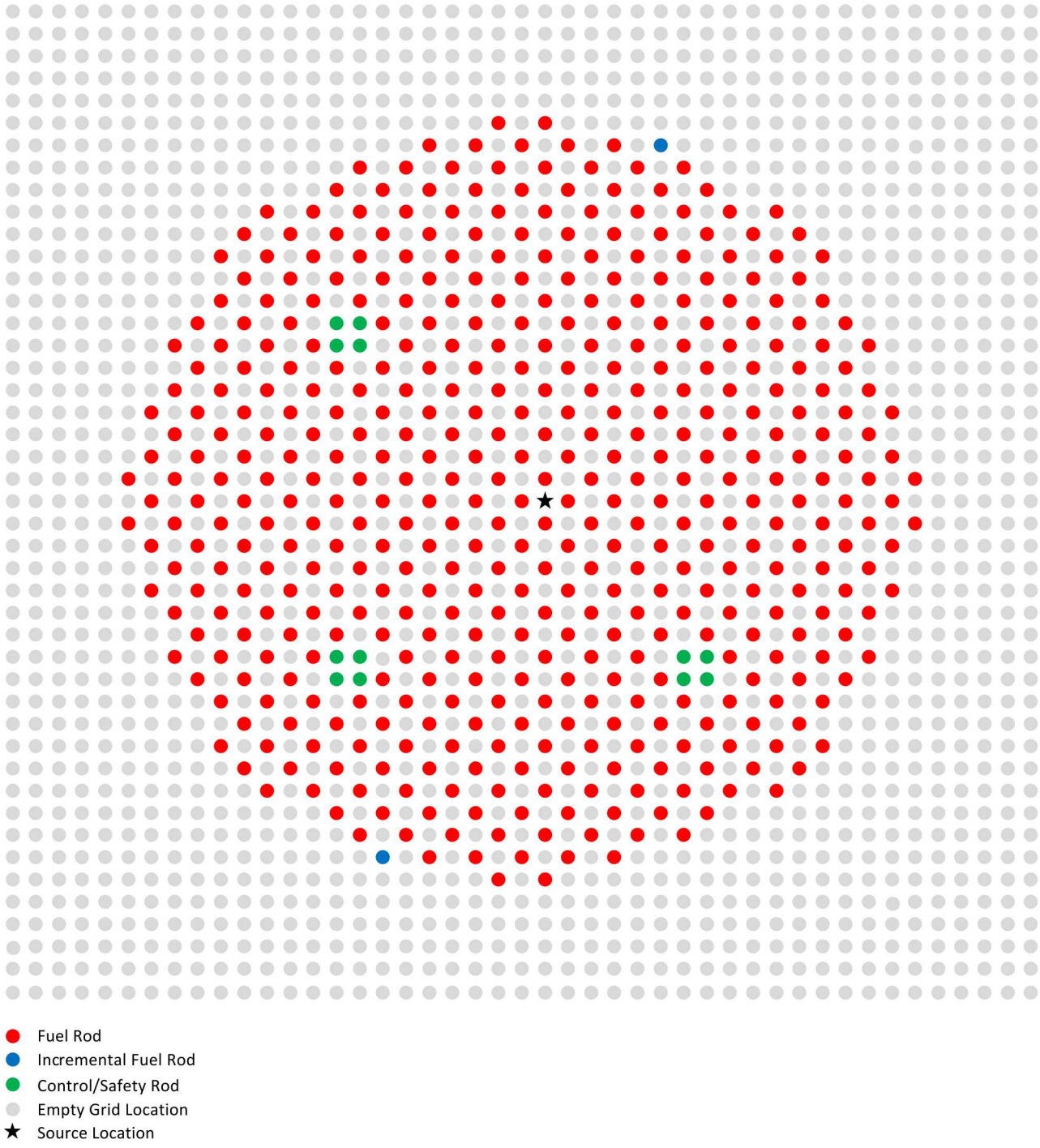

Figure 30. Fuel Rod Layout of the Largest Array Measured for Case 12.

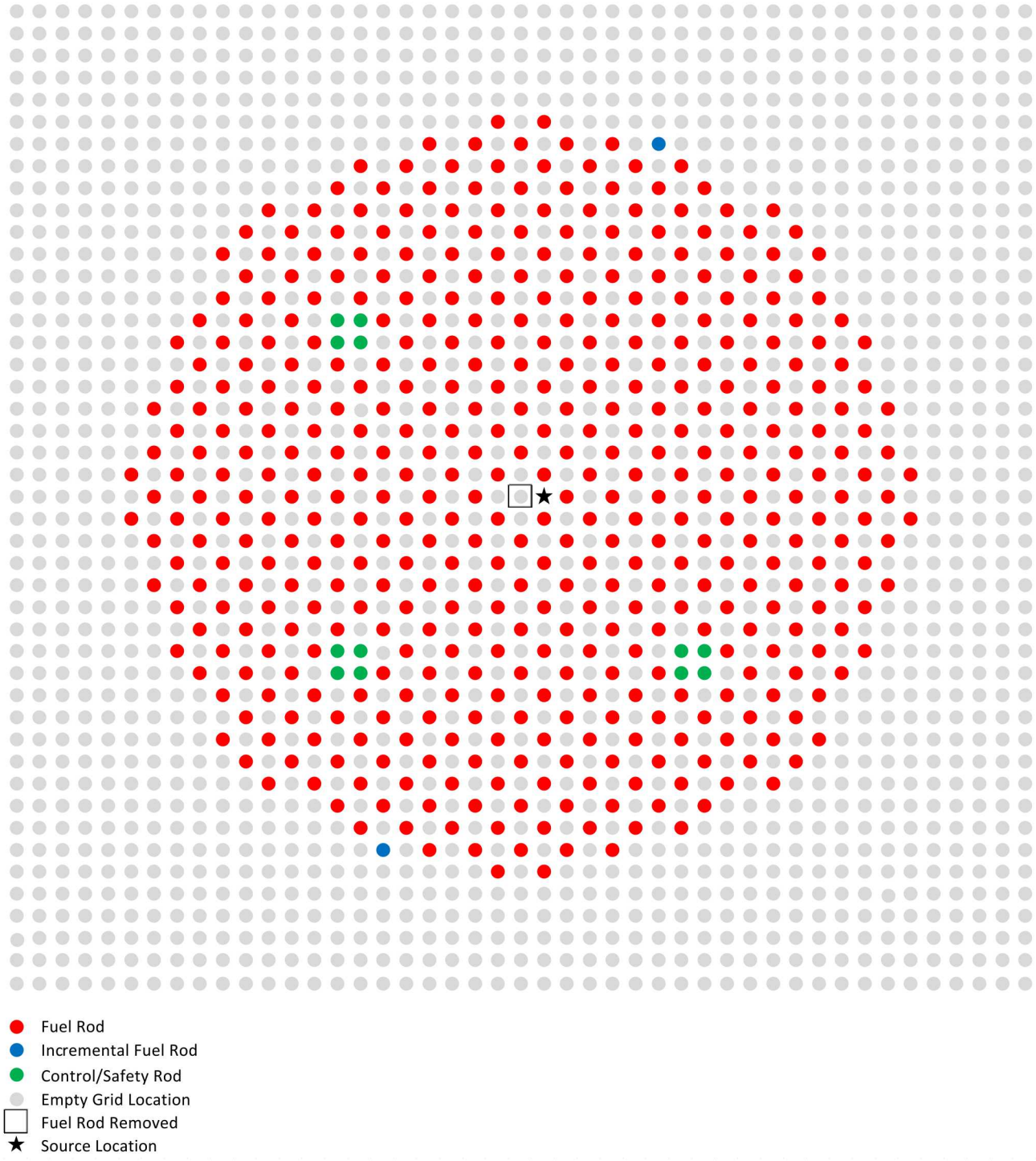

Figure 31. Fuel Rod Layout of the Largest Array Measured for Case 13.

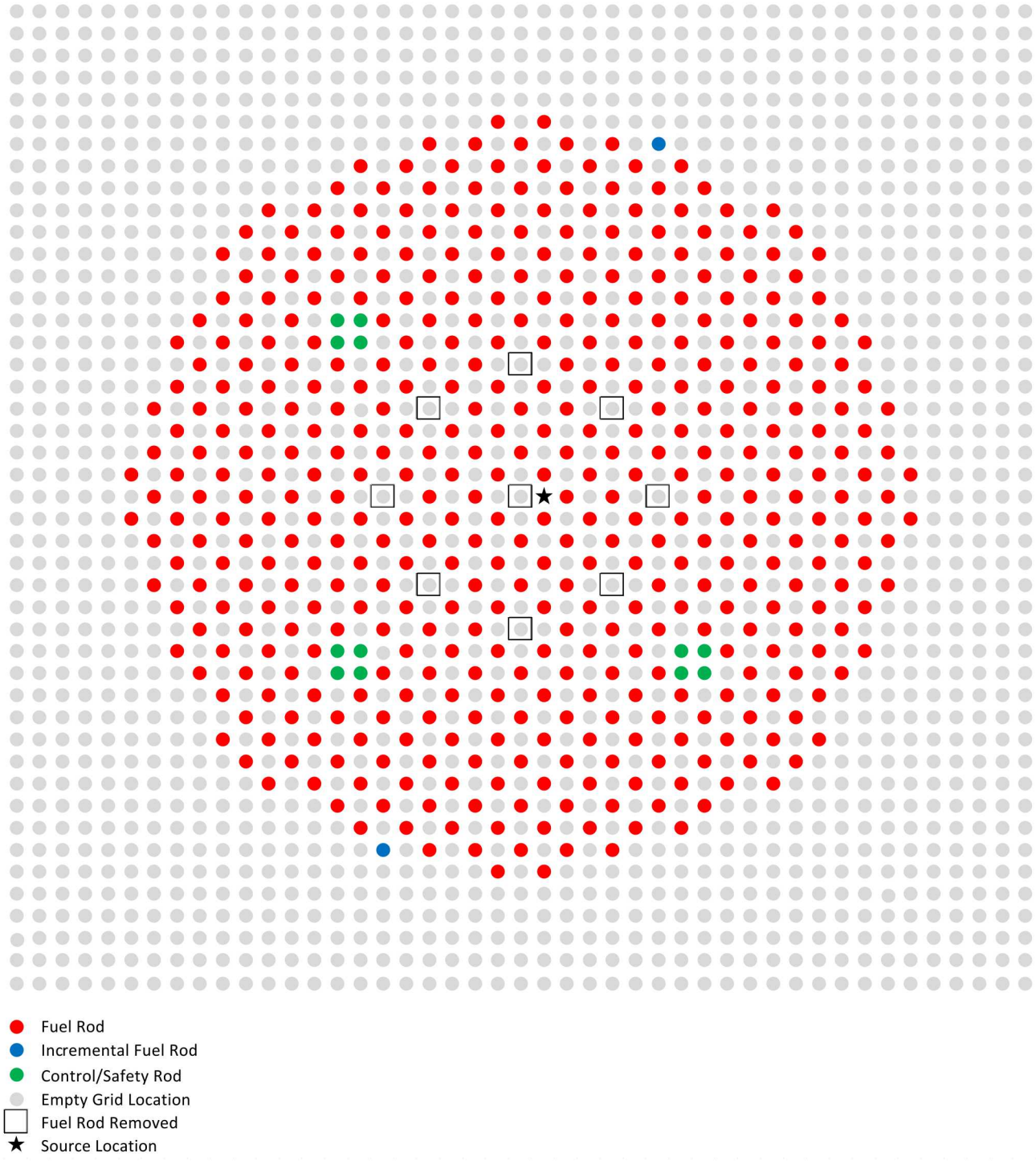

Figure 32. Fuel Rod Layout of the Largest Array Measured for Case 14.

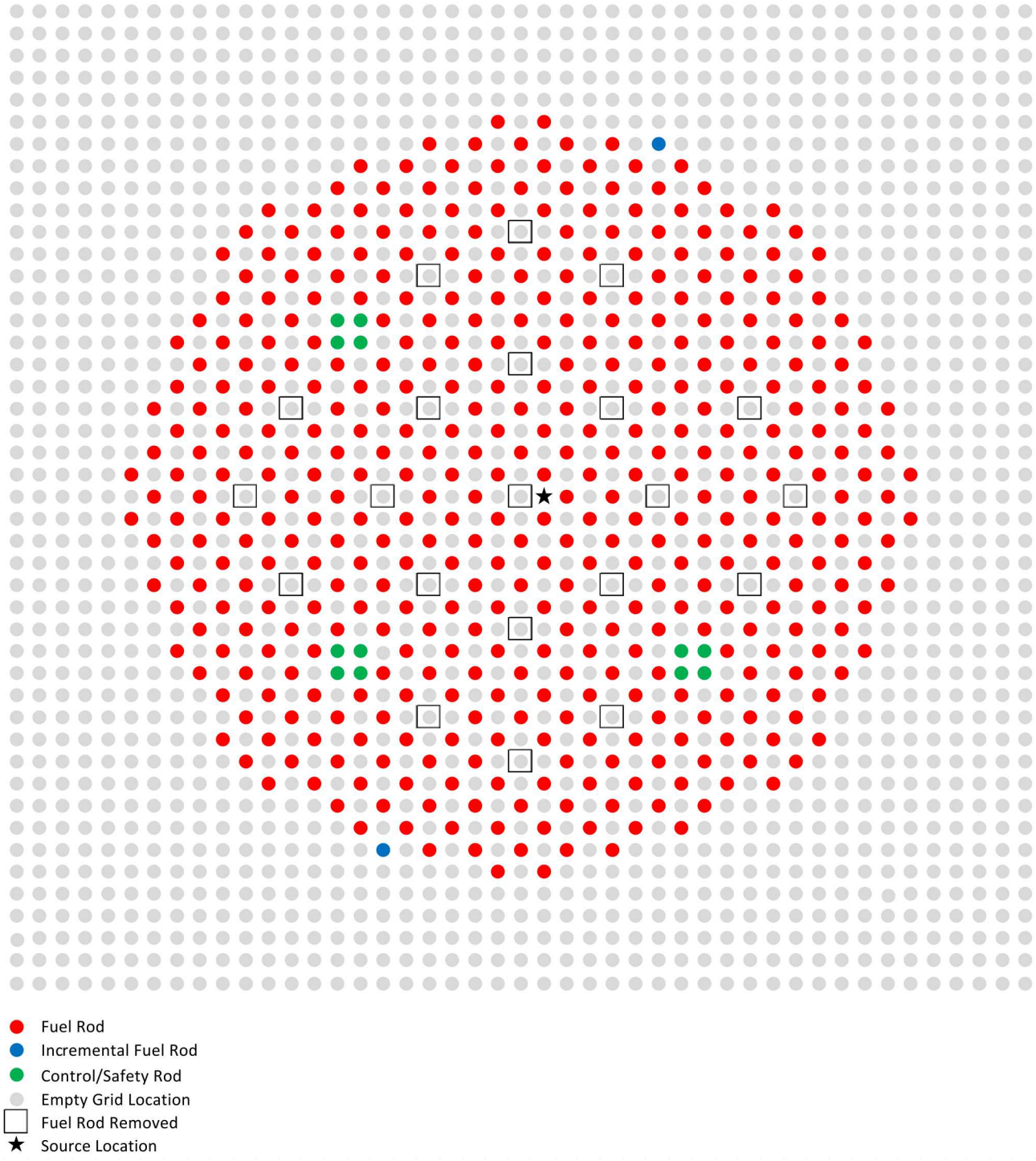

Figure 33. Fuel Rod Layout of the Largest Array Measured for Case 15.

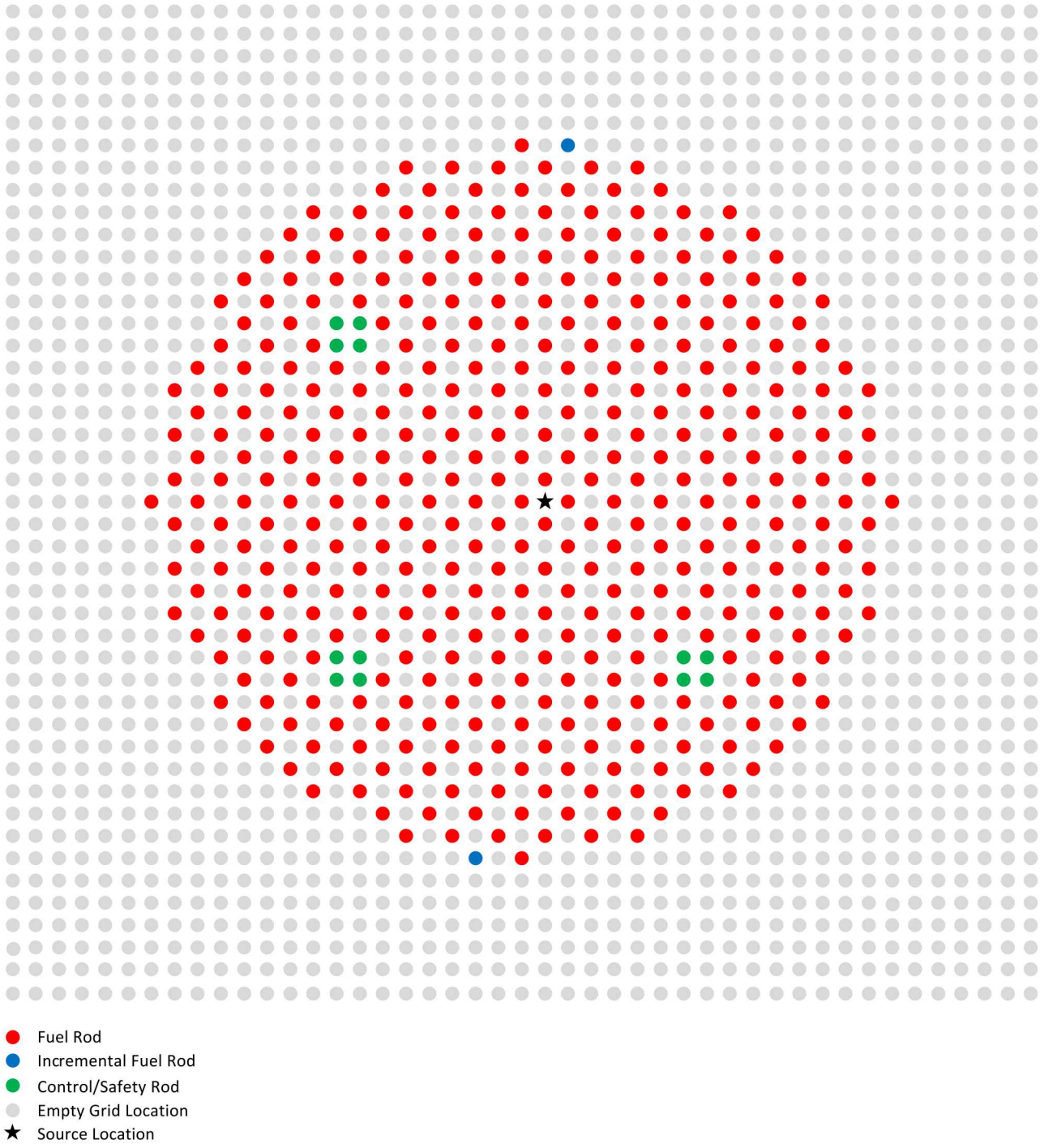

Figure 34. Fuel Rod Layout of the Largest Array Measured for Case 16.

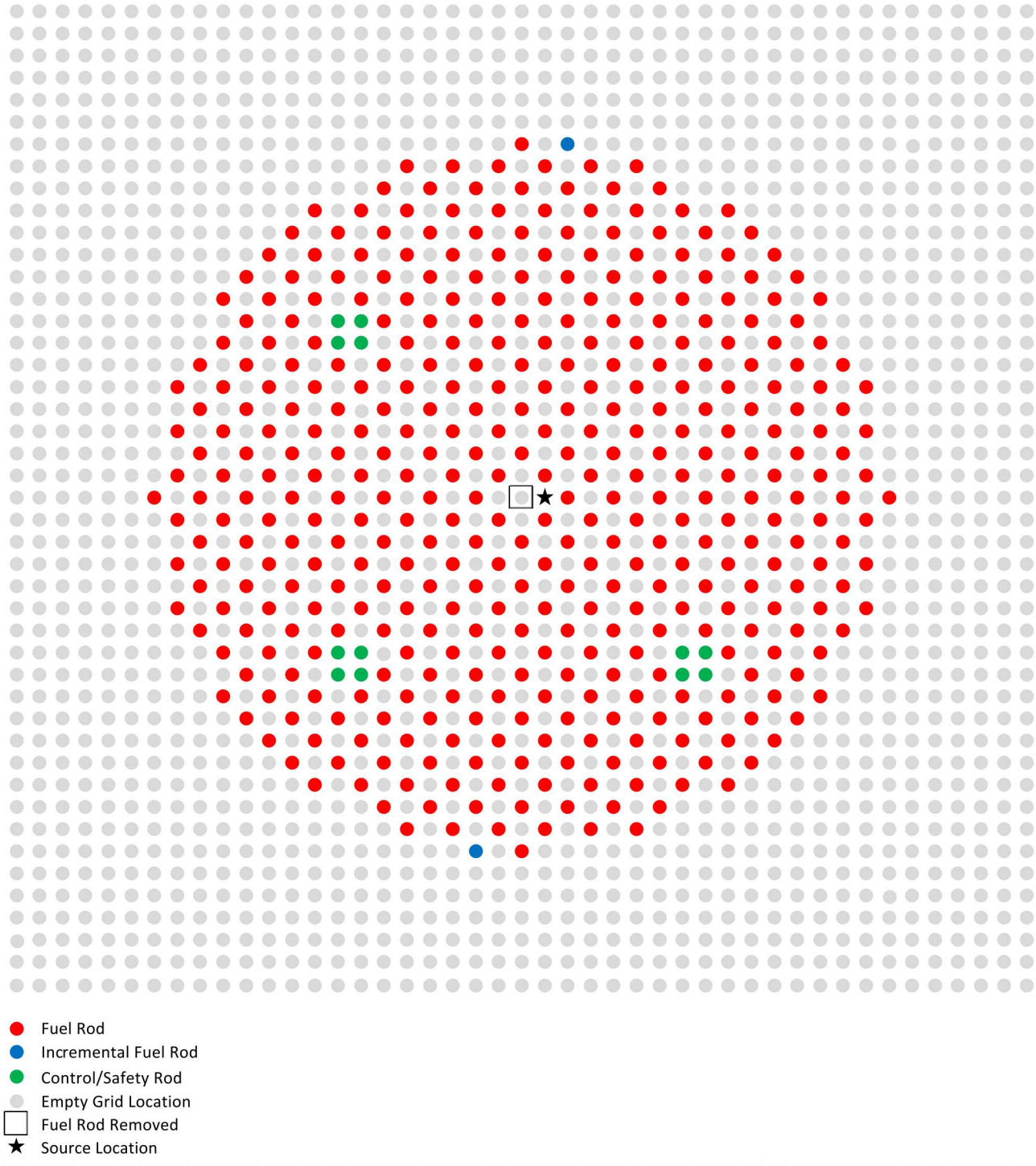

Figure 35. Fuel Rod Layout of the Largest Array Measured for Case 17.

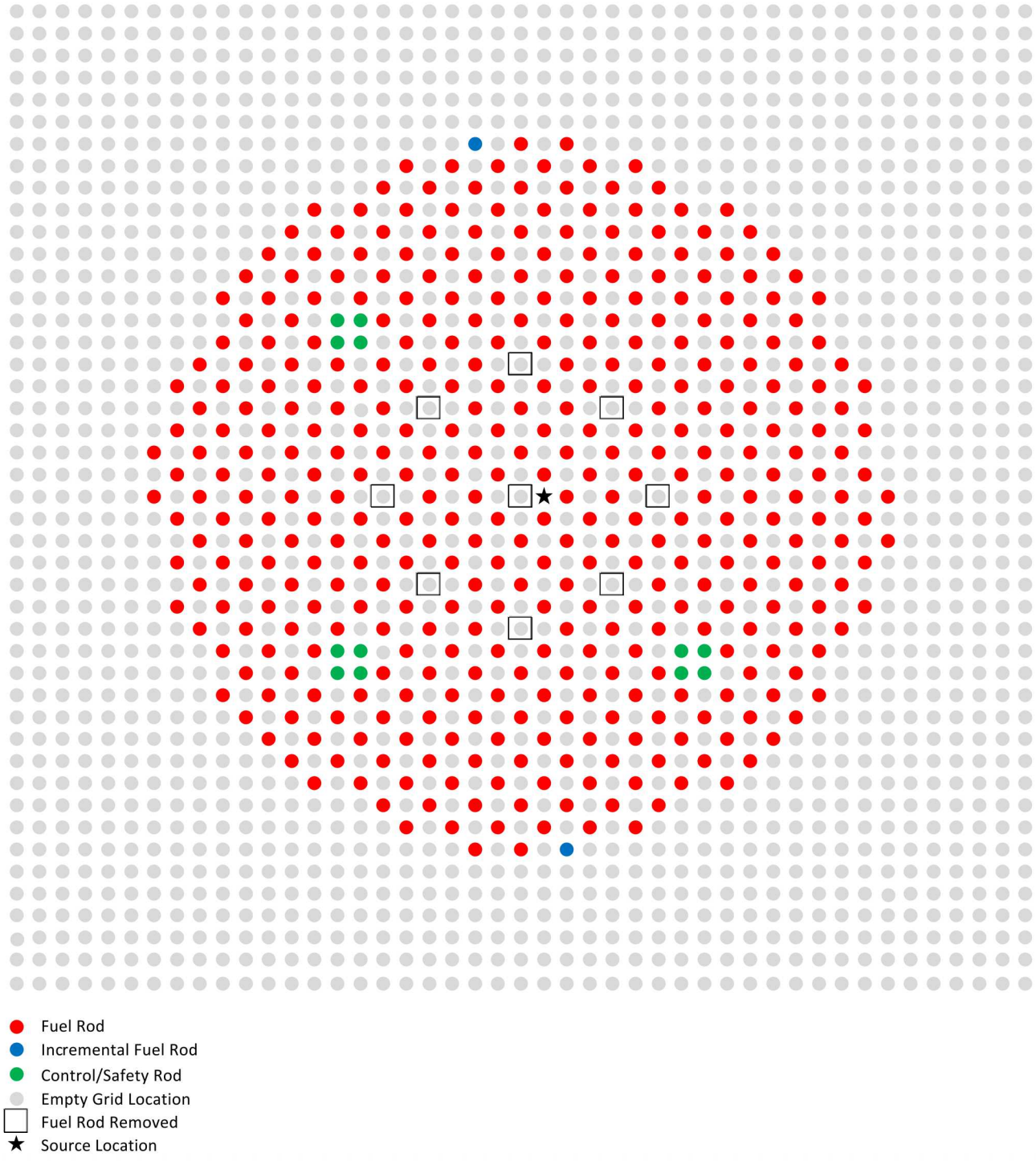

Figure 36. Fuel Rod Layout of the Largest Array Measured for Case 18.

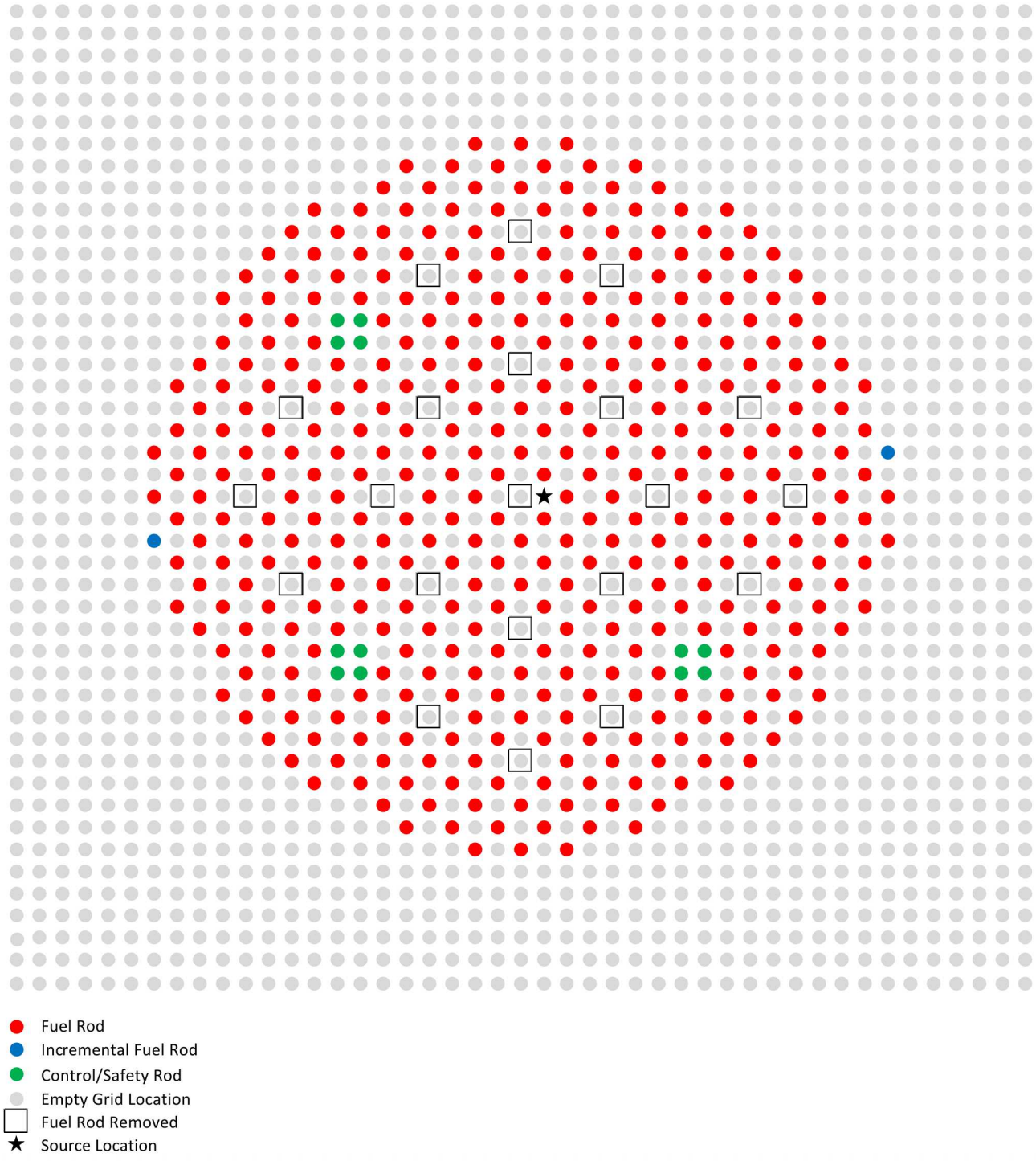

Figure 37. Fuel Rod Layout of the Largest Array Measured for Case 19.

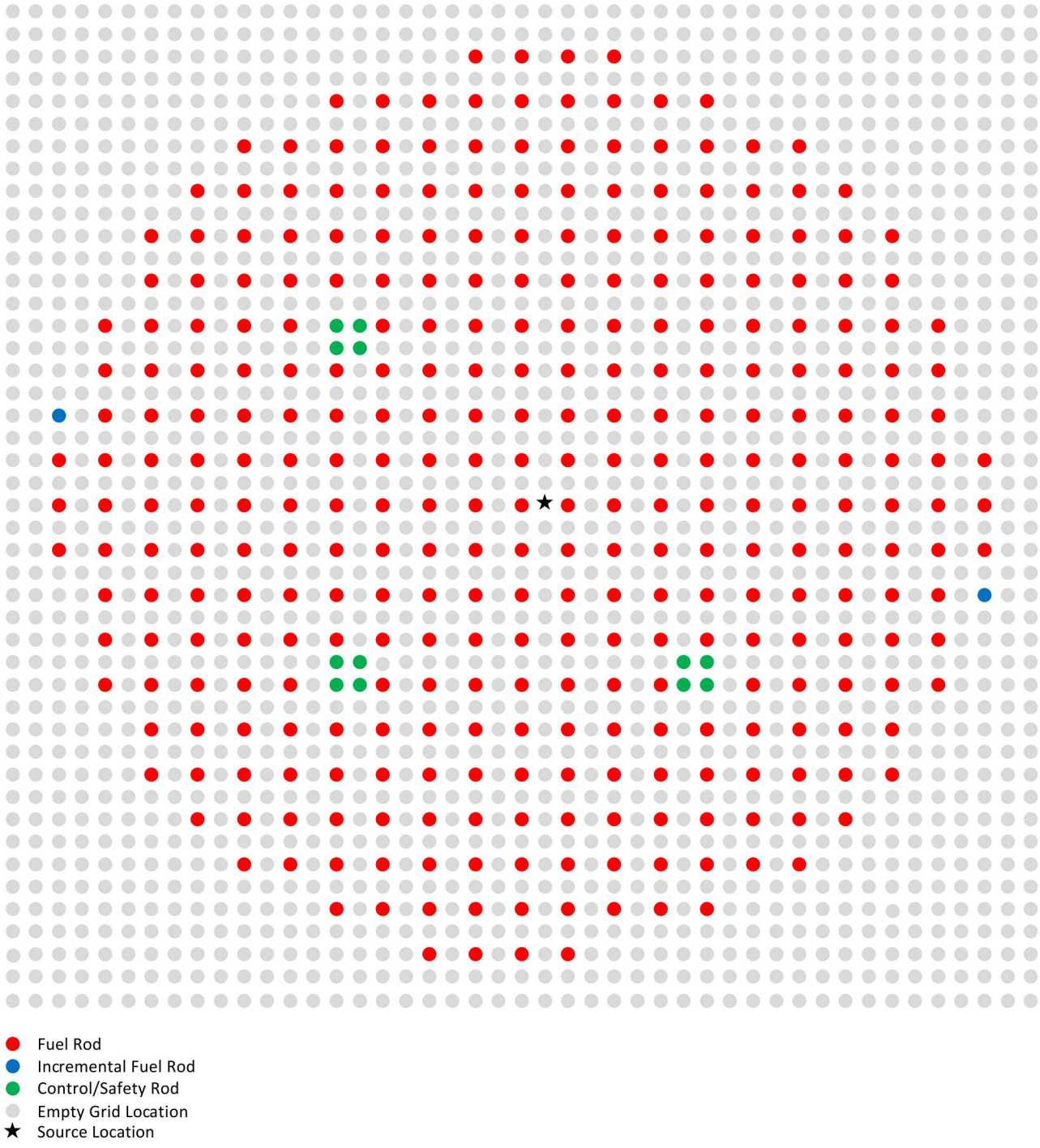

Figure 38. Fuel Rod Layout of the Largest Array Measured for Case 20.

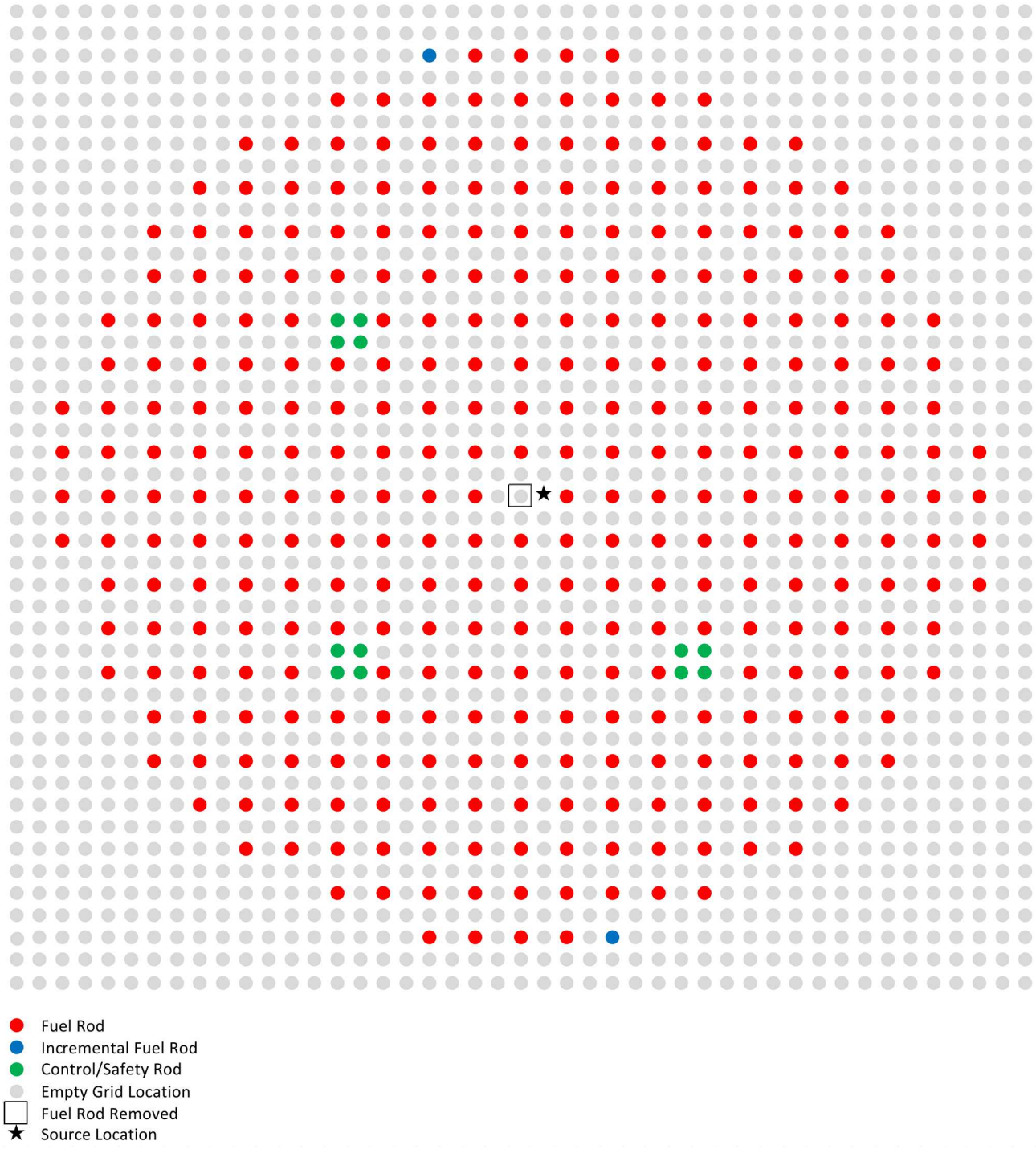

Figure 39. Fuel Rod Layout of the Largest Array Measured for Case 21.

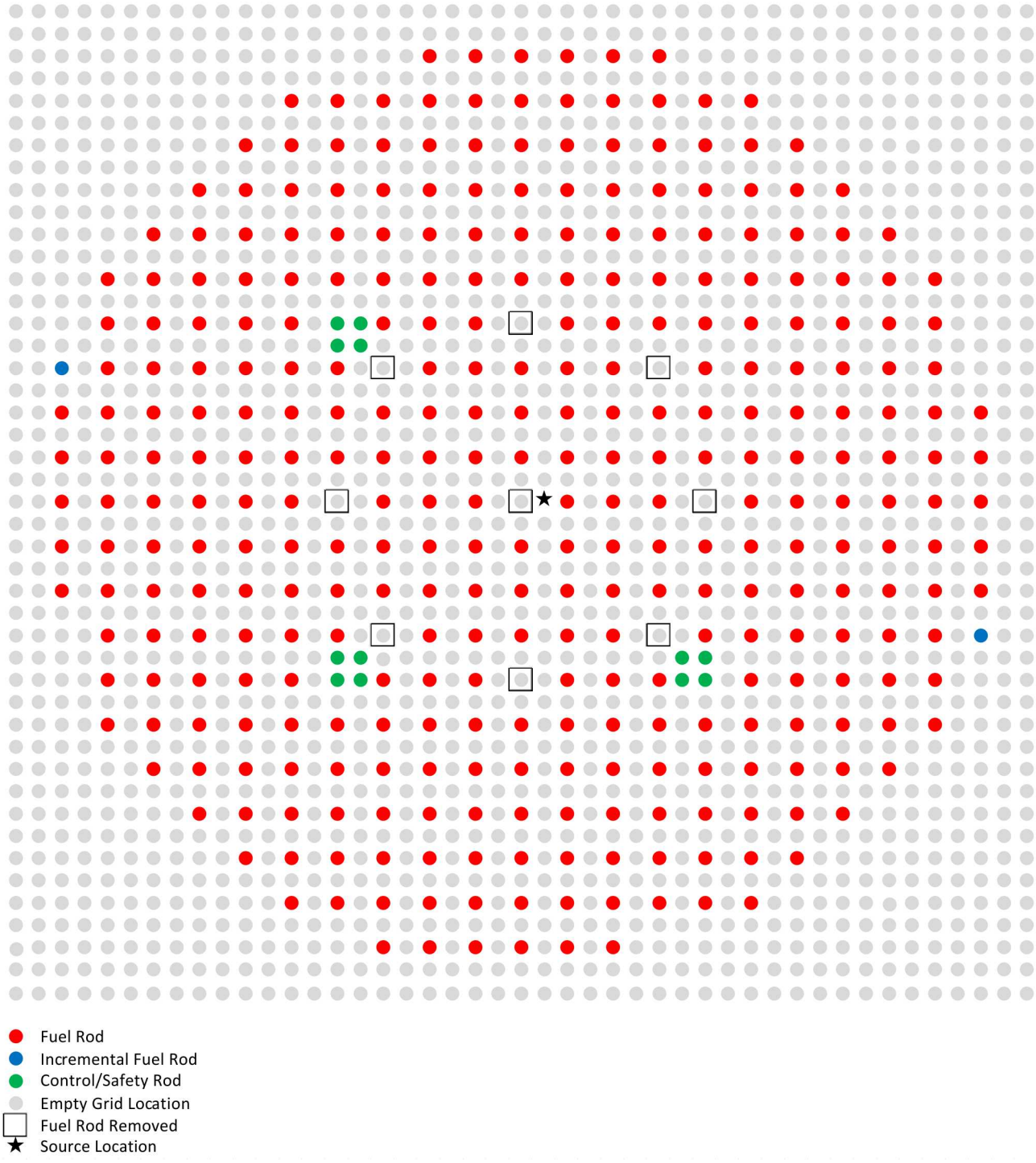

Figure 40. Fuel Rod Layout of the Largest Array Measured for Case 22.

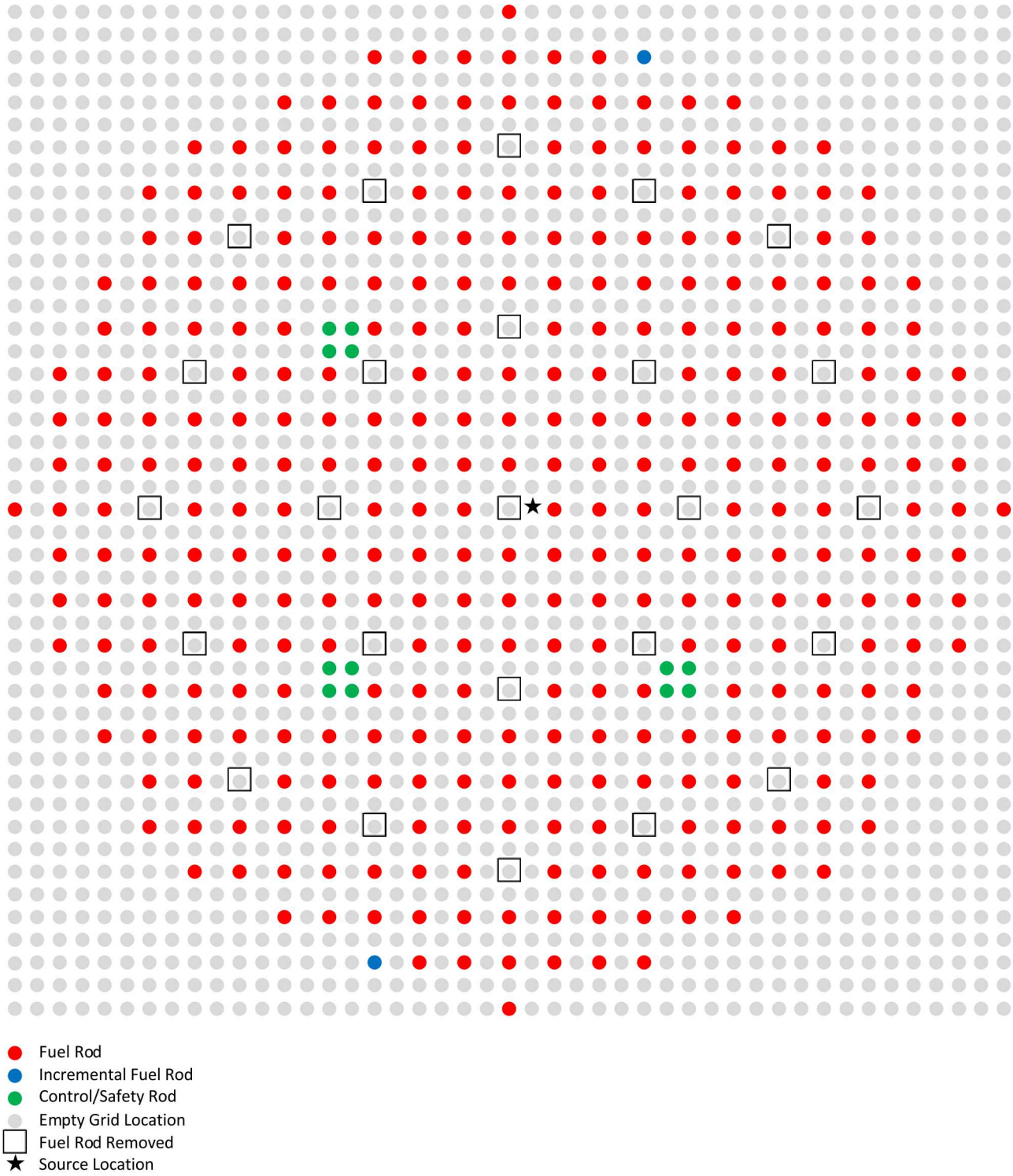

Figure 41. Fuel Rod Layout of the Largest Array Measured for Case 23.

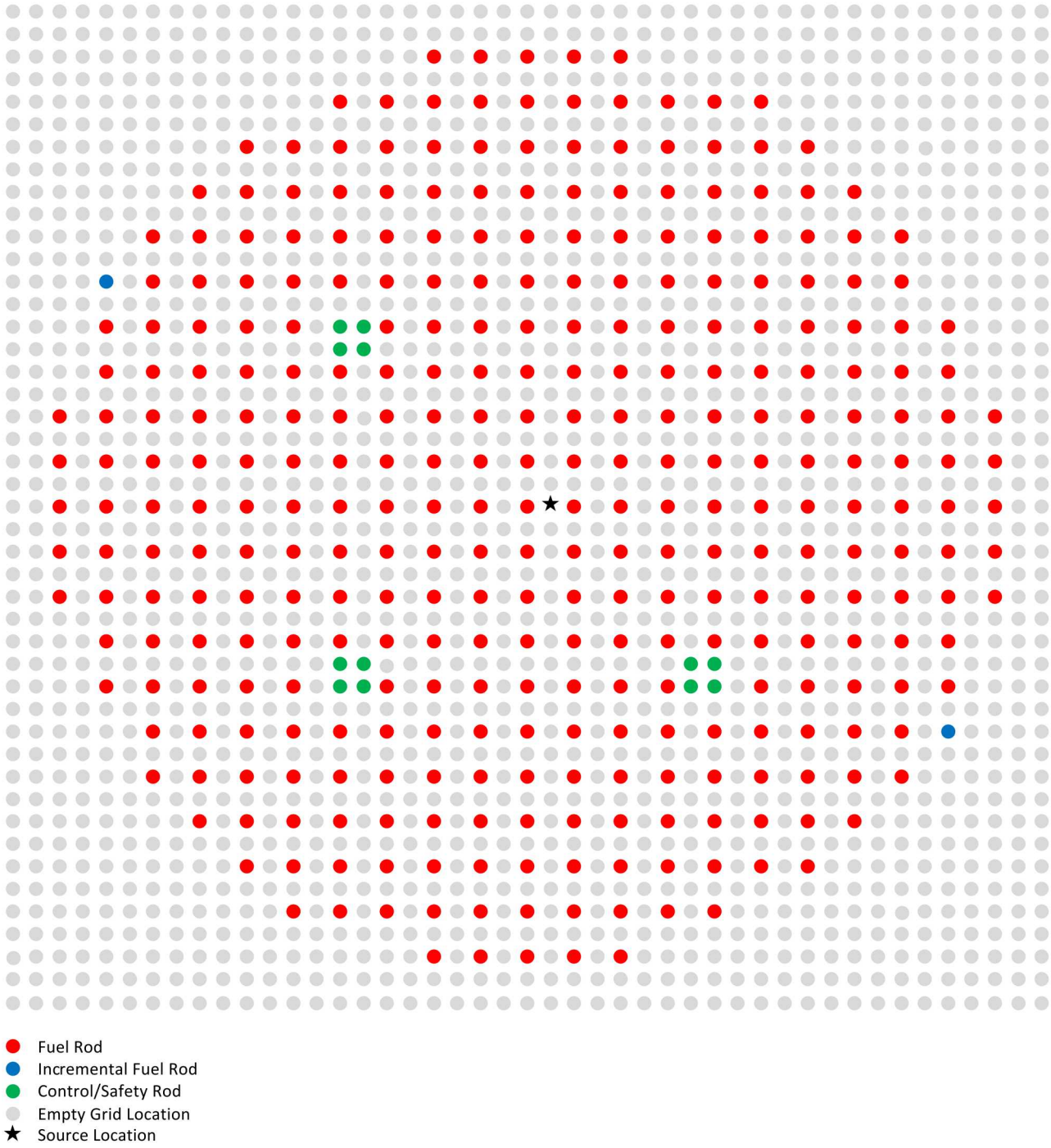

Figure 42. Fuel Rod Layout of the Largest Array Measured for Case 24.

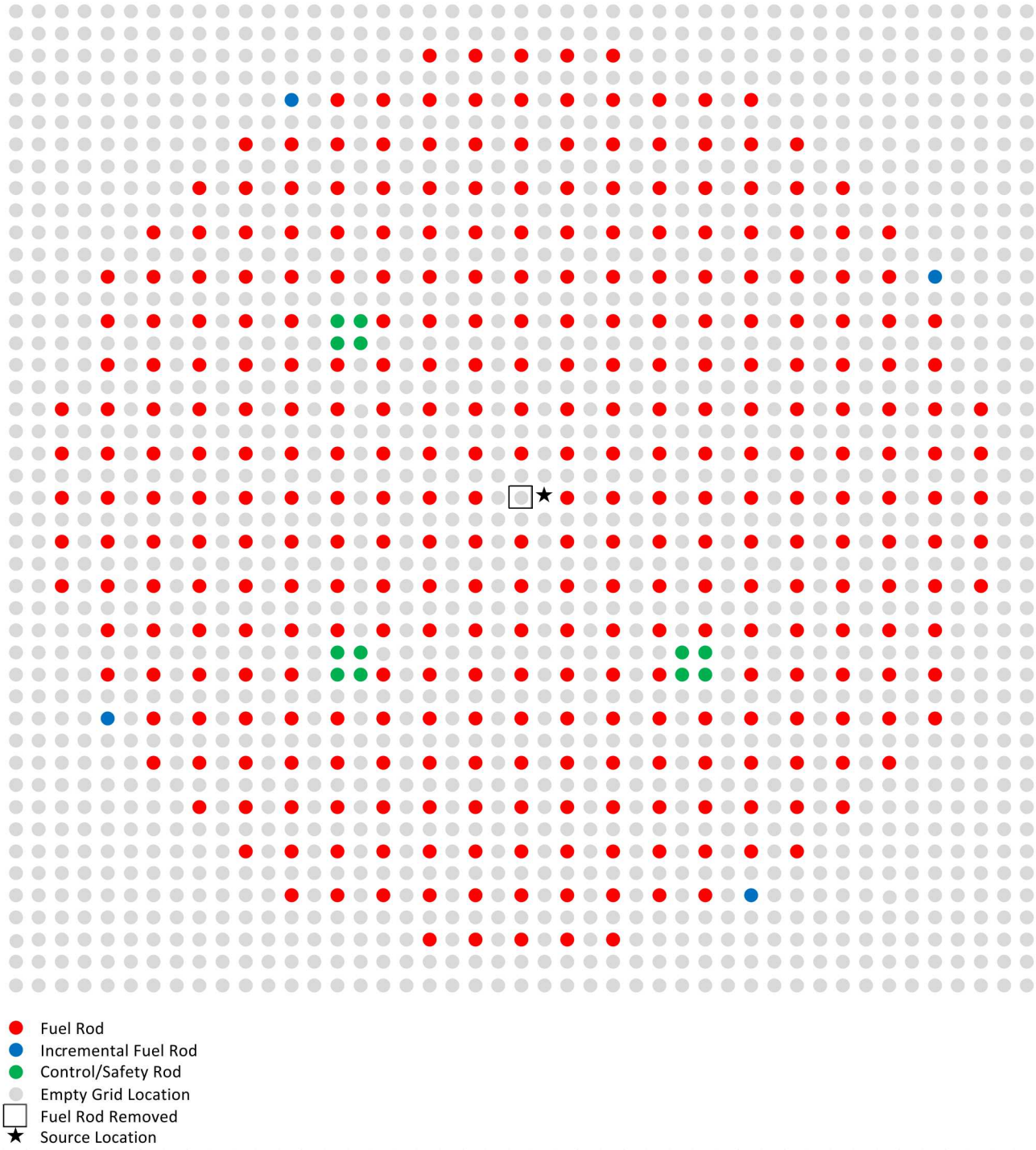

Figure 43. Fuel Rod Layout of the Largest Array Measured for Case 25.

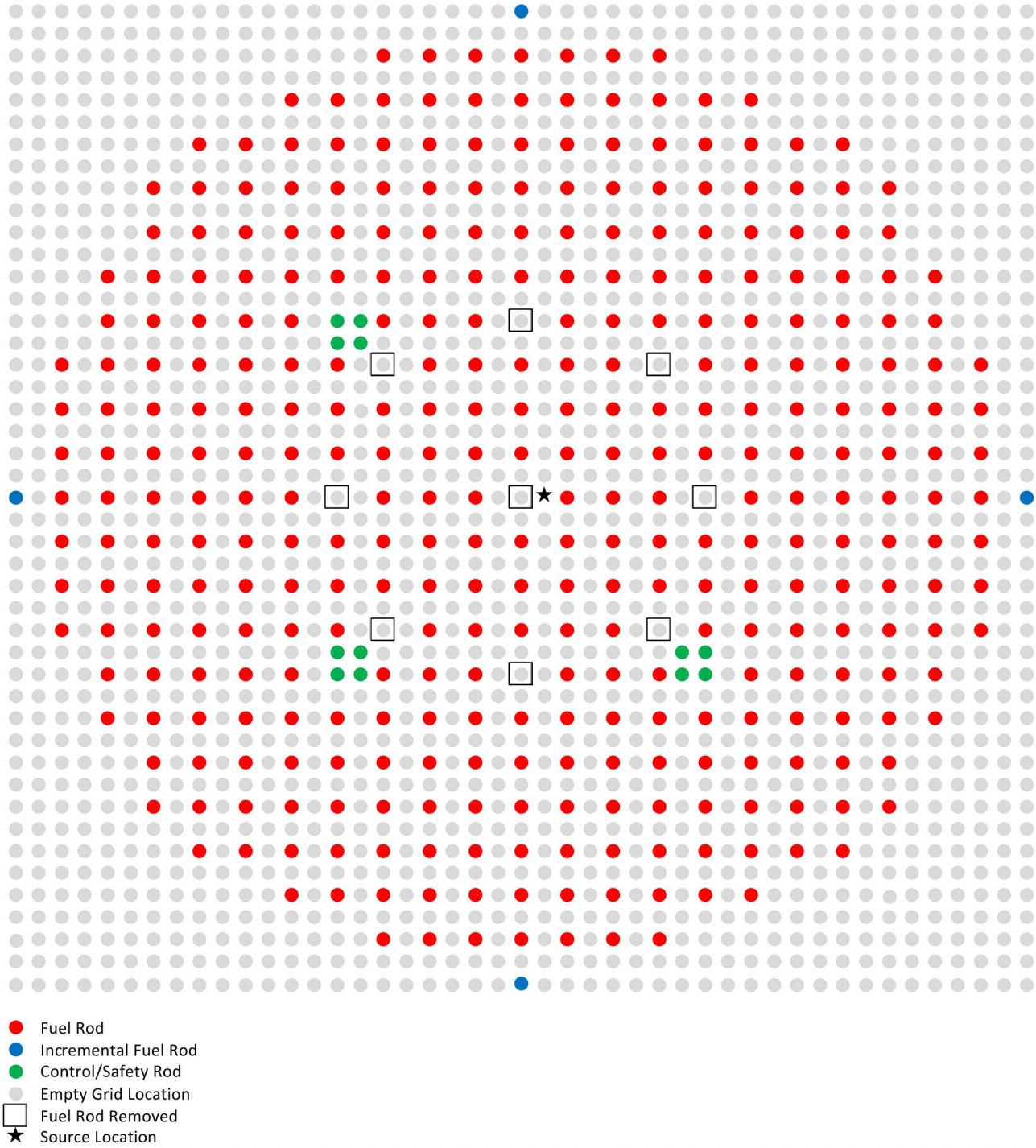

Figure 44. Fuel Rod Layout of the Largest Array Measured for Case 26.

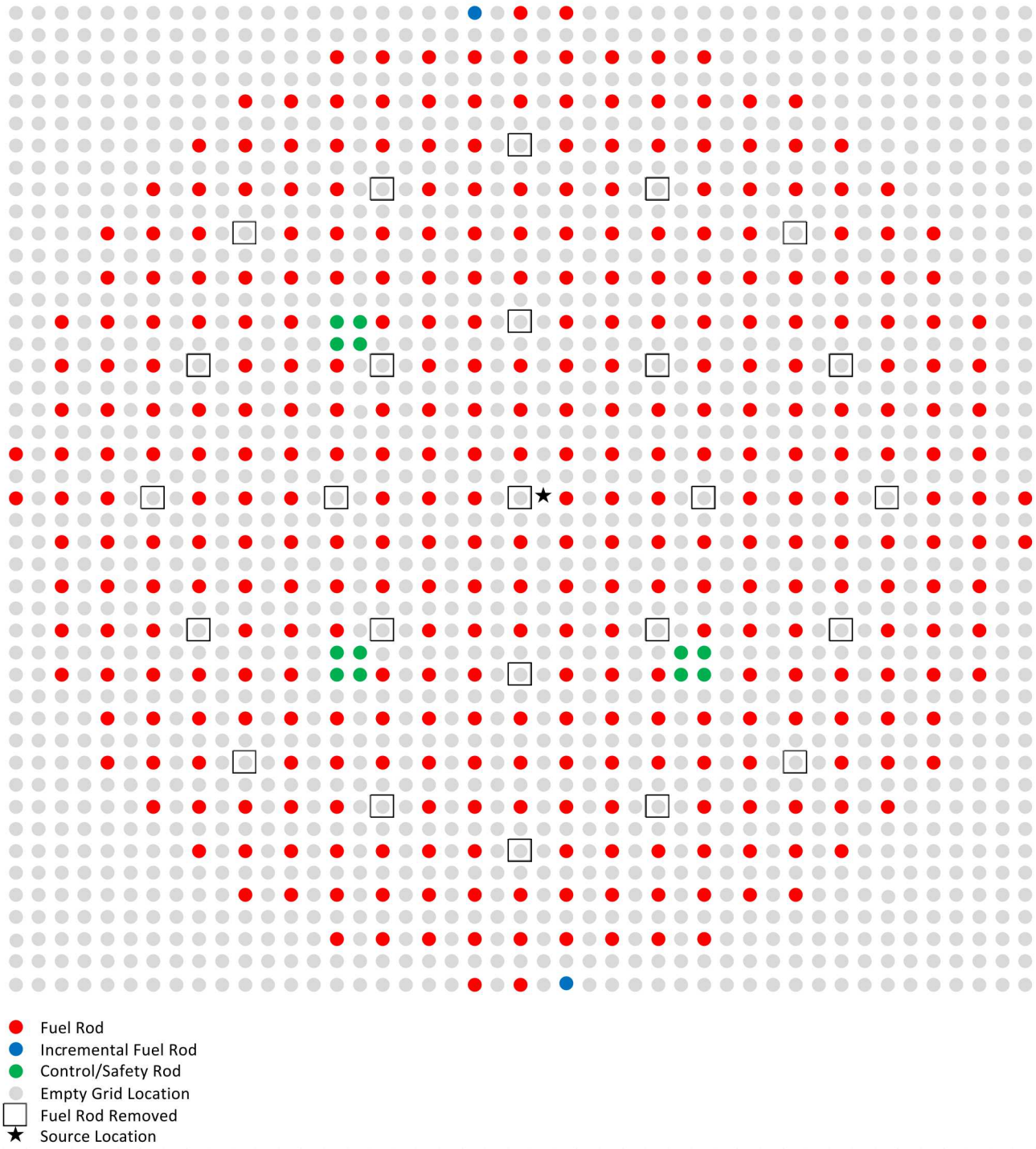

Figure 45. Fuel Rod Layout of the Largest Array Measured for Case 27.

1.3 Description of Material Data

1.3.1 UO_2 Fuel – The fuel pellets used in the fuel rods were drawn from the fuel stock that was removed from fuel elements obtained from The Pennsylvania State University. The uranium isotopic data were measured for ten randomly-selected fuel pellets from the pool of fuel pellets used in the fuel rod fabrication using a high-resolution multi-collector inductively coupled plasma mass spectrometer (ICP-MS). The measured uranium isotopic data are given in Table 10. The uncertainties shown with the mass fractions are the standard deviations for the ten measurements. The systematic uncertainties were estimated by the laboratory that made the isotopic measurements.

Table 10. Isotopic Composition of Uranium in 6.90 % Enriched UO_2 Fuel Pellets.

Uranium Isotope	Wt. % [(a)]	Systematic Uncertainty (Wt. %) [(b)]
^{234}U	0.02814 ± 0.00008	0.00013
^{235}U	6.9034 ± 0.0046	0.0069
^{236}U	0.06336 ± 0.00012	0.00063
^{238}U	93.0051 ± 0.0046	-
Total	100.000	-

(a) The uncertainties given are the standard deviations for ten measurements.
(b) The systematic uncertainties are given at the one-standard-deviation level.

The oxygen to uranium ratio was not measured.

Metallic impurities were also obtained during the ICP-MS measurements of the ten fuel pellets. The results of the impurity measurements are shown in Table 11.

Table 11. Results of the Fuel Impurity Measurements.

Element	Average[(a)] (g/g)	Standard Deviation[(a)] (g/g)	Maximum[(b)] (g/g)	Minimum[(c)] (g/g)	Reported Detection Limit[(d)] (g/g)	Measurements Above Detection Limit
Ag	1.61E-07	2.19E-07	6.67E-07	2.24E-08	2.24E-08	9
B	4.17E-07	4.73E-07	1.56E-06	2.24E-08	2.24E-08	9
Cd	2.25E-07	3.98E-07	9.36E-07	2.21E-08	2.27E-08	5
Co	2.06E-07	5.67E-08	3.13E-07	1.27E-07	-	10
Cr	2.11E-05	1.06E-05	4.03E-05	1.31E-05	-	10
Cu	2.19E-06	1.59E-06	4.95E-06	2.26E-07	2.26E-07	9
Fe	9.31E-05	4.31E-05	1.79E-04	5.27E-05	-	10
Mn	2.52E-06	1.04E-06	4.51E-06	1.50E-06	-	10
Mo	1.93E-06	1.85E-06	5.19E-06	6.34E-07	-	10
Ni	3.32E-05	1.13E-05	5.73E-05	2.31E-05	-	10
V	1.22E-07	2.33E-08	1.56E-07	9.71E-08	-	10
W	1.07E-07	1.14E-08	1.23E-07	8.53E-08	-	10
Sm	5.31E-08	-	5.31E-08	2.21E-08	2.27E-08	1
Dy	-	-	-	-	2.27E-08	0
Eu	-	-	-	-	2.27E-08	0
Gd	-	-	-	-	2.27E-08	0

(a) The impurities were reported as mass of impurity per unit UO_2 fuel pellet mass. Averages and standard deviations are reported for the measurements that were above the detection limit for the element. Measurements at the detection limits were not included in the averages or the calculation of the standard deviations. Because only one measurement was above the detection limit for Sm, no value is reported for the standard deviation.

(b) Reported maximum measured value. No value is included when all measurements were at the detection limit.

(c) Reported minimum measured value when all ten measurements were above the detection limit. Minimum of the reported detection limits when one or more measurements were below the detection limit. No value is included when all measurements were at the detection limit.

(d) The detection limit varied slightly from sample to sample. The maximum detection limit is recorded. Where all measurements were above the detection limit, no value is entered.

1.3.2 Fuel Rod Cladding – The fabrication drawings for the fuel rods specify the material for the clad tubing and end plugs as aluminum alloy 3003. The composition of the material used was not measured. The specification for the composition of aluminum alloy 3003 is given in Table 12. The density of the cladding material was not measured.

Table 12. Chemical Composition Limits of Aluminum Alloy 3003.

Element	Weight % [(a)]
Si	0.6 max
Fe	0.7 max
Cu	0.05 – 0.20
Mn	1.0 – 1.5
Zn	0.10 max
Other Elements Each	0.05 max
Other Elements Total	0.15 max
Al	Remainder

(a) From ASTM B210-04

1.3.3 Aluminum Grid Plates – The upper and lower grid plates were fabricated from 1.00 in (2.54 cm) thick plates of aluminum alloy 6061-T651. The measured composition of the grid plates is compared with the 6061 aluminum specification in Table 13. The density of the grid plate material was not measured.

Table 13. Chemical Composition Limits of Aluminum Alloy 6061 Compared to the Measured Composition of the Grid Plates.

Element	Weight %	
	6061 spec [(a)]	Measured
Si	0.40 – 0.8	0.72
Fe	0.7 max	0.62
Cu	0.15 – 0.40	0.31
Mn	0.15 max	0.09
Mg	0.8 – 1.2	1.04
Cr	0.04 – 0.35	0.20
Zn	0.25 max	0.12
Ti	0.15 max	0.02
V	–	0.01
Zr	–	0.00
Other Elements Each	0.05 max	–
Other Elements Total	0.15 max	0.06
Al	Remainder	Remainder

(a) From ASTM B209-10

1.3.4 Aluminum Guide Plate – The composition of the aluminum tooling plate used in the guide plate was also measured. That composition is given Table 14. The density of the guide plate material was not measured.

Table 14. Chemical Composition of the Aluminum Tooling Plate used in the Guide Plate.

Element	Weight %
Si	0.50
Fe	0.60
Cu	1.2
Mn	0.75
Mg	1.6
Cr	0.06
Zn	3.00
Other Elements Total	0.06
Al	Remainder

1.3.5 Water – The water moderator in the assembly was taken from the de-ionized water supply in the facility. Samples of the moderator were taken during the experiment and archived. No chemical analysis was done on the water samples.

The facility water is taken from the Albuquerque municipal water supply. The deionizer is fed from that source. The Albuquerque municipal water system is divided into nineteen distribution regions. The water quality is monitored in each distribution region. Table 15 lists the impurities detected in the water for the year 2017. Both the city-wide average and the maximum level across the system are listed in the table. Table

16 lists the elements for which testing was done but that were not detected in the system along with the detection limit for those elements.

Table 15. Impurities Measured in the Albuquerque Municipal Water Supply in the Year 2017.

Element	Units [a]	City-Wide Average [b]	Maximum Detected in the Water System [b]
As	PPB	2	9
Ba	PPM	ND [c]	0.2
Cr	PPB	1	8
U	PPB	2	9
Fe	PPM	0.004	0.036
Ca	PPM	50	67
Cl	PPM	33	48
Mg	PPM	5.5	8.8
K	PPM	3.2	7
Na	PPM	28	86

(a) Parts Per Million (PPM) or Parts Per Billion (PPB) by mass.
(b) Data obtained from http://www.abcwua.org/Water_Quality_by_Distribution_Zone.aspx on June 13, 2018.
(c) ND: Not Detected

Table 16. Impurities Tested but not Detected in the Albuquerque Municipal Water Supply in the Year 2017.

Element	Units [a]	Detection Limit [b]
Sb	PPB	1
Be	PPB	1
Cd	PPB	1
Hg	PPB	0.2
Se	PPB	5
Tl	PPB	1

(a) Parts Per Billion (PPB) by mass.
(b) Data obtained from www.abcwua.org/Substances_Not_Found.aspx on June 13, 2018.

1.3.6 Stainless Steel – The source capsule was fabricated from 316L stainless steel. The specific composition of the material used in the source was not measured. The specification for the composition 316L stainless steel is listed in Table 17. The density of the stainless steel was not measured.

Table 17. Composition of 316L Stainless Steel.

Element	Weight % [a]
C	0.030 max
Mn	2.00 max
P	0.045 max
S	0.030 max
Si	1.00 max
Cr	16.0 – 18.0
Ni	10.0 – 14.0
Mo	2.00 – 3.00
Fe	Remainder

(a) From ASTM A276-10

The composition of the corrosion-resistant steel springs in the fuel rods is listed in the manufacturer's catalog as "stainless steel." No further composition data were available on the springs.

1.3.7 Polyethylene – The fuel rods included polyethylene in the part of the rod that was in the reflector. The annuli surrounding the radiation detector dry wells were also polyethylene. Polyethylene has the basic molecular formula CH_2.

1.3.8 Boron Carbide – The boron carbide powder used to fill the absorber sections of the control and safety elements was mixed from two lots of powder mixed equally before loading into the absorber sections. The composition data for the two lots of boron carbide are given in Table 18

Table 18. Composition and Particle Size Data for the Boron Carbide.

Quantity		Lot 1 [(b)]	Lot 2 [(b)]
Boron Mass Fraction (%)		77.0	77.0
Carbon Mass Fraction (%)		21.7	21.6
B_2O_3 Mass Fraction (%)		0.1	0.1
Silicon Mass Fraction (%)		<0.010	<0.010
Iron Mass Fraction (%)		0.10	0.10
Nitrogen Mass Fraction (%)		0.04	0.07
^{10}B Isotopic Abundance (atom %)		20.02	20.01
Particle Size Distribution (micron) [(a)]	3 %	11.23	158.2
	50 %	7.251	80.13
	94 %	3.140	40.47

(a) The particle size above which the specified fraction of the material falls.
(b) The mass fractions do not sum to 100 %. The remainder is unknown and is treated as void.

1.4 Temperature Data

The water temperature in the experiment was measured at three different heights in the reflector of the assembly with thermocouples. The average measured temperature for each case is shown in Table 8.

1.5 Supplemental Experimental Measurements

Additional experimental measurements were not performed.